Eindhoven University of Technology

MASTER

Modeling respiratory induced variations in blood pressure

Diepen, S.

Award date:
2006

Link to publication

Disclaimer
This document contains a student thesis (bachelor's or master's), as authored by a student at Eindhoven University of Technology. Student theses are made available in the TU/e repository upon obtaining the required degree. The grade received is not published on the document as presented in the repository. The required complexity or quality of research of student theses may vary by program, and the required minimum study period may vary in duration.

General rights
Copyright and moral rights for the publications made accessible in the public portal are retained by the authors and/or other copyright owners and it is a condition of accessing publications that users recognise and abide by the legal requirements associated with these rights.

- Users may download and print one copy of any publication from the public portal for the purpose of private study or research.
- You may not further distribute the material or use it for any profit-making activity or commercial gain

Eindhoven University of Technology
Department of Electrical Engineering
Signal Processing Systems

TU/e

Modeling respiratory induced variations in blood pressure

by S. Diepen

Master of Science thesis

Project period: 14-2-2005 – 29-3-2006
Report Number: 15-06

Commissioned by: Prof.dr. H.H.M. Korsten

Supervisors:
Prof.dr. H.H.M. Korsten
Dr.ir. J.A. Blom

Additional Commission members:
Prof.dr.ir. J.W.M. Bergmans
Prof.dr.ir. P.F.F. Wijn

The Department of Electrical Engineering of the Eindhoven University of Technology accepts no responsibility for the contents of M.Sc. theses or practical training reports

Preface

This thesis describes the results of my graduation project at the MBS/SPS group of the department of electrical engineering at the Eindhoven University of Technology, in cooperation with the Catharina Hospital in Eindhoven. The project marks the end of my study period which started in September 2000. The project itself started in February 2005. The main research was finished in February 2006.

During the project I had the opportunity to present parts of this work and results (the new method to quantify the respiratory induced variations in systemic arterial blood pressure) at the annual conference of the European Society of Computing and Technology in Anesthesia and Intensive Care (ESCTAIC) in Aalborg, Denmark. I am very grateful for this experience.

Sincere gratitude goes to my supervisors and coaches (Prof.dr. H.H.M. Korsten, Dr.ir. J.A. Blom, and H.M. Kuipers). Furthermore, I would like to mention Herman Ossevoort. We spent a lot of time together working on the casus for Biomedical Engineering and the Publieksdag. During these times we often had nice off-topic discussions. Also, I want to thank my (former) colleagues at 3.31, who created a nice working atmosphere and gave critical notes on my project, the ESCTAIC presentation and on my thesis.

Thanks go to the staff of the intensive care unit and operating rooms of the Catharina Hospital, Eindhoven. In particular Dr. A.J.G.H. Bindels and Dr. A.N. Roos who helped me out and gave useful background information.

Finally, I wish to express my thanks to my family and friends for their support during the years that I spent at the university. And last but certainly not least Anja for her patience and support.

Eindhoven, March 2006
Sjoerd Diepen

Summary

During surgery or in the intensive care hypovolemia (or hypovolemic shock; a too small circulating blood volume), is easily correctable by fluid loading therapy, yet very difficult to assess. Clinicians are aware of the risks of (hypovolemic) shock and often start with this therapy. However, approximately 50% of the patients does not respond positively and fluid loading may result in overfilling the circulation, which is harmful as well. Currently, there is no method to reliably predict a patient's response to this therapy. The scope of this thesis is to develop such a method. The method consists of a coupled model of the respiratory and circulatory system and the finding that during positive pressure ventilation variations in arterial blood pressure, which are related to the filling status of a patient, can be observed.

During positive pressure ventilation, the varying intrathoracic pressure causes variations in preload which, in turn, cause variations in stroke volume. The latter are reflected as variations in arterial blood pressure and may be used as indicator for fluid loading responsiveness: high amplitudes indicate significant changes in stroke volume for changes in preload. An increase in preload due to volume loading will then result in a significant increase in stroke volume and cardiac output. Successive values used for indication can fluctuate highly, resulting in inconsistent successive indications. Therefore, a new approach is introduced. Currently, maximum and minimum systolic pressures, pulse pressures, and stroke volumes during one respiratory cycle are used. In the new approach, systolic pressures, pulse pressures, and stroke volumes are thought of as samples of modulation envelopes. When the maximum and minimum values of these envelopes are used, successive indications are more consistent. Although a consistent value for the variations in stroke volume can be obtained now, the clinical value is unclear since changes in preload are unknown.

A coupled physiological model of the respiratory and circulatory systems is derived, based on models of both systems that already exist and the most significant influences causing the variations in arterial blood pressure (as mentioned in literature). Eventually, the model may assist the clinician in assessing fluid loading responsiveness based on the (variations in) preloads and stroke volumes as calculated by the model. Only a qualitative verification of the model was performed. Ventilator settings and total blood volume were changed and the trends in simulations and patient data were compared. The latter were both measured and obtained from literature. For the measurements, a system was developed.

For all ventilator setting changes as well as for changing the blood volume, the trends in simulation results are consistent with the trends found in patient data. However, the ventilation periods used in the model differed with the periods in patient data as they were extended. The extended periods were used because it was found that the shape and phase of the modulation envelopes in the model depend on the respiratory period. Two recordings during which the respiratory periods were varied seem to confirm this dependency. Whether the (changes in) shape and phase are valuable information in clinical practice yet remains unclear and needs further research. An aspect that needs further research as well is a parameter estimation routine which is necessary to do a quantitative verification and make the model usable in clinical practice. Furthermore, further research on an unexpected high-frequency component that was observed in the model's modulation envelopes is necessary.

Contents

List of Acronyms

ABP	Arterial Blood Pressure
AWP	Airway Pressure
BMTV	Body Mass scaled Tidal Volume
CO	Cardiac Output
EDF	European Data Format
FSM	Finite State Machine
ICU	Intensive Care Unit
LBM	Lean Body Mass
OR	Operating Room
PEEP	Positive End Expiratory Pressure
PPV	Pulse Pressure Variation
PPM	Pulse Pressure Modulation
RMV	Respiratory Minute Volume
SPM	Systolic Pressure Modulation
SPV	Systolic Pressure Variation
SV	Stroke Volume
SVM	Stroke Volume Modulation
SVV	Stroke Volume Variation

chapter 1

Introduction

1.1 Background

During major surgery and intensive care, a patient's blood flow can become too low. This means that too little oxygen will be supplied to the body's peripheral tissue and organ sites. Also too little carbon dioxide will be taken out of these sites. Especially during surgery, the low blood flow may be due to a too small circulating blood volume, resulting from e.g. inevitable losses of blood. Situations in which a patient's blood volume is too small are called hypovolemia or hypovolemic shock. Hypovolemia is not the only possible cause of shock. Problems with the functioning of the heart and infections may cause shock as well. Situations in which the functioning of the heart is the cause are called cardiogenic shock, whereas situations in which infections are the cause are called septic shock. Shock may result in irreversible organ failure and damage to peripheral tissue. Therefore, it is important to diagnose and counteract shock. According to Shoemaker et al. [1999], almost half of the 2.1 million annual deaths in the United States are patients who die acutely from shock and/or organ failure.

Clinicians want to prevent and, if necessary, counteract cases of shock. A common question that clinicians standing at the bedside therefore often face is "Can I improve the patient's well being by means of fluid loading?" [Perel, 2003]. Fluid loading involves adding fluid (i.e. blood/solutions) to the circulating blood volume. In this manner clinicians want to increase the volume of blood that the heart pumps into the body each minute. This volume is called Cardiac Output (CO). Since the CO is a volume per unit of time, it is a measure of the blood flow. Thus, by means of fluid loading the clinician wants to increase the blood flow.

Fluid loading is not the only available therapy to counteract shock. Medications supporting the heart and its function can also be used [Michard and Teboul, 2002]. For hypovolemic patients or patients with septic shock, these drugs may have an adverse effect [Beale et al., 2004]. Adequate fluid loading is therefore a prerequisite for successful and appropriate use of such medications. Unfortunately, the desired increase in CO does not necessarily materialize with fluid loading. Besides on blood volume, CO depends on the functioning of the heart and of the rest of the circulatory system. For example, if a patient has a very stiff (or non-compliant) heart, the addition of fluid does not improve the heart functioning and CO will not increase significantly. In this case, the patient does not respond positively to fluid loading.

According to Perel [2003], only 50% of the patients in intensive care respond positively to fluid loading. For the negative responders, often patients with a malfunctioning heart, the addition of too much fluid results in hypervolemia, a situation where the system contains too much blood. Hypervolemia, in turn, may result in harmful situations such as pulmonary oedema, a life-threatening situation in which fluid accumulates in the lungs, making it difficult for the lungs to expand and to exchange gases. Therefore, it is of great importance to assess a patient's responsiveness to fluid loading before one starts with this therapy. Unfortunately, there is no general way to predict a patient's response to fluid loading therapy accurately. Traditionally, clinicians assess the response by determining whether the CO increases significantly during stepwise fluid loading, a time-consuming invasive procedure [Perel, 2003].

Responsiveness to fluid loading mainly depends on the functioning of the heart. This functioning is usually expressed in terms of preload and Stroke Volume (SV; CO = heart rate x SV). Preload is defined as the tension in the heart muscle due to the blood volume in the ventricle just before the muscle contracts. SV is the volume of blood that the heart ejects during a heart cycle. Fluid loading usually results in increased preload and knowledge of the value of preload might therefore be helpful in assessing fluid loading responsiveness. Since preload cannot be measured in vivo, approximations of preload such as cardiac filling pressures and cardiac dimensions must be used. However, although these parameters contribute to preload, they do not reflect the correct preload value [Norton, 2001]. Furthermore, the parameters alone have minimal clinical value for the assessment of fluid loading responsiveness [Michard and Teboul, 2002]. Therefore, using these parameters of preload to predict a patient's response to fluid loading is not favorable.

Most cases of shock occur in operating room and intensive care unit settings. In these settings, patients are usually fully sedated and therefore cannot breathe themselves. Artificial breathing is ensured by a ventilator. During a respiratory cycle the ventilator pumps a mixture of gases containing oxygen into the patient's lungs, after which the patient can expire passively. To ensure gas inflow into the patient's lungs, a positive pressure compared to the pressure inside the lungs is applied in the patient's trachea. For this reason, the artificial breathing is called positive pressure ventilation. In literature positive pressure ventilation is usually referred to as mechanical ventilation.

It was found that during mechanical ventilation variations in arterial blood pressure (ABP) can be observed [Massumi et al., 1973]. ABP is the blood pressure measured in the large arteries that transport oxygen-rich blood from the heart to the periphery. The pressure waveform is usually measured invasively, although non-invasive measurement is also possible [Blom, 2004]. The variations in ABP result from variations in SV, which, in turn, result from variations in preload [Michard, 2005]. The variations in preload are due to the periodical increases in lung and thorax pressures resulting from the ventilation. Artificial respiration thus induces variations in ABP.

Since the variations in ABP reflect variations in SV, they depend on the functioning of the heart and can hence be used as indicators for the assessment [Michard, 2005]. They are generally accepted as appropriate indicators [Bendjelid and Romand, 2003; Michard, 2005]. However, according to Boldt et al. [1998], only one percent of clinicians use them. This can be explained by four reasons:

1) **Variations in preload:**
   The variations in ABP reflect variations in SV. However, the variations in preload are not known. Therefore, a clear indication of the functioning of the heart cannot be obtained if only the

variations in ABP are used.

2) **Fluctuations:**
The variations in ABP for successive respiratory cycles can fluctuate highly. This means that when the amplitudes are used for assessing fluid loading responsiveness, a patient could be found a positive responder after one respiratory cycle and, strangely, a negative responder after the next. So, although two commercially available monitors are capable of quantifying the variations in ABP each respiratory cycle (PulseCo by LiDCO Ltd. and PiCCO by Pulsion Medical Systems GmbH[1] [Parry-Jones and Pittman, 2003]), clinicians may not obtain consistent information.

3) **Threshold:**
The amplitude of the variations in ABP depend on ventilator settings and patient specific parameters. Since these settings and parameters may differ from patient to patient, it is difficult to determine a threshold for the variations in ABP in order to discriminate between positive and negative responders of fluid loading.

4) **Availability:**
Except for the previously mentioned monitors, the variations in ABP are not presented by most patient monitors. They only present a filtered version of the ABP waveform that does not contain the respiratory induced variations anymore. The assessment of the response to fluid loading based on manual processing of the respiratory induced variations in ABP as proposed by Gouvêa and Gouvêa [2005] is then not possible.

From these four reasons, the first one is the most important. If variations in preload can be measured, the combination of the respiratory induced variations in ABP or SV and the preload variations should give a clear indication of the functioning of the heart and response to fluid loading can be determined reliably, so more clinicians will use them. In this thesis a coupled model of the respiratory and circulatory system is developed. By using the model's estimates of (variations in) preload, the model might assist a clinician in assessing a patient's responsiveness to fluid loading.

In order to be valuable, the model parameters need to be adjusted in order to accurately match model signals and measured signals. The respiratory induced variations in the model's ABP should then match the measured respiratory induced variations in ABP. A system is therefore developed to calculate these variations. In order to compare them to the variations in the model's ABP, the problem of the fluctuations has to be resolved. A solution to this problem is given in the thesis.

The model is not fully validated yet. However, a preliminary qualitative verification shows promising results. If these results are confirmed by a full validation, the model may indeed be used for assisting the clinician in assessing a patient's fluid loading responsiveness. The threshold and availability problems may then not be an issue anymore.

1.2 Problem definition and research objectives

In order to assess responsiveness to fluid loading, a clinician needs to know how the heart of a patient is functioning. During mechanical ventilation variations in ABP can be observed which reflect

[1] PiCCO does not quantify the variations in ABP based on one respiratory cycle, but uses the maximum and minimum values seen during the last 30 seconds [Berkenstadt et al., 2001].

variations in SV. To assess the responsiveness reliably, simultaneous variations in preload need to be available because then the functioning can be determined. However, as said before, preload cannot be measured directly.

If the relation between the measured respiratory pressure and ABP is modeled accurately, tuning the parameters of the resulting model in order to tune the simulation signals to best match the measured patient signals might provide helpful diagnostic information. The estimation of preload as given by the model would then be valuable. Ultimately, a real-time system based on such a model could assist the clinician at the bedside in assessing a patient's response to fluid loading based on respiratory induced variations in preload and SV during mechanical ventilation.

The research objectives of this project are as follows:

a) Modeling the respiratory induced variations in ABP by means of a coupled model of the respiratory and circulatory systems.

b) Calculating the respiratory induced variations in ABP by measuring ABP and airway pressure waveforms. Since the signals may contain artifacts, they need to be validated. Using the validated signals the indicators of the respiratory induced variations in ABP can be calculated.

c) Adding a parameter estimation routine to the coupled model that uses available patient signals to estimate the patient-specific parameters in order to match the simulation signals with measured patient signals.

Patient-specific parameters will have to be estimated in short periods of time during which only limited data can be obtained, therefore, the model cannot contain too many parameters. On the other hand, with too few parameters, the model might not be able to produce reliable (and usable) results. There is thus a design trade-off between accuracy and complexity.

A system needs to be implemented that is able to process the patient data and calculate the respiratory induced variations in the measured ABP. An implementation of the model is also necessary. Ultimately, both implementations should run in one program to match the variations in the modeled ABP to measured variations in ABP.

1.3 Report outline

Background information on the circulatory system, the respiratory system as well as well as influences of the respiratory system on the circulation during mechanical ventilation are described in Chapter 2. Currently used measures of the respiratory induced variations in ABP are described in Chapter 3. In Chapter 4, a new approach to measure these variations is presented. A coupled model of the respiratory and circulatory systems is developed in Chapter 5. In Chapter 6 aspects of the model implementation and simulation results are presented. Limitations for obtaining patient data are listed in Chapter 7. Due to limitations experiments were not possible. Only passive recordings were obtained. Results obtained from these recordings can be found in Chapter 8. Results of the project are presented in Chapter 9. Finally, based on the project results, conclusions are drawn and recommendations are given in Chapter 10.

The emphasis of the project lies on the modeling part, therefore, the emphasis of the report lies on the modeling too. However, because a system to process patient signals online was needed for the project, much attention was paid to constructing such a system as well. A description of this system and how it is constructed is presented in Appendix B.

chapter 2

Anatomy and physiology

Blood is one of the body's main transport media. Besides delivering oxygen and nutrients throughout the body, carbon dioxide and other waste products are taken to areas where they can be disposed of. In order to perform its tasks, blood circulates through the cardiovascular system.

In the lungs the carbon dioxide is taken out of the blood and leaves the body, whereas freshly inhaled oxygen comes into the blood. The respiratory system ensures the supply of oxygen and the drainage of carbon dioxide through the airways.

This chapter describes the main anatomical and physiological aspects of both systems: the circulation and the respiration. It then continues with influences of the respiration on the circulation during mechanical ventilation.

2.1 Circulation

2.1.1 Heart

The main part of the cardiovascular system is the heart. This is a hollow muscle located in the thoracic cavity and pumps blood by contracting and relaxing (quasi-)periodically. Without the pumping of the heart, blood would not be able to circulate through the body. If there is no circulation of blood, the body will not get oxygen and nutrients, while at the same time carbon dioxide and other waste products pile up in the body's periphery.

A schematic version of the heart is depicted in Figure 2.1.[1] From the picture it can be seen that the heart is divided into two sides, each containing an atrium and a ventricle. The ventricles are the main pumping elements. The atria only improve ventricle filling with about twenty percent [Guyton and Hall, 2000]. The blood enters the left atrium through the pulmonary vein and is ejected from the left ventricle into the systemic artery, called the aorta. On the right side, blood enters the atrium through the vena cava and is ejected from the ventricle into the pulmonary artery. The systemic and pulmonary circulations are described in Section 2.1.2 and Section 2.1.3, respectively.[2] Valves between the atria and ventricles as well as between the ventricles and the arteries ensure uni-directional flow of blood.

[1] Frontal drawing, so the left side of the heart is drawn on the right.

[2] There is also a third circulation, the coronary circulation, which is meant to supply the heart muscle with blood.

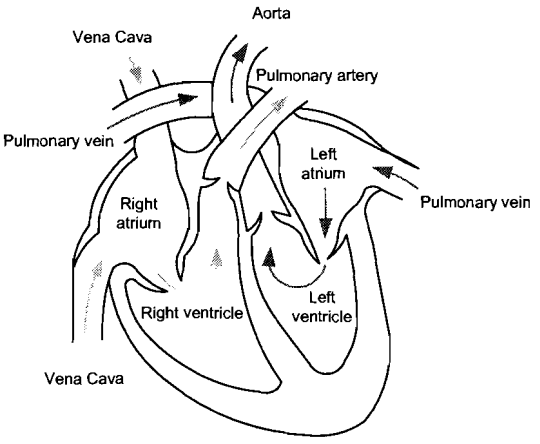

Figure 2.1: *Schematic drawing of the heart with flow directions of the blood. Oxygen-rich blood (dark arrows) enters the left atrium from the pulmonary vein. The left atrium fills the left ventricle and from here the blood is ejected into the systemic artery (aorta). Carbon dioxide-rich blood (light arrows) enters the right atrium from the vena cava. The right atrium fills the right ventricle and from here blood is injected into the pulmonary artery. Valves between atria and ventricles as well as between ventricles and arteries ensure uni-directional flow of blood (adapted from Guyton and Hall [2000]).*

The pumping of the ventricles can be split up into four phases: filling, isovolumetric contraction, ejection, and isovolumetric relaxation. When the ventricle is relaxed, blood flows from the atrium into the ventricle. The blood volume of the ventricle increases, while the pressure in the ventricle increases only slightly. The relationship between the ventricle's pressure P and blood volume V is called a PV-loop, because it is cyclic. A typical example of such a loop and its previously mentioned phases is depicted in Figure 2.2. Furthermore, the difference between the volumes during isovolumetric contraction and relaxation, the Stroke Volume (SV), is also shown in this figure.

At some point in time the atrium contracts, resulting in the previously mentioned extra filling. Not long after this the ventricle also contracts. The pressure in the ventricle now becomes higher than the pressure in the atrium, so the valve between atrium and ventricle closes. Since the pressure is lower than the arterial pressure, the valve between ventricle and artery is also closed, so blood cannot flow out of the ventricle now. The blood volume in the ventricle thus remains constant. However, because the ventricle contracts, the pressure keeps increasing. Since the blood volume remains constant, the contraction is called isovolumetric.

During the next phase, the pressure in the ventricle becomes higher than the pressure in the artery. The valve between the artery and the ventricle now opens and blood is ejected into the circulation.

After some time of ejection, the ventricle relaxes again. This causes the ventricle's pressure to drop below the pressure in the artery, so the valve between ventricle and artery closes and no blood flows out anymore. The pressure keeps dropping until the valve between the atrium and the ventricle opens again since the pressure in the ventricle becomes lower than the atrial pressure. Like the contraction phase, this phase of relaxation is called isovolumetric, as the volume remains constant throughout the phase. When the pressure in the ventricle drops below the atrial pressure, the cycle starts over again.

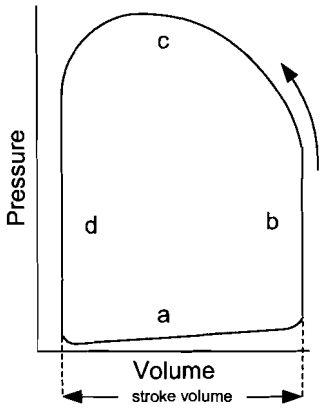

Figure 2.2: *The pressure volume relationship of the ventricle (PV-loop) consists of four phases: (a) filling, (b) isovolumetric contraction, (c) ejection and (d) isovolumetric relaxation. The difference between the volumes during contraction and relaxation is the stroke volume.*

2.1.2 Systemic circulation

From the ventricle, blood is ejected into the large arteries the large arteries. The pressure measured in these arteries is the called the arterial blood pressure (ABP) and is referenced to atmospheric pressure. The arteries successively branch into smaller vessels. Blood then enters the capillary section, in which the smallest vessels, the capillaries, are located. In this section oxygen is supplied to the tissue and carbon dioxide is taken out. At the end of this section vessels join again into veins. All veins together form the venous section. This section forms the blood reservoir from which the right atrium is filled with blood again. This reservoir normally contains around 64% of the body's circulating blood volume [Guyton and Hall, 2000]. Changes in the circulating blood volume will normally only affect the volume contained in this reservoir.

To ensure flow of blood, positive pressure gradients between the different sections are necessary. In Figure 2.3 (normal) blood pressures are shown for the three sections. Since the blood has to be pumped through the whole body, the pressures in the arterial section are much higher than the pressures in the venous section. While in the arterial section big fluctuations due to the pumping of the heart are clearly present, these are completely damped in the venous section.

Unlike the heart, only parts of the systemic circulation are located in the thoracic cavity. For example, the abdominal aorta, as the name implies, is located in the abdomen instead of the thoracic cavity, whereas the vena cava is almost entirely included in the thoracic cavity.

2.1.3 Pulmonary circulation

Like the systemic circulation, the pulmonary circulation consists of an arterial, a capillary and a venous section. However, as the blood in this circulation does not have to be transported through the whole body, the pressures in the arterial and capillary sections are much lower than those in the systemic circulation. For example, the systolic and diastolic pressures of the pulmonary artery are approximately 30 mm Hg and 15 mm Hg, compared to 120 mm Hg and 80 mm Hg in the systemic arteries [Guyton and Hall, 2000].

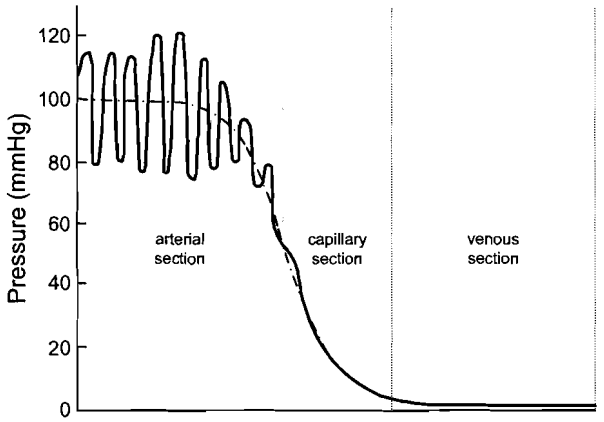

Figure 2.3: *Blood pressures in the main sections of the systemic circulation (adapted from Guyton and Hall [2000]).*

Besides the differences in blood pressures, the main function of this circulation differs from the systemic one. While the systemic circulation is responsible for transporting oxygen to the capillaries and carbon dioxide away, the pulmonary circulation transports carbon dioxide to the lung capillaries and exchanges it there with freshly inhaled oxygen.

Like the heart, the pulmonary circulation is entirely encapsulated in the thoracic cavity.

2.1.4 Closing the loop

The blood circulation is a closed loop system. The left ventricle ejects the blood into the aorta. Blood then flows through the systemic circulation from the vena cava (both superior and inferior) into the right atrium. When it is then ejected from the right ventricle, it enters the pulmonary artery. At the end of the pulmonary circulation, the oxygen-rich blood flows from the pulmonary vein into the left atrium. So the loop is closed.

In healthy persons approximately 84% of the blood is contained in the systemic circulation, 9% in the pulmonary circulation, and 7% in the heart [Guyton and Hall, 2000].

2.2 Respiration

2.2.1 Airways and lungs

In order to perform their tasks, cells in the body need oxygen and have to lose carbon dioxide. In the previous section it was mentioned that the flow of blood ensures transport of these gases. It was also mentioned that in the pulmonary circulation carbon dioxide in the blood is exchanged with oxygen in the lungs. Oxygen flows into the lungs from the mouth and/or nose (i.e. the inspiratory phase) and carbon dioxide has to flow vice versa (i.e. the expiratory phase).

After gas is inhaled through mouth and/or nose it travels through the trachea. The trachea branches into two airways, the left and right bronchi. Like the arteries of the blood circulation that branch successively into smaller vessels, the bronchi branch into smaller bronchi. An overview of this branching, called a bronchial tree, is shown in Figure 2.4. If one calls the trachea generation 0, then the branching stops

at generation 23, called the alveoli. Until the generation 17 generation there is only transport of gas. From this generation on, gas exchange with the blood takes place.

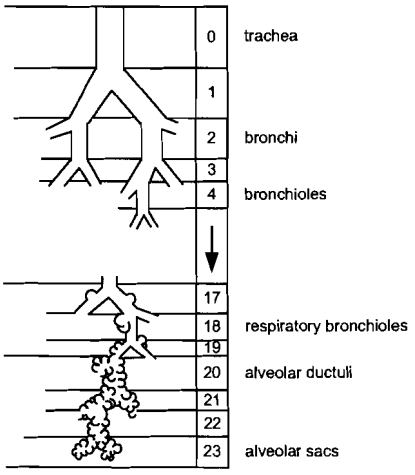

Figure 2.4: *The generations of the bronchial tree. Generations 0 to 16 transport gas. Gas exchange takes place in generations 17 to 23 (adapted from Blom [2004]).*

2.2.2 Spontaneous breathing

During the inspiratory phase of spontaneous breathing, respiratory muscles contract. The contraction results in a volume increase of the thorax and therefore also of the lungs. This change of volume causes the pressure inside the lungs to decrease, so gas is 'sucked' into the lungs.

Although the inspiration is active, the expiration can be both passive and active. If the previously mentioned muscles relax, the volumes of the thorax and the lungs decrease, so the gas flows out of the lungs. This is a passive process. During active expiration the previously mentioned muscles also relax, however, at the same time other muscles contract. The contraction of these muscles causes the thoracic volume to decrease much faster.

2.2.3 Artificial breathing

There are cases where spontaneous breathing is not possible. For example, during surgery, where the muscles (including the respiratory muscles) of a patient are relaxed due to anesthetics. Since shortage of oxygen can quickly become lethal, such patients need artificial breathing or mechanical ventilation.

Mechanical ventilation ensures the flow of gas into the lungs by applying either a (time-varying) pressure or a (time-varying) flow. The pressure needs to be positive during inspiration in order to create a positive pressure gradient between trachea and lungs. Since the intrathoracic pressure, which is negative at rest, becomes less negative or even positive due to the positive pressure applied to the trachea. The outflow of gas from the lungs is usually passive, until a certain end pressure is reached. If this end pressure is positive, it is called positive end expiratory pressure. This pressure may also be zero, in which case it is called zero end expiratory pressure. The end expiratory pressure is used to

keep the lungs inflated.

2.3 Respiratory induced variations in ABP

As mentioned before, the respiratory system and parts of the circulatory system are contained within the thoracic cavity. In Figure 2.5 a horizontal cross section of the thorax at the height of the lungs is shown. The left and right lungs are enclosed by the visceral pleura. The inside of the ribs is enclosed by the parietal pleura. The space between these pleurae is called the intrapleural space. Furthermore, the image shows that the heart, the bronchi, and the esophagus are surrounded by the lungs. Although not shown in the image, the same holds for the pulmonary circulation, in which the blood flows from the heart, through the lungs, back to the heart.

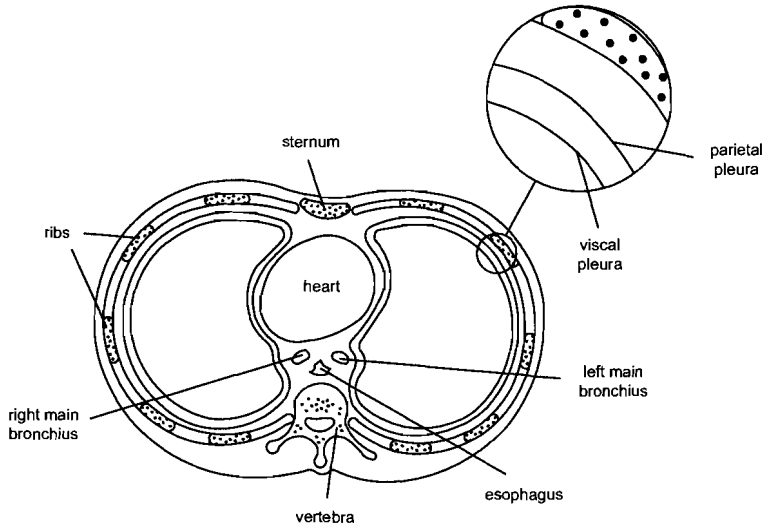

Figure 2.5: *Horizontal cross section of the thorax at the height of the lungs. Ribs are located at the edge of the thorax. The inside of the ribs is enclosed by the parietal pluear. The bronchi that transport gas, as well as the esophagus and the heart are enclosed by the two lungs. The lungs are enclosed by the vicseral pleura (adapted from Blom [2004]).*

The changes in volume and pressure during breathing result in changes of the environment in which the heart, the pulmonary circulation, and part of the systemic circulation. The latter changes cause respiratory influences on the circulation. Especially during mechanical ventilation, the positive pressure in the lungs and the increased pressure in the thorax compresses the blood vessels contained in the thoracic cavity. Blood volume in these vessels therefore gets squeezed out. Of course this can only happen if there is an exit. Near the inflow valves of the heart, this can only happen if the pressure in the venous sections is higher than the pressure inside the ventricle. Depending on the hemodynamic state of the patient and the type of vessel, some vessels can even collapse fully.

Compressed vessels and squeezing of blood is not the case during spontaneous breathing, because then the intrathoracic pressure is negative and the swings in alveolar (lung) pressure are not as high. Also, alveolar pressure is negative during inspiration. An example of the difference in alveolar

pressures and intrathoracic pressures during spontaneous breathing and ventilation is depicted in Figure 2.6.[3]

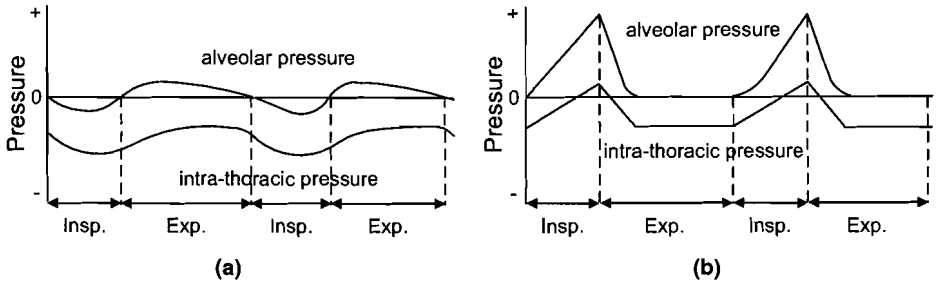

Figure 2.6: *Difference in alveolar and intrathoracic pressure during (a) spontaneous breathing and (b) ventilation. When breathing spontaneously, alveolar pressure becomes negative during inspiration. Intrathoracic pressure is negative. During mechanical ventilation, alveolar pressure is always positive and intrathoracic pressure is increased (adapted from Oczenski et al. [1996]).*

The respiratory influences on the circulation during mechanical ventilation, cause variations in systemic ABP. This is because SVs vary [Michard, 2005]. The variations in SV can be explained by the Frank-Starling curve as shown in Figure 2.7 [Guyton and Hall, 2000]. The Frank-Starling curve describes the relation between a ventricle's preload and the SV. As can be seen, this is not a linear relation. It can be split up into two parts: the steep part and the plateau part. A change in preload on the steep part results in a larger change in SV than a similar change in preload on the plateau part. During positive pressure ventilation, variations in preload occur, which result in variations in SV. The ABP depends on the SV, so respiratory induced variations in ABP can be observed.

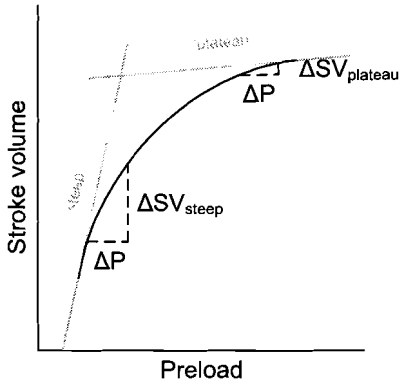

Figure 2.7: *Typical example of a Frank-Starling curve with a steep part and a plateau part. Similar changes in cardiac preload result in larger changes in SV in the steep part than in the plateau part.*

With fluid loading, the clinician wants to increase the preload in order to increase the SV and thereby the Cardiac Output (CO; CO = heart rate x SV). The Frank-Starling curve for a stiff heart (or ventricle) is shown in Figure 2.8. The curve mainly consists of a plateau part. Therefore, for patients with a stiff

[3]The original image uses intra-pulmonary and intra-pleural pressure. For convenience, these are substituted by alveolar pressure and intrathoracic pressure, respectively.

heart, fluid loading usually does not increase the Cardiac Output (CO; CO = heart rate x SV), since increased preload will not result in a significant increase in CO.

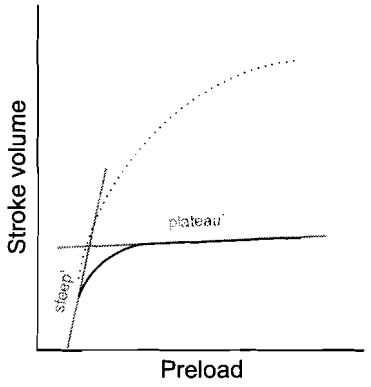

Figure 2.8: *Typical example of a Frank-Starling curve of a stiff heart (solid sline). Similar changes in cardiac preload still result in larger changes in SV in the steep part than in the plateau part. However, compared to the Frank-Starling curve of a normal heart (dotted line), the shape is ratter flat and mainly consists of a plateau part.*

Fluid loading generally results in increased cardiac preload. The variations in ABP can therefore be used to detect on which part of the Frank-Starling curve the heart is working. Therefore, the variations in ABP can be used as a good indication for fluid loading responsiveness. For patients with stiff ventricles it will also be clear that volume loading (and the increase in preload) will not increase the SV and thereby the CO.

2.4 Summary

In this chapter a brief overview of the human blood circulation and the respiratory system was given. Furthermore, the influences that the latter have on the former were mentioned.

Blood is pumped from the left part of the heart through the systemic circulation to the right side of the heart. In this part of the systemic circulation, the body exchanges the oxygen in the blood with carbon dioxide. Also waste products are obtained and delivered to sections where they can be disposed of. From the right side of the heart, blood flows back to the left part through the pulmonary circulation. In this part of the circulation carbon dioxide is exchanged with freshly inhaled oxygen in the lungs.

The respiratory system enables inhalation of oxygen-rich gas and exhalation of carbon dioxide-rich gas from the lungs. In spontaneous breathing, the 'pumping' of this system is caused by the in- and expiratory muscles. During the inspiratory phase a negative pressure is created in the lungs, so air flows through the nose (or mouth) and trachea to the lungs. During expiration, either passive or forced, gas contained in the lungs flows back.

During mechanical ventilation the flow into the lungs is ensured by either creating a positive pressure drop between mouth and lungs (pressure controlled ventilation) or by forcing a gas to flow through the trachea (flow controlled ventilation). The flow of gas out of the lungs is usually passive, until a certain

end expiratory pressure is reached.

Since the respiratory system and parts of the circulatory system are contained within the thoracic cavity, the respiratory system has influences on the circulatory system. This is especially the case during mechanical ventilation, where the positive pressure in the lungs and thorax result in variations in preloads and SVs. The variations in SV are reflected in variations in ABP.

chapter 3

Currently used measures of respiratory induced variations in arterial blood pressure

In the previous chapter it was mentioned that, during mechanical ventilation, respiratory induced variations in arterial blood pressure (ABP) reflect variations in Stroke Volume (SV). If the amplitudes of the variations in SV are high, the heart is likely to be working on the steep part of the Frank-Starling curve. The Cardiac Output (CO; CO = heart rate x SV) will then most likely increase significantly with fluid loading, because fluid loading increases preload. Therefore, a clinician can use the variations in ABP as an indicator for a patient's fluid loading responsiveness.

This chapter describes the currently used measures of respiratory induced variations in ABP. It continues with drawbacks of these measures and factors that influence their values.

3.1 Systolic Pressure Variation

A close look at the ABP waveform shows that the peak pressures (called systolic pressures) vary during the respiratory cycle. From the start of the cycle, the pressure peaks can rise above the first peak and fall below it. The difference between the maximum and minimum systolic pressures during one respiratory cycle is called the Systolic Pressure Variation (SPV) [Rick and Burke, 1978]. An example of the varying systolic pressures and the corresponding SPV value is shown in Figure 3.1(a).

According to Michard [2005], the pulse pressure, which is defined as the difference between a pressure peak and the preceding pressure valley (called diastolic pressure), depends on the SV. Since the systolic pressure depends on the pulse pressure, it depends on the SV as well. Variations in systolic pressure therefore reflect variations in SV, and hence they can be used as indicator for a patient's fluid loading responsiveness.

To clearly discriminate between variations in ABP seen during inspiratory and expiratory phases, Perel et al. [1987] proposed to decompose the SPV into a $\triangle_{up}$ component and a $\triangle_{down}$ component. Here $\triangle_{up}$ is defined as the difference between the maximum systolic peak seen during the respiratory cycle and a baseline systolic pressure. The $\triangle_{down}$ component is defined as the difference between the baseline pressure and the minimum systolic pressure seen during the respiratory cycle. The baseline systolic pressure is the systolic pressure that can be measured after a short period of apnea (i.e. after a period when breathing is stopped). In Figure 3.1(b) the decomposition of the SPV from Figure 3.1(a) is shown.

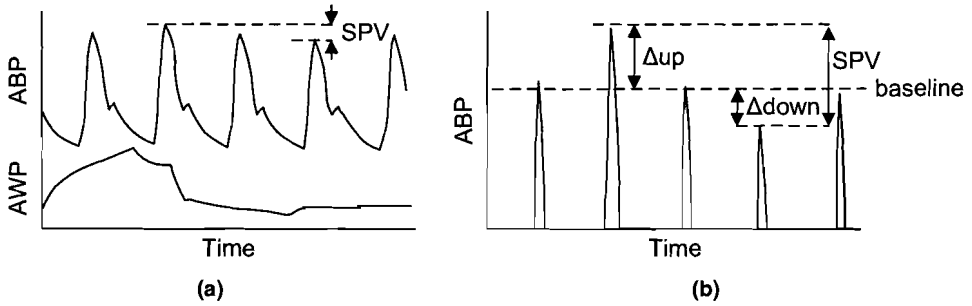

Figure 3.1: *(a) Simultaneous tracings of arterial blood pressure (top) and airway pressure (bottom) waveforms during one respiratory cycle. The SPV is the difference between the maximum and minimum systolic pressures during one respiratory cycle. (b) The decomposition of the SPV into $\triangle_{up}$ and $\triangle_{down}$ components for the same respiratory cycle using a baseline systolic pressure.*

Although Perel et al. [1987] showed that the $\triangle_{down}$ component was a better indicator for fluid loading responsiveness than the SPV, determining the baseline systolic pressure is somewhat cumbersome since the ventilator must be turned off [Schwid and Rooke, 2000]. Therefore, Schwid and Rooke [2000] proposed to use the end-expiratory systolic pressure as a surrogate. Using this surrogate and an approach somehow similar to the one described in the next chapter, Fujita et al. [2004] were able to show that the SPV and $\triangle_{down}$ values are equally sensitive indicators for assessing fluid loading responsiveness.

3.2 Pulse Pressure Variation

As said before, the pulse pressure is directly proportional to the SV [Michard, 2005]. Therefore, Michard et al. [1999] proposed to measure the respiratory induced variations in ABP as the variations that can be seen in pulse pressure, because variations in pulse pressure reflect variations in SV more directly than the variations in systolic pressure.

Whereas the SPV is based on the maximum and minimum systolic pressures during one respiratory cycle, the Pulse Pressure Variation (PPV) is based on the maximum and minimum pulse pressures during the cycle. In Figure 3.2 the maximum and minimum pulse pressures seen during a respiratory cycle are highlighted. However, instead of the absolute difference between maximum and minimum pulse pressures, the PPV is defined as the difference between the maximum and minimum pulse pressures expressed as a percentage of their average.

Like the decomposition of the SPV, a decomposition of the PPV using a baseline pulse pressure was proposed [Morelot-Panzini et al., 2003]. However, contrary to the SPV's $\triangle_{down}$ component, the equivalent component of the PPV was found to be as sensitive for assessment of fluid loading responsiveness as the PPV itself. According to Michard [2005], this emphasizes the minimal role of the inspiratory increase in left ventricular SV in the respiratory induced variations in SV.

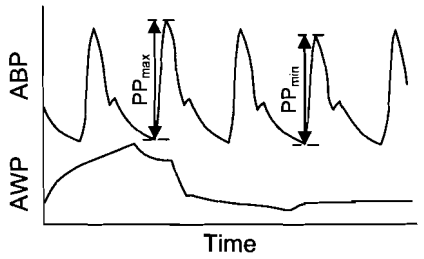

Figure 3.2: *Simultaneous tracings of arterial blood pressure (top) and airway pressure (bottom) waveforms during one respiratory cycle. The maximum and minimum pulse pressures (PP_{max} and PP_{min}) are necessary for calculation of PPV.*

3.3 Stroke Volume Variation

It was stated earlier that the respiratory induced variations in ABP reflect respiratory induced variations in SV. A clinician is interested in the latter type of variations, because they give information about the functioning of the heart. Instead of measuring the respiratory induced variations in ABP it would thus be better to measure the respiratory induced variations in SV. Unfortunately, measuring the variations in SV using maximum and minimum SVs of one respoiratory cycle is not always possible since measurement of true beat-to-beat SVs has limited use [Magder, 2004].

Different methods have been proposed that can estimate beat-to-beat SVs based on the ABP waveform: (improved) pulse contour analysis [McDonald, 1974; Wesseling et al., 1983] and Modelflow [Wesseling et al., 1993]. In pulse contour analysis, the SV is computed using the systolic area (A_{sys}) of a pressure pulse: $SV = A_{sys} / Z_{ao}$, where Z_{ao} is the characteristic impedance of the aorta. In Figure 3.3 the systolic area of a pressure pulse is shown. It is defined as the area between a pressure pulse and the diastolic pressure level during the blood ejection period. Since the characteristic impedance of the aorta is not constant (it depends on pressure, age and pulse wave velocity which increases with age), Wesseling et al. [1983] developed a correction formula for Z_{ao} to improve the pulse contour analysis' outcome.

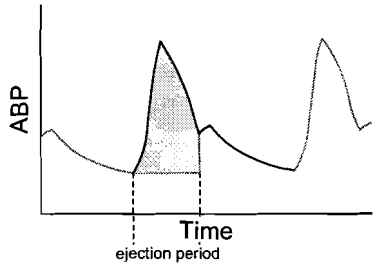

Figure 3.3: *The systolic area of a pressure pulse (highlighted area) is defined as the area between the pressure pulse and the diastolic pressure level during the blood ejection period.*

Modelflow [Wesseling et al., 1993] uses aortic pressure and the three-element model shown in Figure 3.4 to compute aortic flow. The three elements (aortic characteristic impedance Z_0, buffer compliance C_w, and peripheral resistance R_p) depend on pressure, time, and patient specific parameters. With the known ABP waveform P(t) and the computed elements, the aortic flow $\dot{Q}(t)$ can be computed. In turn,

the SV can be found if this flow is integrated over the blood ejection period.

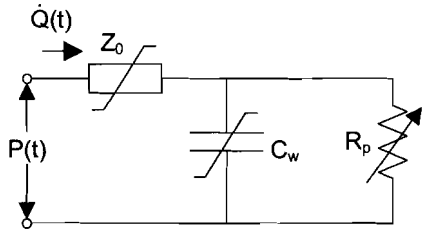

Figure 3.4: *Three-element model for aortic (in-)flow $\dot{Q}(t)$ computation using known ABP waveform P(t), aortic impedance Z_0, buffer compliance C_w, and peripheral resistance R_p.*

When the approximated SVs are compared to the 'golden standard' of cardiac output measurements based on dilution techniques, errors are mostly systematic [Jansen et al., 2001]. As the Stroke Volume Variation (SVV) is the difference between the maximum and minimum stroke volumes during a respiratory cycle expressed as a percentage of the average of the two, the errors are proportional and will thus be canceled in the SVV.

3.4 Drawbacks of the indicators and influencing factors

If the SPV, PPV, and SVV values of successive respiratory cycles are compared, it can be seen that they can fluctuate highly. An example of such fluctuations in the SPV values of six successive respiratory cycles is shown in Figure 3.5.

When the fluctuating values are used as indicators for fluid loading responsiveness, the clinician may get inconsistent indications. For example, during one respiratory cycle a value may indicate that a patient is a positive responder, whereas the value during the next cycle indicates that he or she is a negative responder. If for the successive SPV values that are shown in Figure 3.5 a threshold of 6 mm Hg is used to discriminate between positive responders (SPV > 6 mm Hg) and negative responders (SPV <= 6 mm Hg), the indication would indeed almost alter each respiratory cycle between positive and negative responder. Similar inconsistencies in indication can be observed when successive PPV and SVV values are used. The inconsistency in indications is a major drawback of the currently used indicators of respiratory induced variations in ABP. The source of the fluctuations and a solution to increase the consistency are described in the next chapter.

Another major drawback is the fact that the indicators only reflect variations in SV and that the variations in preload are not known. Therefore, it is impossible to say whether the heart is working on the steep part of the Frank-Starling curve or on the plateau part.

The fact that respiratory induced variations in ABP can only be used as indicators for fluid loading responsiveness when patients are fully sedated and ventilated is a drawback as well. However, this is considered a minor drawback only, since the assessment of this responsiveness is often only important in situations where the patients are critically ill, in which case they usually are fully sedated and ventilated.

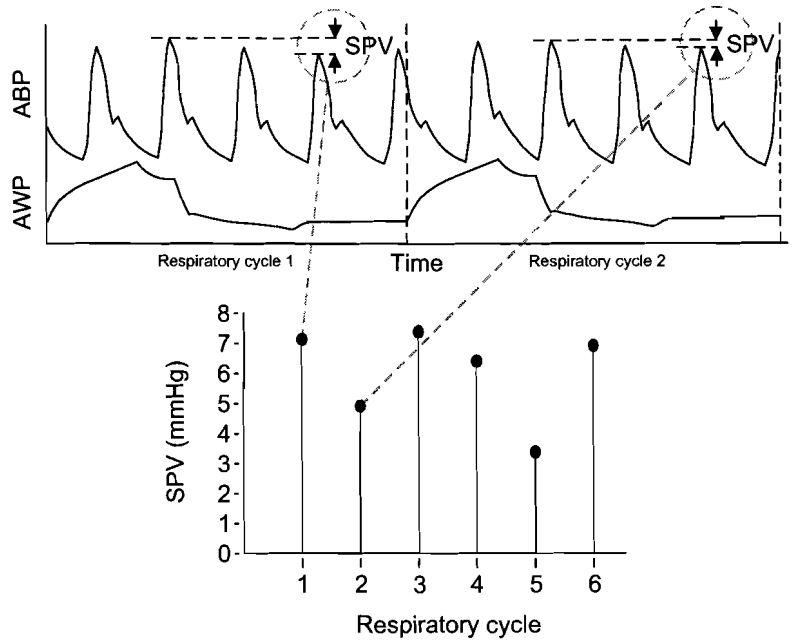

Figure 3.5: *SPV values for successive respiratory cycles can fluctuate highly. The top graph shows how the first two SPV values of the bottom graph are calculated.*

The threshold value for the SPV of 6 mm Hg as described above was chosen arbitrarily. However, clinicians do not have specified values to use as thresholds [Michard, 2005]. This is mainly because the magnitude of the variations in ABP highly depends on patient specific parameters and ventilator settings which usually differ per patient/situation. For example, increases in tidal volume result in increases in SVV [Reuter et al., 2003].[1] Other factors that influence the measures of respiratory induced variations in ABP are the patient's lung and chest wall compliances and the level of positive end expiratory pressure [Michard, 2005].

3.5 Summary

Currently used measures of respiratory induced variations in ABP are the SPV, the PPV, and the SVV. Each respiratory cycle, the SPV is the difference between the maximum and minimum systolic pressures during the respiratory cycle. The PPV is the difference between the maximum and minimum pulse pressures during the cycle, expressed as a percentage of the average of the two pressures. The SVV is defined as the difference between the maximum and minimum stroke volumes during the cycle expressed as a percentage of the average of the two volumes. Beat-to-beat stroke volumes cannot always be measured directly, but can be approximated using a three-element model and the ABP waveform.

[1] Perel et al. [2005] proposed a manoeuvre to reduce or even cancel out the influence of the tidal volume, consisting of several (three to four) successive incremental pressure-controlled breaths. The minimal systolic values following the breaths are plotted against their respective airway pressures, producing the Respiratory Systolic Variation Test slope. This test manoeuvre was shown to be as predictive as the PPV [Preisman et al., 2005].

Successive SPV, PPV, and SVV values can fluctuate highly and therefore indications of fluid loading responsiveness may vary each respiratory cycle. The fact that indications are not consistent is a major drawback. Another major drawback of the SPV, PPV, and SVV values is that they only reflect changes in SV and that changes in preload are not known. Determining the heart's working area on the Frank-Starling curve accurately is therefore not possible. Full sedation and ventilation are requirements on usage of the respiratory induced variations in ABP as indicators for fluid loading responsiveness. However, this is considered a minor drawback since most patients for which assessment of fluid loading responsiveness is important are fully sedated and ventilated. A more important drawback is the fact that the SPV, PPV, and SVV values are influenced by patient specific parameters and ventilator settings.

chapter 4

Measures of respiratory induced variations in arterial blood pressure based on modulation envelopes

In the previous chapter it was stated that the currently used measures of respiratory induced variations in arterial blood pressure (ABP) may result in inconsistencies because their values for successive respiratory cycles can fluctuate highly. These inconsistencies limit their indicative value in the assessment of fluid loading responsiveness. A new approach to measure the respiratory induced variations in ABP resulting in more consistent successive values is presented in this chapter.

In the first section the source of the fluctuations is discussed. Hereafter, the new approach is presented. A comparison between the SPV approach and the new approach applied to systolic pressures is given in Chapter 9.

4.1 Source of fluctuations in successive indicator values

Since the ventilation signal is cyclic, the influences of the respiration on the circulation during mechanical ventilation are cyclic as well. The ventilation rate and heart rate are usually not synchronized, because the ventilation rate is artificial and the heart rate is not. This implies that if one looks at two successive respiratory cycles, the heart beats that occur during the first respiratory cycle have different timings with respect to the start of the cycle than the heart beats in the second respiratory cycle. Similar respiratory influences will thus have different effects on the circulation during these cycles and the variations in preload, Stroke Volume (SV), and ABP will be different. Therefore, the successive values of the measures of respiratory induced variations in ABP can fluctuate for these cycles.

4.2 Reducing fluctuations in successive indicator values

4.2.1 Averaging

In some studies the problem of the fluctuations in successive indicator values is solved by averaging the values across several successive respiratory cycles [Szold et al., 1989; Pizov et al., 1990; Preisman et al., 1997]. This means that there can be situations in which values above a responsiveness threshold are observed, while the mean value is below the threshold. Thus, although indications of positive response to fluid loading are present, the average indication shows that the patient will not respond positively to fluid loading. Averaging may therefore result in false indications.

4.2.2 Modulation envelopes

Based on the source of the fluctuations, it was assumed that the respiratory influences on the circulation have a periodicity that is equal to the ventilation period. The variations are then part of a cyclic process as well. If the periodicity of this cyclic process is the same as that of the ventilation signal, the values used for measuring the respiratory induced variations in ABP (systolic pressures, diastolic pressures, and stroke volumes) can be seen as samples of signals that have the same periodicity as the respiration, implying that these signals can be seen as modulation envelopes of systolic pressures, diastolic pressures, and stroke volumes. The fluctuations in successive indicator values can then be reduced by using the minimum and maximum values of the envelopes instead of the minimum and maximum values seen during each respiratory cycle. This is because for successive respiratory cycles the envelopes should not change, at least not for stationary situations.

For systolic pressures, Diepen et al. [2005] called the modulation approach 'Systolic Pressure Modulation'(SPM). Similarly, Pulse Pressure Modulation (PPM) and Stroke Volume Modulation (SVM) can be defined for the modulation approach applied to pulse pressures and stroke volumes, respectively.

In Figure 4.1 the concept of this approach is shown for systolic pressures. In the top graph the SPV values for two successive respiratory cycles are indicated. It can be seen that SPV_1 and SPV_2 are not equal. In the bottom graph the cyclic envelope signal for these two cycles is drawn. Using the minimum and maximum values of this envelope, the SPM can be calculated. Whereas the SPV values for the separate cycles are different, the SPM is equal for both respiratory cycles.

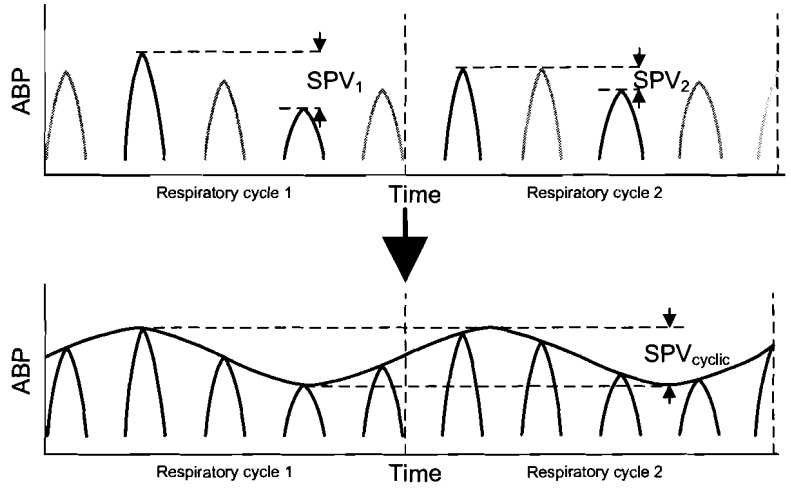

Figure 4.1: *Instead of calculating SPV_1 and SPV_2, the SPM should be calculated using the minimum and maximum systolic pressures of the modulation envelope which is described by all systolic pressures of both respiratory cycles. Whereas SPV_1 and SPV_2 are different, SPV_{cyclic} is the same for both respiratory cycles.*

An example of approximated envelopes for systolic and diastolic pressures that were constructed after neural influences were filtered out (see Section 4.2.4) is shown in Figure 4.2. The envelopes (solid black lines) are constructed using the systolic and diastolic pressures (dots) that were seen in respiratory cycles during the last 75 seconds. The SPM's history window was thus 75 seconds. The

ABP waveform during the most recent respiratory cycle is also included (dotted gray line).

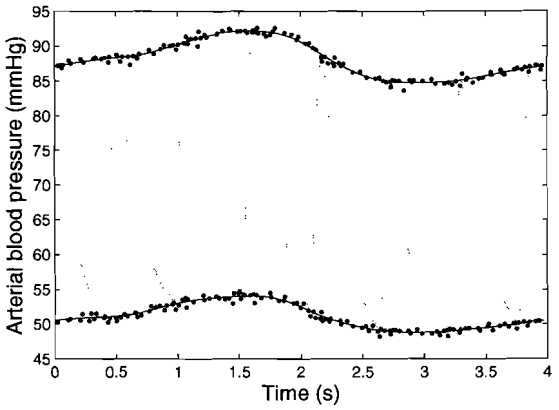

Figure 4.2: *Systolic and diastolic pressures (dots) from the past 75 seconds indicate existence of systolic and diastolic modulation envelopes (solid black lines). For convenience, the arterial blood pressure waveform that was seen during the most recent respiratory cycle is also shown (dotted gray line).*

One could argue that the modulation approach is limited to patients that do not have cardiac arrhythmias, because if such arrhythmias occur variations in preload are not solely induced by the respiration. However, the currently used measures are also affected if such arrhythmias occur. In fact, according to Cannesson et al. [2005], respiratory induced variations in ABP should not be used at all to indicate responsiveness to fluid loading when such arrhythmias occur. This limitation thus applies to all forms of assessing fluid loading responsiveness based on these variations.

4.2.3 Increasing the sample rate and approximating the envelopes

The frequency with which the envelopes are sampled (i.e. the heart rate) is relatively low. This means that the maximum and minimum values (systolic pressures, diastolic pressures, and stroke volumes) that are seen during a respiratory cycle are not necessarily the maximum and minimum values of the envelopes. Unfortunately, one cannot just ask the patient to increase the heart rate. Therefore, the heart rate has to be increased artificially.

Since the envelopes have the same periodicity as the respiratory signal, samples of different respiratory cycles describe the same signal. Due to the non-synchronicity, the sample rate can therefore be increased if the samples of multiple respiratory cycles are combined. In other words, the different cycles are projected on to one combined respiratory cycle. A conceptual example of this for systolic pressures is drawn in Figure 4.3.

An interpolation algorithm can be applied to the samples of the combined respiratory cycle in order to approximate the envelopes. The actual shape of the envelopes is not known and, as will be seen in Chapter 8, seems to depend on the respiratory period. Also, when the samples of multiple successive respiratory cycles are combined and projected on to one respiratory cycle, they are not necessarily equidistant. The chosen interpolation algorithm is able to interpolate curves of which the exact shape is unknown using data that is sampled inequidistantly [Reinsch, 1967].

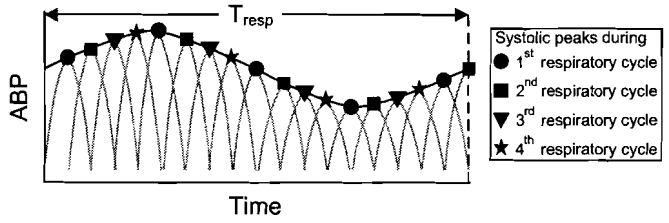

Figure 4.3: *The periodicity of the systolic pressure envelope is the same as that of the respiration signal: T_{resp}. To increase the sample rate with which the systolic pressure envelope is sampled, systolic pressures measured during four successive respiratory cycles are combined and projected on to one respiratory cycle. Together, the pressure points form the cyclic systolic pressure envelope.*

Samples of successive respiratory cycles are used and therefore the state of the patient should be stable during these cycles. Because of this, the window length cannot be too long.

Fujita et al. [2003] used a somehow similar approach for calculation of SPV and called the approximated envelope the 'Systolic Pressure Curve'. However, although they perform a projection of systolic pressures as well, this projection is not onto one respiratory cycle.

4.2.4 Neural influences

Besides the respiratory induced variations in ABP, also neural influences act on the cardiovascular system [Malpas, 2002]. These influences may be clearly present as low-frequency oscillations in the ABP. Guyton and Harris [1951] found waves in the ABP in the range of 0.03–0.06 Hz that were clearly visible in animals who had lost 20–25% of their blood volume. The amplitudes of these waves were in the order of 20–40 mm Hg. In Figure 4.4 an extreme example of such low-frequency distortions on the ABP is shown. The ABP signal was recorded from a hypovolemic patient who was diagnosed brain dead. The combination of hypovolemia and brain death may have caused the extreme amplitude of the low-frequency distortions.

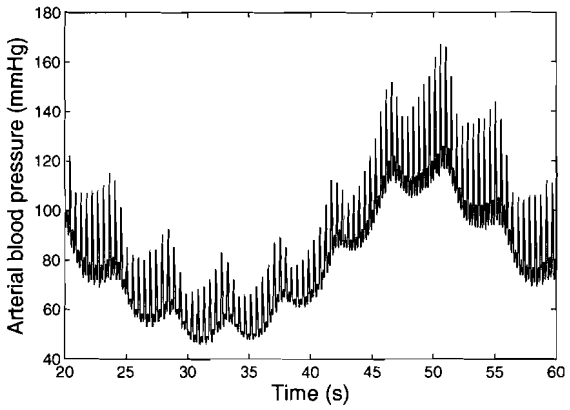

Figure 4.4: *Besides the respiratory induced variations in ABP ($\approx$ 0.2 Hz) a neural related low-frequency component ($\approx$ 0.03 Hz) distorts the ABP significantly.*

Although the neural related influences are usually not as extreme as the ones that distort the ABP

shown in Figure 4.4, such low-frequency components have to be filtered out before the envelopes can be constructed/approximated.

4.3 Summary

Since the respiratory rate and the heart rate are not synchronized, respiratory influences on preload for successive respiratory cycles are reflected differently as variations in ABP, which can result in fluctuating SPV, PPV, and SVV values for these cycles. Averaging these values reduces the fluctuations, however, due to this averaging wrong indications for fluid loading responsiveness may be given.

Instead, the systolic pressures, diastolic pressures, and stroke volumes of these cycles can be thought of as samples of modulation envelopes. Calculation based on the maximum and minimum values of these envelopes should result in similar successive values, because the envelopes have the same periodicity as the ventilation signal. With the reduced fluctuations, inconsistencies in successive indications of fluid loading responsiveness should be reduced as well.

Since the envelopes have the same periodicity as the ventilation signal, systolic pressures, diastolic pressures, and stroke volumes of successive cycles can be projected onto one cycle to increase the sample rate of the envelope signals.

chapter 5

Modeling respiratory induced variations in arterial blood pressure

The main objective of the project is to model the respiratory induced variations in arterial blood pressure (ABP). This chapter describes the derivation of a physiological model for these variations in ABP. First, a general description of the goals of a model is presented. Next, individual models for the respiratory and circulatory systems is derived. Finally, based on the two individual models and respiratory influences on the circulation as mentioned in literature, a coupled model of both systems is derived.

The modeling was done in cooperation with E.P.A. Verheijen. He is a fellow Master of Science graduate student and is working on modeling respiratory induced variations in intrathoracic blood flows.

For the physiological modeling, physiological domains of fluid and gas transport are transferred into the domain of electricity transport. The correspondences between these domains are shown in Table 5.1. Based on these correspondences, the model can be constructed using electric circuit elements.

Table 5.1: *Correspondence between domains of fluid and gas transport vs. electrical transport (adapted from Blom [2004]).*

Fluid and gas transport	Electricity transport
pressure (P)	vol tage (V)
flow (F or $\dot{Q}$)	current (I)
volume (V, Q)	charge (Q)
resistance (R)	resistance (R)
inertia (I)	inductance (L)
compliance (C)	capacitance (C)

5.1 Goals of a model

A model has two goals. The first goal is to estimate the values of parameters. This is especially useful if parameters and signals of a system are difficult or impossible to measure. For example, a model of the circulation can be used to monitor ventricular preload volume or ventricular contractility.

If one starts with a certain set of parameter values and an input signal is fed into both the system and the model, the output of the system can be compared to the output of the model. The error in model

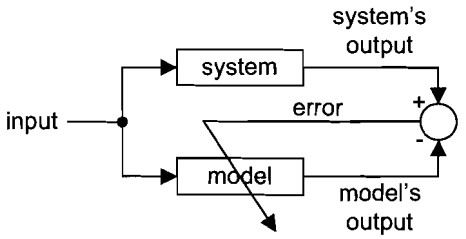

Figure 5.1: *If the same input signal is fed into the system as well as the model, the error of the model is the difference in system output and model output. The error can be used to adjust the model parameters.*

output, which is the difference between the outputs of the system and the model, can then be used to adjust parameter values, until the error is minimized. This concept is depicted in Figure 5.1.

In addition, to the purpose described in the few lines above, a model should be usable for prediction. Tests which may or cannot be performed on the real system can be performed on an already validated model in order to predict how the system will react. For example, a coupled model of the respiration and circulation can be used to determine the response to fluid loading.

5.2 Physiological model of the respiratory system

According to Schott [2005], a simple two-element model can be used to model the respiratory mechanics. The friction between air flowing through the airways and the walls of the airways, can be modeled by a resistance R_{aw}. The combined compliance of the lungs and thorax can be modeled by a capacitance C_{lt}. The pressure and flow that can be measured at the mouth or trachea are denoted by P_{aw} and F_{aw}, respectively. The model is shown in Figure 5.2.

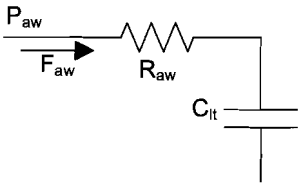

Figure 5.2: *Simple model of airways, lungs and thorax. R_{aw} models the friction of air flowing through the airways, C_{lt} is the combined lung/thorax compliance. P_{aw} is the pressure measured in the airways (trachea) and F_{aw} the flow in the airways (adapted from Schott [2005]).*

Since the resistance of the airways during inspiration is usually not the same as the resistance during expiration, the model needs to be adapted. This can be done by replacing the resistance R_{aw} with the circuit shown in Figure 5.3. The inspiratory flow F_{aw_insp} and expiratory flow F_{aw_exp} can be calculated using the inspiratory and expiratory parts of the flow F_{aw}. For this, the two diodes D_{insp} and D_{exp} are assumed ideal.

It must be noted that the model shown in Figure 5.2 is based on the assumption that resistances and compliances for left and right lungs are equal, which may not be the case for critically ill patients.

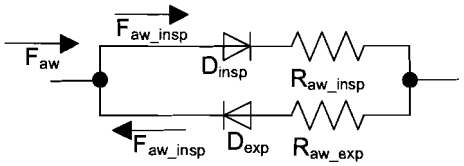

Figure 5.3: *Replacing circuit of R_{aw} to model inspiratory resistance R_{aw_insp} and expiratory resistance R_{aw_exP} separately.*

However, according to Schott [2005], the shown model is sufficient and gives satisfactory results.

When mechanically ventilated, the patient is connected to a ventilator. A model of a mechanically ventilated patient is shown in Figure 5.4. According to Schott [2005], this general model is widely used. In the model, a switch S is used to model the different phases of ventilation: inspiration (1), inspiratory pause (2) and expiration (3). The resistances R_{v_insp} and R_{v_exp} model the resistances of the inspiratory and expiratory hoses through which the patient is connected to the ventilator. The ventilator-imposed pressure is modeled by P_{insp}. The parameter PEEP models the level that the pressure in the lungs would reach when the expiratory phase lasts infinitely long. This pressure, usually called positive end expiratory pressure (PEEP) is used to keep the lungs inflated. Also zero end expiratory pressure is used.

During inspiration, the gas flow F_{aw} flows through the inspiratory resistances R_{v_insp} and R_{aw_insp} and charges capacitor C_{lt}. The flow is measured at the mouth or trachea. During an inspiratory pause, gas cannot flow out of the lungs and P_{aw}, the pressure measured in the airways, is the same as the lung pressure $P_{alveoli}$. At expiration lungs empty over the expiratory resistances R_{aw_exp} and R_{v_exp}.

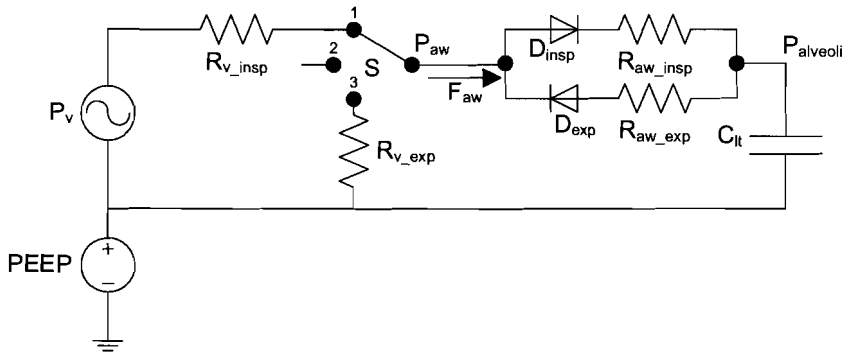

Figure 5.4: *Physiological model of a mechanically ventilated patient (adapted from Schott [2005]). The three-position switch models inspiration, inspiratory pause and expiration. At inspiration (position 1) capacitance C_{lt} is charged with flow F_{aw} which flows through R_{v_insp} and R_{aw_insp}. At inspiratory pause (position 2) P_{aw}, the pressure measured at the trachea, equals alveolar pressure $P_{alveoli}$. At expiration (position 3) the lungs discharge over R_{aw_exp} and R_{v_exp}. If expiration is continued infinitely long, $P_{alveoli}$ reaches PEEP.*

Patient specific parameter values as well as $P_{alveoli}$ can be estimated based on the model and the measured signals P_{aw} and F_{aw}. According to Michard [2005], both alveolar and intrathoracic (intrapleural) pressure have influence on the intrathoracic blood flows which result in variations in preload. Therefore,

the model has to be extended in order to obtain the intrathoracic pressure as well.

Since the lungs are a pressure/volume chamber within another pressure/volume chamber, the thorax, separate modeling of lung compliance and thorax compliance would result in a series connection of two capacitances. Since approximately 50% of the alveolar pressure is transferred to the thorax [Niranjan et al., 1999; Pybus; Blom, 2004; Aben, 2003],[1] these capacitances have the same value. The intrathoracic pressure is then the pressure measured at the junction of these capacitances. Although such models exist in literature [Niranjan et al., 1999; Aben, 2003], this intrathoracic pressure is not well defined. The junction pressure is only the pressure that is transferred to the thorax, the actual intrathoracic pressure is a sum of the transferred pressure and the intrathoracic pressure at rest (approximately 4 mm Hg below atmospheric pressure [Smith, 2003]). Furthermore, if the two compliances are connected in series, a DC-value of the ventilator (PEEP) would not be transferred to the thorax, while in the real system such values are transferred.

In the remainder of this thesis the respiratory model of the mechanical ventilated patient will only be used in simulations and not for estimation of alveolar/intrathoracic pressure based on patient data. Therefore, no more attention will be paid to modeling the intrathoracic pressure. This pressure will be calculated as half the alveolar pressure (the 50% pressure transfer) minus 4 mm Hg (the resting pressure).

5.3 Physiological model of the circulatory system

In the eventual application, patient-specific parameters have to be estimated quickly using limited data only. Therefore, the model of the circulation cannot contain too many parameters. Otherwise it would be difficult to validate its correctness and find a unique solution. On the other hand, the circulatory model needs to have some minimal complexity. It should reflect the main hemodynamic signals and parameters reliably and it should not be based on too many assumptions.

Numerous models of the circulatory system have been proposed already [Beyar et al., 1987; Ferrari et al., 1992; Sun et al., 1997; Kentgens, 2001; Smith, 2003]. Most of them describe the circulation using arterial, venous, and heart sections only. The sections themselves are usually constructed as Windkessel circuits (i.e. circuits that separate elastic properties from the fluid dynamics; a (rigid) tube models fluid dynamics and a compartment with a pressure-volume relation models a vessel's compliance) [Tsitlik et al., 1992]. By using (series of) Windkessel circuits, fluid flow governing equations do not become too complex [Smith, 2003]. Furthermore, if necessary, complexity of the system can usually be added by increasing the number of Windkessel circuits.

Smith [2003] proposed a minimal hemodynamic model of the heart and circulation for clinical application. Despite its minimal complexity, it is able to capture main hemodynamic trends reliably for varying situations. The model consists of six compartments that have a pressure-volume relation. Compartments are then connected using resistances and inductances to make the model a closed-loop. The separate pressure-volume and flow dynamics modeling resembles the Windkessel approach. A similar approach will be followed here.

[1] One should keep in mind that this is a good approximation for healthy persons only.

As mentioned before, in the Windkessel approach the pressure-volume relation of a compartment models the compliance of a vessel. In Chapter 2 it was derived that both the pulmonary and systemic circulation can be subdivided into three separate sections: the arterial, capillary, and venous sections. Since relatively little blood is contained within the capillary sections [Guyton and Hall, 2000], only the arterial and venous sections will be assigned a pressure-volume compartment.

With the inverse of compliance, elastance (E), a compartment's transmural pressure[2] P(t) can be calculated when the compartments volume V(t) is known:

$$P(t) = E \cdot V(t). \tag{5.1}$$

It is assumed that the elastance E is constant. For arterial sections this a good approximation, whereas linearizing the pressure-volume relations in veins is difficult [Blom, 2004]. One of the reasons that this is difficult is venous collapse, which may happen if the outside pressure is higher than the pressure inside a vein. However, such collapses most likely will not occur in the systemic venous section, since during positive pressure ventilation this section will be a growing pool of blood. Although pulmonary veins may be collapsed during the respiratory cycle, flow of blood through the pulmonary circulation will already be decreased, reducing the importance of venous collapse in these veins. Therefore the pressure-volume relation as presented in Equation 5.1 will be used for the arterial and venous sections of the systemic and pulmonary circulation. The relation first needs to be extended because, like a balloon, the compartments have a certain volume below which no transmural pressure is generated [Guyton and Hall, 2000]:

$$P(t) = \begin{cases} E \cdot (V(t) - V_0) & \text{, for } V(t) \geq V_0, \\ 0 & \text{, for } V(t) < V_0. \end{cases} \tag{5.2}$$

Here V_0 is the volume of the compartment below which no transmural pressure is generated. Since E and V_0 are assumed constant, Equation 5.2 can be rewritten using $P_0 = E \cdot V_0$:

$$P(t) = \begin{cases} E \cdot V(t) - P_0 & \text{, for } V(t) \geq V_0, \\ 0 & \text{, for } V(t) < V_0. \end{cases} \tag{5.3}$$

Using Equation 5.3, the pressure-volume relation can be modeled as a compliance C in series with a constant pressure source P_0. The resulting circuit of the model is shown in Figure 5.5. Note that the circuit only holds for $V(t) \geq V_0$.

To ensure flow of blood between two compartments, they have to be connected. In the Windkessel approach, the connections are tubes. Usually, these tubes are modeled as (constant) resistances, resembling the friction forces acting on the blood [Smith, 2003]. The blood flow $\dot{Q}(t)$ then becomes:

$$\dot{Q}(t) = \frac{P_1(t) - P_2(t)}{R}. \tag{5.4}$$

Here $P_1(t)$ - $P_2(t)$ is the pressure drop over the tube and R the resistance of the tube. The latter can be found using Poiseuille's law [Smith, 2003]:

$$R = \frac{8\eta l}{\pi r^4} \tag{5.5}$$

[2] Transmural pressure is the pressure inside a compartment minus the pressure outside. In other words this is the pressure over the wall of the compartment.

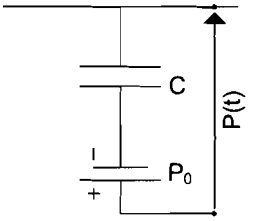

Figure 5.5: *Model of the pressure-volume relation of a compartment. The pressure in the compartment P(t) is equal to the volume in the compartment times the elastance (1/C) minus a constant pressure.*

where η, l and r are the blood viscosity, the length and radius of the tube, respectively.

The definition for blood flow does not take into account inertial effects. Especially near the heart valves, where the flow of blood stops periodically, such effects play an important role. In all other parts of the circulation, the effects can be neglected. Also, the effect of time varying resistances are not taken into account. Time varying resistances play an important role in the arteries near the heart [Smith, 2003], but a minor role in the total arterial sections. Therefore, this effect is neglected as well.

The in- and outflow of blood changes the blood volume V(t) contained within a compartment:

$$\frac{dV(t)}{dt} = \dot{Q}_{in}(t) - \dot{Q}_{out}(t) \tag{5.6}$$

where $\dot{Q}_{in}$ and $\dot{Q}_{out}$ are the chamber's blood in- and outflow, respectively.

The last part of the circulation that needs to be modeled is the heart and its pumping capability. Without pumping of the heart, blood would keep on redistributing on all compliances until a certain equilibrium is reached. Since the atria only improve ventricular filling, the heart will be modeled as two ventricular compartments only. There are three ways to model a ventricle: one can see it as a pressure or a flow source, or as a time-varying compliance. However, if one of the sources is used, the model becomes an open loop, while the circulation is a (semi-) closed loop system. Physiologically, the ventricle is just a pressure-volume compartment that contracts repeatedly (i.e. the compliance varies). Therefore, modeling the ventricle as a time-varying compliance[3] seems the most correct physiological solution in order to model the closed loop system.

The time-varying compliance has to ensure that the ventricle produces proper pressure-volume relations (i.e. PV-loops, as shown in Figure 2.2). For given maximum elastance and heartbeat duration, Senzaki et al. [1996] defined a normalized elastance curve of the ventricle, which was later slightly modified [Segers et al., 2000]. The normalized curve describes the instantaneous elastance over the given maximum elastance as a function of time. The time t is normalized in such a way that the maximum value of the normalized elastance (i.e. one) occurs when the normalized time equals one.

A more common approach uses the end systolic and end diastolic pressure-volume relations which are weighted by a periodic driver function e(t) [Smith et al., 2004, 2005]. Whereas the end systolic pressure P_{es} is assumed to be related linearly to the end systolic ventricular volume as described in

[3]Actually, the name 'time-varying elastance' is a more proper name, because that describes the (active) capability of contraction, whereas compliance is due to passive characteristics of the tissue [Blom, 2004].

Equation 5.3, the end diastolic pressure P_{ed} is calculated as an exponential function of the end diastolic ventricular volume:

$$P_{ed}(t) = P_0(\exp(\lambda(V(t) - V_0)) - 1). \tag{5.7}$$

Here the constant parameters P_0, λ and V_0 define gradient, curvature, and volume at zero pressure of the end diastolic pressure volume relation [Smith, 2003].

The cardiac cycle has periodicity T_h. Therefore, at time t, the timing within the cardiac cycle t_h is defined as:

$$t_h = t \bmod T_h. \tag{5.8}$$

Using t_h, the periodic driver function is defined as:

$$e(t) = exp(-80(t_h - \frac{T_h}{2})^2). \tag{5.9}$$

The ventricular pressure $P_v(t)$ can now be written as a weighted sum:

$$P_v(t) = e(t)P_{es}(t) + (1 - e(t))P_{ed}(t). \tag{5.10}$$

As described in Chapter 2, ventricles are preceded and followed by valves. The valves ensure unidirectional flow of blood. In the electrical analogy, the valves can be treated as diodes. Although the valves have resistances, the diodes are assumed ideal. This is because the resistances of the valves are only important when the valves are open. In this case, the valve resistance is connected in series with a section's resistance. Therefore, the valve resistance will be taken as part of the section's resistance. Since inertial effects near the valves will most likely not have significant influence on the respiratory induced variations in ABP, they are omitted. The resulting circuit that models one side of the heart is shown in Figure 5.6.

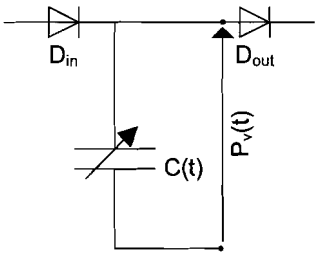

Figure 5.6: *Model of one side of the heart. The ventricular pressure $P_v(t)$ can be calculated with the ventricular volume and varying compliance C(t). The heart in- and outflow valves are modeled by diodes D_{in} and D_{out}, respectively.*

The two sides of the heart are contained within a pressure compartment called the pericardium. In turn, this compartment is located inside the thorax. Smith [2003] describes the pressure of the pericardium as a function of its volume (which is the sum of the left and right ventricular volumes) using the pressure-volume relation of Equation 5.7. Since the pressure in the pericardium depends on the volume of both ventricles, the pressure inside the ventricles depend on each other. The ventricles thus interact.

The pericardium is not the only cause of ventricular interaction. Between the ventricles there is a flexible wall called the septum. Due to its flexibility, the septum can move. Movements of the septum cause the ventricles to interact as well [Van den Berg, 1991; Smith, 2003]. However, because the septal deflections are approximately ten times smaller than the pericardial deflections [Smith, 2003] and because Michard [2005] does not mention them as contributors to the respiratory induced variations, the ventricular interaction due to septum movements is omitted.

The total circulatory model can now be constructed using the mentioned compartment and connection types. The model is shown in Figure 5.7. The left part of the heart consists of the in- and outflow diodes D_{li} and D_{lo} and the capacitance C_{lv}. From here, blood flows through diode D_{lo} into the systemic arterial section, consisting of resistance R_{sa}, capacitance C_{sa} and source P_{sa}. From the arterial section, blood flows through the systemic capillary resistance R_{sc} into the systemic venous section, which consists of resistance R_{sv}, capacitance C_{sv} and source P_{sv}. From the systemic venous section, blood flows through diode D_{ri} into the right side of the heart, consisting of diodes D_{ri} and D_{ro} and capacitance C_{rv}. Blood that is ejected by the right side of the heart flows through diode D_{ro} into the pulmonary arterial section consisting of resistance R_{pa}, capacitance C_{pa} and source P_{pa}. From this section, blood flows through the pulmonary capillary resistance R_{pc} into the pulmonary venous section consisting of resistance R_{pv}, capacitance C_{pv} and source P_{pv}. From here blood flows into the left side of the heart again through diode D_{li}. The flow of blood is ensured by the varying capacitances C_{lv} and C_{rv}. The total blood volume is modeled by the sum of the charges on the capacitances.

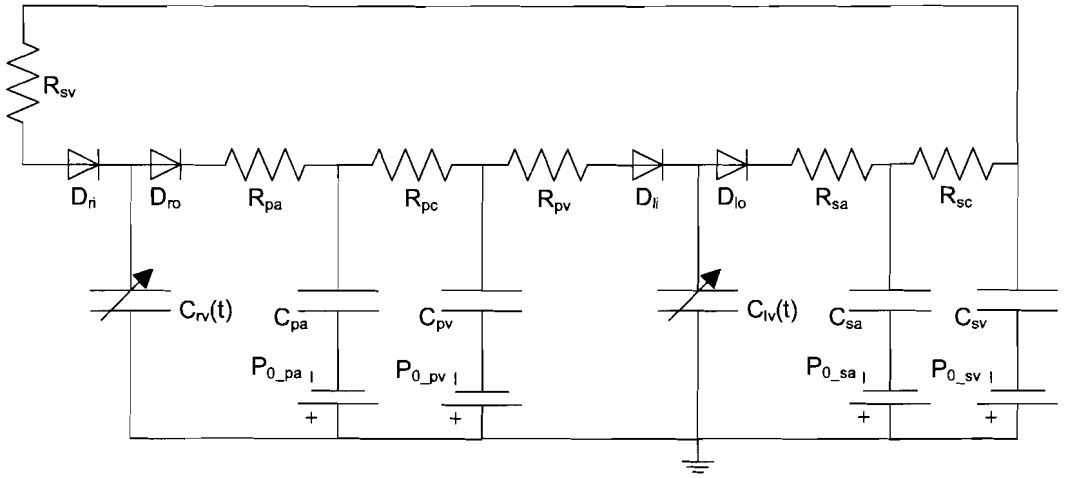

Figure 5.7: *Physiological model of circulation. Due to varying capacitances C_{lv} and C_{rv} blood can flow around. The total blood volume is modeled by the sum of the charges on the capacitances. The diodes represent the heart's in- and outflow valves which ensure uni-directional flow of blood. The combination of compliance and source represents a pressure-volume compartment. Systemic arterial, capillary and venous sections are denoted by subscripts sa, sc and sv, respectively. Pulmonary arterial, capillary and venous sections are denoted by subscripts pa, pc and pv, respectively. The reference pressure is extracorporeal (atmospheric) pressure.*

In the previous chapter it was discussed that neural influences act on the circulatory system. An important factor that is often mentioned when talking about such influences, is the (arterial) baroreceptor or pressoreceptor control [Guyton et al., 1973]. Changes in ABP result in changes in firing rates of the receptors. Through a complex control by the central nervous system, these ABP changes eventually result in changes in heart rate. Also changes in peripheral vascular resistance and heart contractility

occur [Milnor, 1990; Lu et al., 2001; Smith, 2003]. For example, for significant losses of blood, ABP drops. The control system can then try to recover the old level of the ABP by increasing the peripheral (systemic) vascular resistance. In 'stable' situations, the vascular resistance and heart contractility do not alter too much and the control paths are rather slow compared to the control path affecting the heart rate [Lu et al., 2001]. Eventually, the coupled model will have to track the patient signals for 'stable' situations. If these situations change, the model's parameters have to be estimated again. Furthermore, in the observed patient data the heart rate is approximately constant, so implementing such a control only adds unnecessary complexity [Lu et al., 2001]. Therefore, the neural influences will be neglected in the model.

The derived circulatory model is based on several assumptions and simplifications. For example, the relation between the pressure and volume in systemic and pulmonary compartments is assumbed to be linear, which is a huge simplification (e.g. the elastance of the vena cava is volume/pressure dependent [Guyton and Hall, 2000]). However, the model derived by Smith [2003] shows that the linear modeling is sufficient for capturing main hemodynamic trends. The same holds for the resistances which are assumed constant. Also, as already mentioned, the contributions of the left and right atria as well as inertia of blood are neglected. Finally, neural influences, the baroreflex or pressoreceptor control in particular, are neglected. With the eventual application and implementation of the coupled respiratory and circulatory models in mind, all these factors do not have a significant contribution and only add more complexity which makes the coupled model difficult to validate and verify.

Compared to the model proposed by Smith [2003], the presented circulatory model not only differs in modeling of inertia, but also ventricle interdependence due to the septum is omitted [Guyton and Hall, 2000; Van den Berg, 1991; Lu et al., 2001; Smith, 2003]. One would expect that change in septum location is an important factor in the end application (changes in the right ventricular volume are related to changes in left ventricular volume). However, Michard [2005] does not mention its contribution.

5.4 Coupling the respiratory and circulatory models based on respiratory influences on the circulation

The pressure-volume relation of Equation 5.3 defines the transmural pressure of a chamber. For the systemic parts of the circulation the measured pressure (i.e. the pressure inside the chamber referenced to atmospheric pressure) equals the transmural pressure because the pressure outside those parts is the atmospheric pressure.[4] On the other hand, for the parts of the circulation that are contained within the thorax, the outside pressure is not equal to atmospheric pressure but to the (time-varying) intrathoracic pressure. In the model, the sections thus have to be connected to the intrathoracic pressure.

Like Michard [2005] describes, intrathoracic vessels get compressed and/or squeezed. This means that (especially) the pulmonary capillary resistance increases. Although the squeezing would mean a temporary high outflow from the pulmonary capillaries, it was assumed earlier that the capillaries do not contain significant volumes of blood. Therefore, only the capillary resistances will be adjusted. According to Lu et al. [2001], the pulmonary peripheral (capillary) resistance R_{pc} is proportional to the square of the alveolar volume $V_{alveoli}$:

[4] This holds in general, however, parts contained within the abdomen may have a small difference.

$$R_{pc} = R_{pc,0}(\frac{V_{alveoli}}{V_{alveoli,max}})^2. \tag{5.11}$$

Here $R_{pc,0}$ and $V_{alveoli,max}$ are the maximum pulmonary resistance and alveolar volume, respectively. As was mentioned earlier, the intrathoracic pressure depends on the alveolar pressure which in turn is related to the alveolar volume. Therefore, the definition for R_{pc} can be rewritten into the form R_{pc} = f($P_{intrathoracic}$(t)) easily.

The pulmonary arterial and venous resistances will probably also increase. However, because they are much smaller than the capillary resistance, these effects are neglected.

With the influencing elements derived in this section, the combined model of the respiratory and circulatory systems can now be constructed. The model is shown in Figure 5.8.

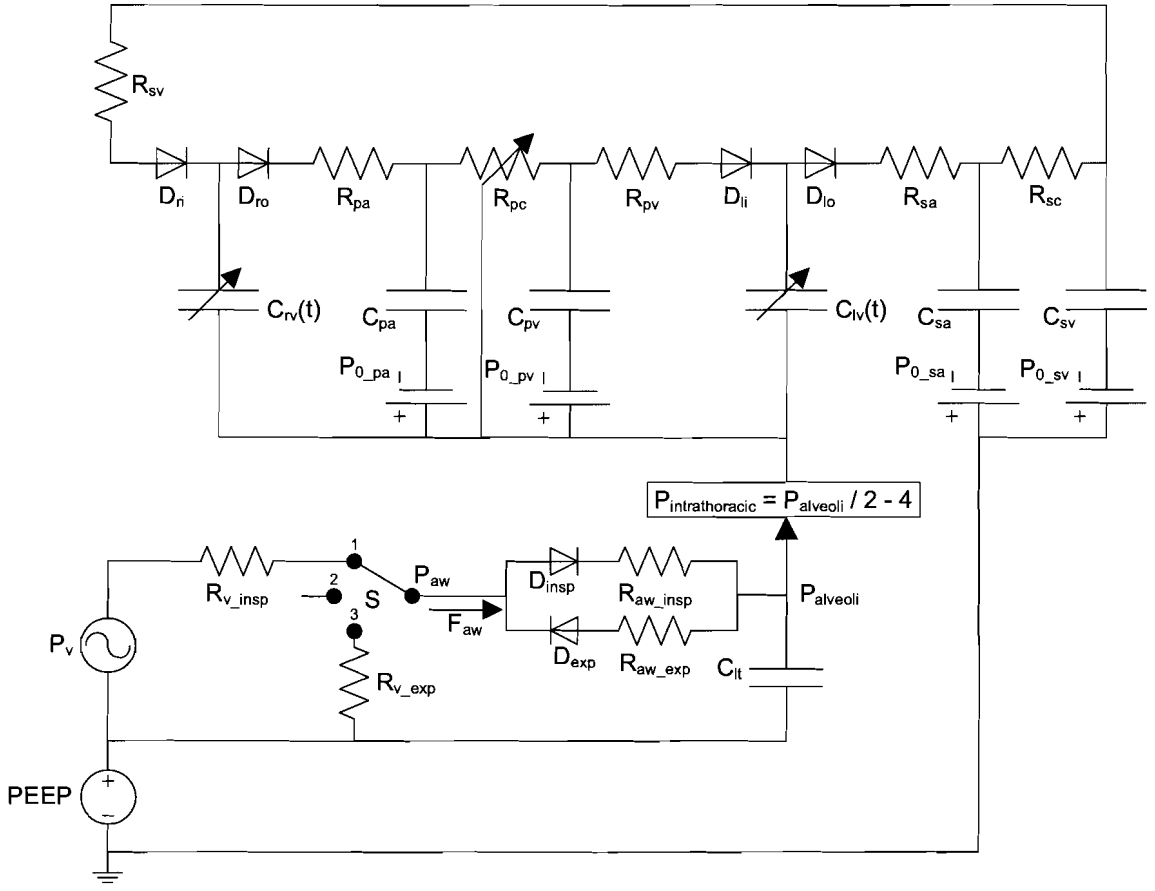

Figure 5.8: *Coupled respiratory and circulatory models. The reference pressure of the intrathoracic compartments is the intrathoracic pressure $P_{intrathoracic}$ instead of atmospheric pressure. Furthermore, the alveolar volume affects the pulmonary capillary resistance. Since the intrathoracic pressure depends linearly on the alveolar volume, the resistance can be changed by the intrathoracic pressure.*

According to Michard [2005], the influence of the alveolar pressure on the pulmonary vascular bed will be less for hypervolemic cases than for hypovolemic ones. This means that the model will probably

not be valid for patients suffering from hypervolemia. However, because one should not add volume to hypervolemic patients at all, these cases will not have to be handled by the model. Hypervolemia should be relatively easy to detect using the decomposition of Systolic Pressure Variation [Perel et al., 1987].

5.5 Summary

The usage of models has two goals. The model has to be used to monitor parameter values, which cannot be measured well in the real system. Furthermore, a correct model can be used to predict responses of the system to situations which are not tested yet.

An already existing and validated model of the respiratory system of a mechanically ventilated patient (including the ventilator) was used. This model can only provide the alveolar pressure and not the intrathoracic pressure. However, for the project it is sufficient to calculate the intrathoracic pressure as half the alveolar pressure plus the intrathoracic resting pressure (approximately 4 mm Hg below atmospheric pressure).

A basic model of the circulatory system was constructed using a Windkessel approach. The model has many resemblances with an already verified 'minimal model' of the circulatory system. However, because not all aspects of the circulatory system have to be captured by the model in detail, aspects of this 'minimal model' were left out.

A coupled model of the respiratory and circulatory systems was constructed based on individual models of both systems and significant respiratory influences on the circulation as mentioned in literature. In this coupled model, the reference pressure of the circulatory sections contained within the thorax is the intrathoracic pressure. The pulmonary capillary resistance is a quadratic function of the intrathoracic pressure.

chapter 6

Implementation and simulation

According to the project objectives, the coupled model of the respiratory and circulatory systems that was derived in the previous chapter, has to be implemented in LabVIEW. Important aspects of the implementation are discussed in this chapter. Also, simulation results of the implemented model are presented. The simulations are divided into two parts. The first part is concerned with the basic model verification: do the basic mechanics work (e.g. the specific patterns in ventricular preload volume during a ventilated breath [Michard, 2005]). The second part describes simulation results related to changes in the respiratory induced variations in arterial blood pressure (ABP) due to changes in (ventilator) settings.

To fully validate the coupled model, qualitative and quantitative comparisons between the model results and patient data have to be made. The quantitative comparisons imply that the model's patient specific parameters need to be estimated reliably. A parameter estimation routine is then necessary to estimate the parameters in short periods of time during which only limited data can be obtained. However, because such a routine was not created in the project, only a qualitative comparison was done.

Parameter values were obtained from literature [Smith, 2003]. Since these values are only modal values, it is difficult to state how 'good' simulation results will be compared to reality. For the qualitative comparison trends are important. In Chapter 9 the trends in simulation results will be compared to trends in patient data (see Chapter 9).

6.1 Implementations

6.1.1 Respiratory system model

In the previous chapter is was stated that the derived respiratory model will only be used for simulations and not for estimation of alveolar pressure $P_{alveoli}$ and intrathoracic pressure $P_{intrathoracic}$ based on patient signals. Furthermore, $P_{alveoli}$ is not necessary because $P_{intrathoracic}$ can be used to calculate the modeled respiratory influences on the circulation. Therefore, only a cyclic function for $P_{intrathoracic}$ was implemented.

The function is based on background knowledge of the intrathoracic pressure and measured intrathoracic pressure waveforms. The funciton can be described using five ventilator settings and two patient-specific parameters. The function and its parameters are shown in Figure 6.1. The length of the

respiratory cycle, the inspiratory rise time and inspiratory pause time are specified by T_{resp}, T_{insp} and T_{pause}, respectively. The level of positive end expiratory pressure (PEEP) is specified by PEEP and the tidal pressure[1]) is specified by P_{tidal}. The expiratory time constant of the lung and airway physiology is specified by τ_{exp} and the thorax resting pressure is specified by P_0.

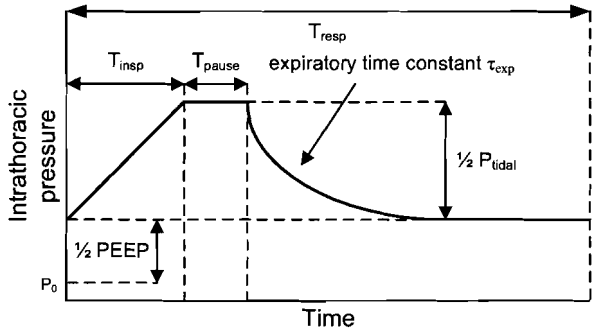

Figure 6.1: *Function for $P_{intrathoracic}$ and its parameters. The respiratory period (T_{resp}) consists of an inspiratory period (T_{insp}), an inspiratory pause (T_{pause}) and an expiratory period. The expiratory time constant τ_{exp} depends on the patient's lung and airway physiology. Resting intrathoracic pressure is given by P_0. The level of positive end expiratory pressure is given by PEEP. The tidal pressure supplied by the ventilator is P_{tidal}.*

6.1.2 Circulatory system model

The derived model for the circulatory system consists of six compartments that have a pressure-volume relation. These compartments are interconnected by resistances. In the implementation, the pressures of the compartments are calculated based on their volumes and external pressures. Changes in volume are calculated using the blood flows between the compartments.

The pressure-volume relations of the chambers as well as the flow relations are based on several parameters. The derived model is very similar to the approach of Smith et al. [Smith, 2003; Smith et al., 2004, 2005].[2] Therefore, the necessary parameter values for the model were obtained from these publications. The parameters and their values are listed in Appendix A.

6.1.3 Coupled model: calculation and order

During each iteration, $P_{intrathoracic}$ has to be calculated. This pressure is a cyclic function with periodicity T_r. Therefore, the timing within the cycle t_r ($t_r = t \bmod T_{resp}$) is calculated first. With t_r, $P_{intrathoracic}$ can be calculated using the intrathoracic pressure function and its parameters:

$$P_{it}(t) = \begin{cases} t_r / T_{insp} * P_{tidal} + P_0 + .5 * PEEP & , 0 \leq t_r < T_{insp}; \\ P_{tidal} + P_0 + .5 * PEEP & , T_{insp} \leq t_r < T_{insp} + T_{pause}; \\ P_0 + .5 * PEEP + P_{tidal} * \exp(-(t_r - T_{insp} - T_{pause})/\tau_{exp}) & , T_{insp} + T_{pause} \leq t_r < T_{resp}. \end{cases} \quad (6.1)$$

[1] Most ventilators supply tidal volume, however, in the model the pressure depends linearly on the volume.

[2] In fact, the derived model is a simplified version of their 'minimal' model.

The circulatory model contains six ordinary differential equations describing the volume(change) of the volume compartments. All of these equations have the following form:

$$V(t) = V(t_0) + \int_{t_0}^{t} (\dot{Q}_{in}(\tau) - \dot{Q}_{out}(\tau))d\tau. \tag{6.2}$$

Here $\dot{Q}_{in}$ and $\dot{Q}_{out}$ are the compartment's in- and outflow of blood, respectively. $V(t_0)$ is the compartment's volume at time $t = t_0$. With a Forward Euler discretization formula, the discrete-time equivalent of the continuous-time equation for the volume becomes:

$$V[n] = V[n-1] + \triangle t(\dot{Q}_{in}[n-1] - \dot{Q}_{out}[n-1]), \text{ where } n\triangle t = t. \tag{6.3}$$

Here a flow $\dot{Q}[n]$ is the time-discrete equivalent of the flow $\dot{Q}(t)$ given in Equation 5.4:

$$\dot{Q}[n] = \frac{P_1[n] - P_2[n]}{R}. \tag{6.4}$$

Before the flow through the pulmonary capillaries can be calculated, the pulmonary capillary resistance R_{pc} has to be calculated using the alveolar volume $V_{alveoli}$:

$$R_{pc}[n] = R_{pc,0}(\frac{V_a[n]}{V_{a,max}})^2. \tag{6.5}$$

However, as described in the previous chapter, this relation can be rewritten into the form $R_{pc}[n] = f(P_{intrathoracic}[n])$.

Based on the volumes and the time-discrete equivalent of Equation 5.2, the pressures of the compartments can be calculated. For the extrathoracic compartments, the pressure-volume relation is:

$$P[n] = E(V[n] - V_0). \tag{6.6}$$

For the intrathoracic arterial and venous sections, the pressure-volume relation becomes:

$$P[n] = E(V[n] - V_0) + P_{intrathoracic}[n]. \tag{6.7}$$

Finally, the time discrete pressure-volume relation for the ventricles is:

$$P[n] = e[n]P_{es}[n] + (1 - e[n])P_{ed}[n] + P_{intrathoracic}[n] + P_{pericardium}[n]. \tag{6.8}$$

Here e[n] is the time-discrete equivalent of Equation 5.9:

$$e[n] = \exp(-80(n_h - \frac{T_h}{2})^2). \tag{6.9}$$

Here T_h is the cardiac cycle's period and n_h the timing within the cycle ($n_h = n\triangle t \bmod T_h$).

Whereas $P_{es}[n]$ can be calculated using Equation 6.6, P_{ed} and $P_{pericardium}[n]$ can be calculated using the time-discrete equivalent of Equation 5.7:

$$P[n] = P_0(\exp(\lambda(V[n] - V_0)) - 1). \tag{6.10}$$

What remains is the time-discrete equivalent of Equation 6.11:

$$P_{it}[n] = \begin{cases} n_r / T_{insp} * P_{tidal} + P_0 + .5 * PEEP & , 0 \leq n_r < T_{insp}; \\ P_{tidal} + P_0 + .5 * PEEP & , T_{insp} \leq n_r < T_{insp} + T_{pause}; \\ P_0 + .5 * PEEP + P_{tidal} * \exp(-(n_r - T_{insp} - T_{pause})/\tau_{exp}) & , T_{insp} + T_{pause} \leq n_r < T_{resp}. \end{cases} \quad (6.11)$$

Here n_r equals $n\triangle t \bmod T_{resp}$.

With Equations 6.3–6.11 one can calculate values for pressures, volumes and flows for a single iteration. The simulation can be performed by repeating this iteration. Due to discretization, certain values have to be known before others can be calculated within the iteration. The order of the calculations is given in pseudo-code below.

```
Initialize Volumes[0]
n = 0
while stopcondition is false {
```

- calculate P_{it}[n]
- calculate R_p[n](P_{it}[n])
- calculate e[n]
- calculate $P_{pericardium}$[n](Volumes[n])
- calculate Pressures[n](Volumes[n],P_{it}[n],$P_{pericardium}$[n],e[n])
- calculate Flows[n](Pressures[n],R_p[n])
- calculate Volumes[n+1](Volumes[n],Flows[n],stepsize)
- n = n + 1

```
}
```

For stable situations, the total blood volume contained within the system (i.e. the sum of the volumes of all sections) should remain constant. However, due to numerical errors, this volume may change. Therefore, in the implementation all volumes, except the volume contained within the systemic venous section, are calculated using Equation 6.3. Next, the vena cava volume is calculated as the total blood volume minus the sum of the volumes of the other sections.

6.2 Simulation

6.2.1 Basic mechanism verification

Increasing the intrathoracic pressure

The circulatory system is based on a model which was already verified [Smith, 2003]. Besides some simplifications, the main difference between the existing model and the current one, is the way the pulmonary resistance is affected by the alveolar pressure. To make sure that However, both models have increasing pulmonary resistance for increasing intrathoracic pressure. Increased pulmonary resistance impedes right ventricular outflow which, after a couple of heartbeats, results in reduced left ventricular SV. Therefore, increasing the intrathoracic pressure in the model should result in an increased right ventricular (pre- and afterload) pressure, while the left ventricular (pre- and afterload)

pressure decreases. The pressures and volumes for the left and right ventricle and their pre- and afterload pressures for two different intrathoracic pressures are drawn in Figure 6.2 and Figure 6.3, respectively.

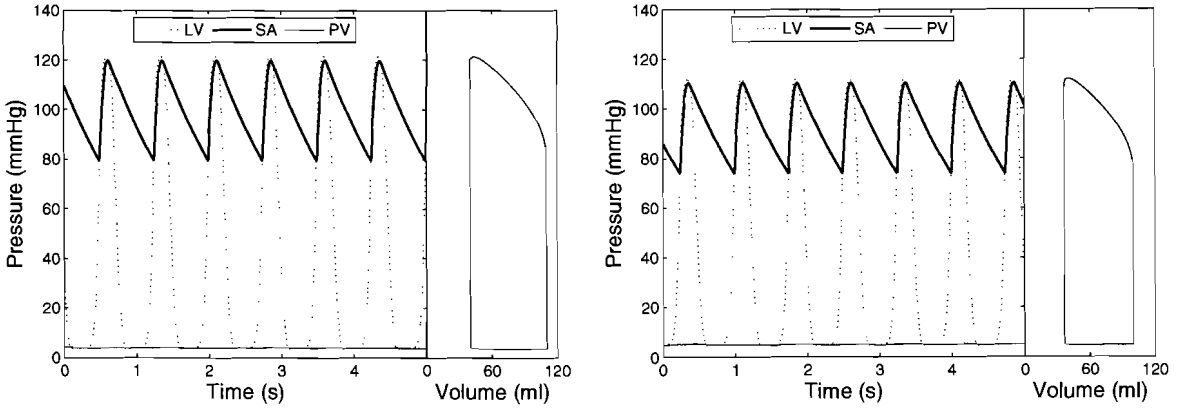

Figure 6.2: *Pressures related to the left ventricle and left ventricular PV-loop for different $P_{intrathoracic}$: (a) -1 mm Hg and (b) 1 mm Hg. Left ventricular pressure is indicated by LV, SA is the systemic arterial pressure and PV the pulmonary venous pressure.*

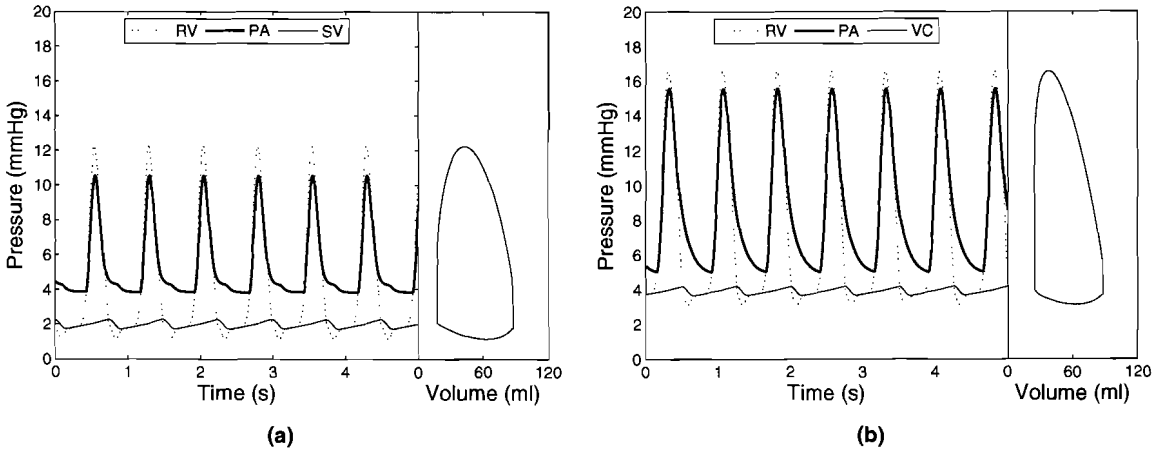

Figure 6.3: *Pressures related to the right ventricle and right ventricular PV-loop for different $P_{intrathoracic}$: (a) -1 mm Hg and (b) 1 mm Hg. Right ventricular pressure is indicated by RV, PA is the pulmonary arterial pressure and SV the systemic venous pressure.*

If one compares the pressures in Figure 6.2b to the ones drawn in Figure 6.2a, it can be seen that the left ventricular afterload pressure indeed decreases for increased intrathoracic pressure. The preload pressure is approximately the same for both situations. In Figure 6.3 it can be seen that the right ventricular pre- and afterload pressures increases for increased intrathoracic pressure (Figure 6.3).

According to Guyton and Hall [2000], the cardiac output (CO) and thus the Stroke Volume (SV) should

decrease for increased $P_{intrathoracic}$ as is the case in the simulation.

Relation between preload and stroke volume

Another aspect the model should be able to reproduce is the heart's preload/SV relation (see Figure 2.7). If this is not the case, the theory behind the variations in ABP will not be applicable to the model. A simulated preload/SV relation of the model's left ventricle is shown in Figure 6.4. The relation was obtained by gradually increasing the total volume contained in the model. In all cases, after redistribution, the increased total volume ensured increases in preload volume. Note that there is not one single relation, but that the actual shape may differ for changing model parameters/variables (e.g. heart rate).

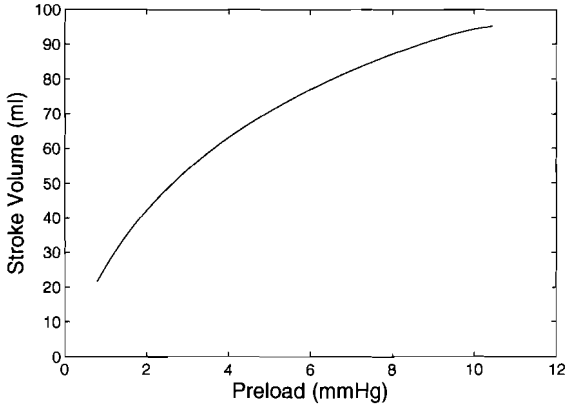

Figure 6.4: *Simulated preload/SV relation of the model's left ventricle. Preload is here defined as the left ventricular end diastolic pressure.*

The relation as drawn in Figure 6.4 shows the preload/SV relation of the model's left ventricle for a normally functioning heart. The model will have to be used to determine whether hypervolemic patients will respond positively to fluid therapy. Hypervolemic negative responders typically have a heart that does not function properly, for example because it is too stiff (non-compliant). For a stiff heart, the preload/SV relation is more flat than for a normally functioning heart. The model's preload/SV relation was therefore also simulated for a heart which was stiffened by increasing the end-diastolic pressure/volume relation (i.e. the value of λ in Equation 6.10 was increased). In Figure 6.5 the simulation results for the preload/SV relation for the model's stiff and normal functioning hearts are shown.

It can be seen that the shape of the preload/SV relation of the model's left ventricle as shown in Figure 6.4 is indeed similar to the expected shape of Figure 2.7. More importantly, in Figure 6.5 one can see that this relation is more flat for the model's stiff heart than for the model's normal heart. The model behavior is thus correct.

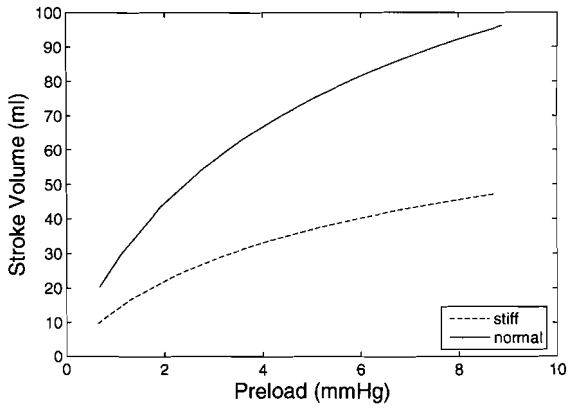

Figure 6.5: *Simulated preload/stroke volume relation of the model's left ventricle for 'normal' and 'stiff' ventricle situations. Preload is here defined as the left ventricular end diastolic pressure.*

Preload patterns during positive pressure ventilation

With the preload/SV relation of the model verified, the model's response to positive pressure ventilation can be simulated. According to Michard [2005], the left and right ventricular preload have a certain pattern during positive pressure ventilation. At the beginning of inspiration, the left ventricular preload increases, while the right one decreases. After a couple of heartbeats, the left ventricular preload decreases. This decrease is accompanied by increases in right ventricular preload. Near the end of expiration, the preloads are returning/returned to their baseline values again.

The capability of the model to reproduce the changing preload patterns was simulated using a ventilation period of six seconds, followed by a period of apnea. The latter was used to make sure that both volumes return to their baseline value. In Figure 6.6 the simulated volumes of the left and right ventricle during the total period are drawn, together with the intrathoracic pressure. Each heartbeat, the preload volume is the top value and the afterload volume the bottom one. SV is the difference between the two volumes. At the beginning of inspiration, the preload volume of the model's left ventricle increases, while the preload volume of the model's right ventricle decreases. After a couple of heartbeats, the preload volume of the model's left ventricle decreases and the preload volume of the model's right ventricle increases. At the end of the respiratory period, the preload volumes of the model's ventricles returned to their baseline values. The preload patterns thus match those mentioned by Michard [2005].

Pulmonary artery pressure pattern during positive pressure ventilation

Much like the preload patterns, the pulmonary pressure seems to have a predefined pattern as well. According to the experimental results of Scharf et al. [1980] and Perel et al. [1987], the systolic and diastolic pulmonary artery pressures follow the shape of the pleural (intrathoracic) pressure. This means that they increase when the intrathoracic pressure increases and that they decrease when the intrathoracic pressure decreases. Also, no clear $\triangle_{down}$ component can be seen in the results.

In Figure 6.7 the pulmonary artery during a ventilatory period of six seconds followed by an apnea together with the intrathoracic pressure is shown. As can be seen in Figure 6.7, the systolic and diastolic pressures indeed increase for increasing intrathoracic pressure and decrease for decreasing

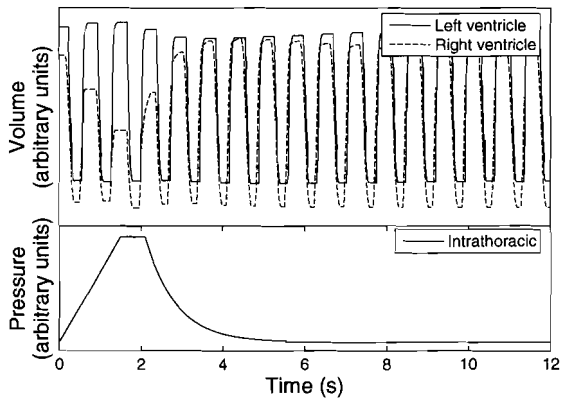

Figure 6.6: *Simulated left and right ventricular volumes during a respiratory period of six seconds followed by a period of apnea.*

intrathoracic pressure. Also, no $\triangle_{down}$ is present. This pattern is thus in accordance with the experimental results.

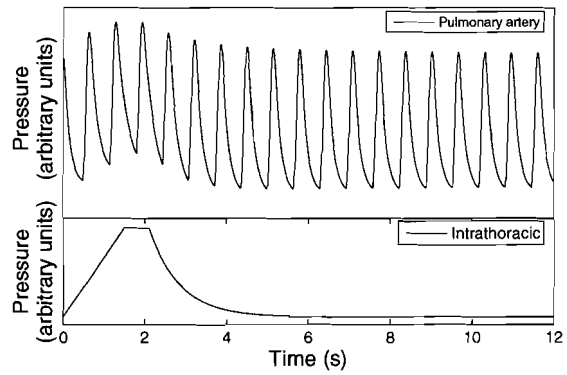

Figure 6.7: *Simulated pulmonary artery pressure during a respiratory period of six seconds followed by a period of apnea.*

6.2.2 Tests during positive pressure ventilation

Now that it is known that the basic mechanisms of the model act as expected, the reaction of the model to positive pressure ventilation can be simulated. Although the preload patterns as drawn in Figure 6.6 correspond to the patterns described in literature, it is not yet clear whether the (qualitative) reaction of the model to changes in (ventilation) conditions resembles reality reliably. Therefore, the conditions have to be altered to be able to do a qualitative validation of the model.

In Chapter 3, it was mentioned that the following conditions may significantly influence the respiratory induced variations in ABP:

- tidal volume;
- lung and chest wall compliance;

- PEEP

It seems logical to simulated the model's response to changes in these conditions. To verify the (qualitative) correctness, tests have to be performed on patients as well. When testing on patients, changing the chest wall compliance can be realized by compressing the chest [Pizov et al., 1989]. However, while keeping in mind that tests and their preparation are time-consuming, they cannot be performed. Also, changes in lung compliance cannot be performed. Tests that can be performed, however, are changes in tidal volume and PEEP conditions. Furthermore, besides the listed aspects, the magnitude of the variations also depend on the total blood volume and maybe also on the ratio of the inspiratory and expiratory times. As will be seen in Chapter 8, no test was carried out. During passive recordings settings were slightly adjusted.

Currently the processing of the signals of the actual patient data is best for the SPM (for further details, see Appendix B). Also, in most literature tests to capture changes in SPV are described. Therefore, in the simulations given below, the SPM values/shapes are given. Since it is already known that increasing the volume results in decreasing modulation values for systolic pressure, pulse pressure and SV, all three modulation types are given for this simulation.

All simulations were performed twice. For each test, the response of the model's normal functioning heart was simulated first. Thereafter, the simulation was done for the model's stiffened heart. The respiratory cycle of all simulation lasted at least twelve seconds. As previously described, the first six seconds of this period was the real ventilatory period, whereas the second part resembled a period of apnea[3] to make sure that the system was able to return to its stationary or equilibrium state.

The period of apnea is used to make sure that no negative $\triangle_{up}$ components could occur. Such values suggest that negative increases in ABP occur during inspiration. Negative values are however mentioned in literature (Pizov et al. [1996]; Weiss et al. [1999]; Jardin [2004]). These negative values can occur when the systolic peaks are still increasing to the baseline level (which they would have reached when the respiratory period was enlarged) when a new respiratory period starts. Therefore, during the inspiration of the new respiratory period, the increasing still plays a role. This even changes the shape of the modulation envelope. All this can be seen in Figure 6.8. Here the same model parameters were used to construct systolic pressure modulation envelopes, except for the (total) ventilation periods: a short ventilation period in which the 'patient' was just able to fully expire, a normal period and an extended period. The baseline that is used for $\triangle_{up}$ calculation is the end-level of the envelope of the extended period. It can be seen that in the short period, a negative $\triangle_{up}$ occurs. Furthermore, when inspiration starts, the envelope is (approximately) at its minimal value. Also, the value of the SPM for the normal period is lower than the extended period, because the equilibrium is not reached yet at the start of inspiration.

[3]Here apnea is defined as extension of the respiratory period while keeping the airway pressure at the level of PEEP, instead of disconnecting the patient from the ventilator or turning off the ventilator [Schwid and Rooke, 2000].

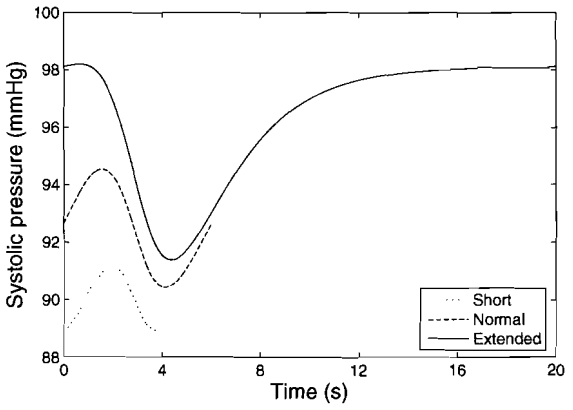

Figure 6.8: *The ventilation period influences the shape and offset of the modulation envelope, especially when the period is too short. In the normal period, the equilibrium is not reached yet, whereas it is reached in the extended period.*

Furthermore, an unexpected high-frequency component that can be observed in the simulation results (see Section 6.2.3), influenced the signals too much when the apnea period was not used.

In Table 6.1 the parameter values of the basic intrathoracic pressure curve (see Figure 6.1) that were used for the simulations are given.

Table 6.1: *Used intrathoracic pressure curve parameter values*

Parameter	Value	Unit
T_{resp}	12	s
T_{insp}	2	s
T_{pause}	1	s
τ_{exp}	0.75	s
P_0	-4	mm Hg
PEEP	6	mm Hg
P_{tidal}	4	mm Hg

Calculation of the modulation envelopes was performed using the algorithm that was used to create the envelopes in patient data (see Appendix B).

Total blood volume

The model's total blood volume was gradually increased from 4500ml to 5500ml with steps of 100ml. The resulting values for Systolic Pressure Modulation (SPM), Pulse Pressure Modulation (PPM), and Stroke Volume Modulation (SVM) are shown Figure 6.9(a, c and e). After stiffening the model's heart, the simulation was performed again. The resulting SPM, PPM, and SVM values for the model's stiff heart are shown in Figure 6.9(b, d and f).

In the drawn curves, it can be seen that for both types of heart, the model results in decreases in SPM, SVM, and PPM values when the total blood volume is increased.

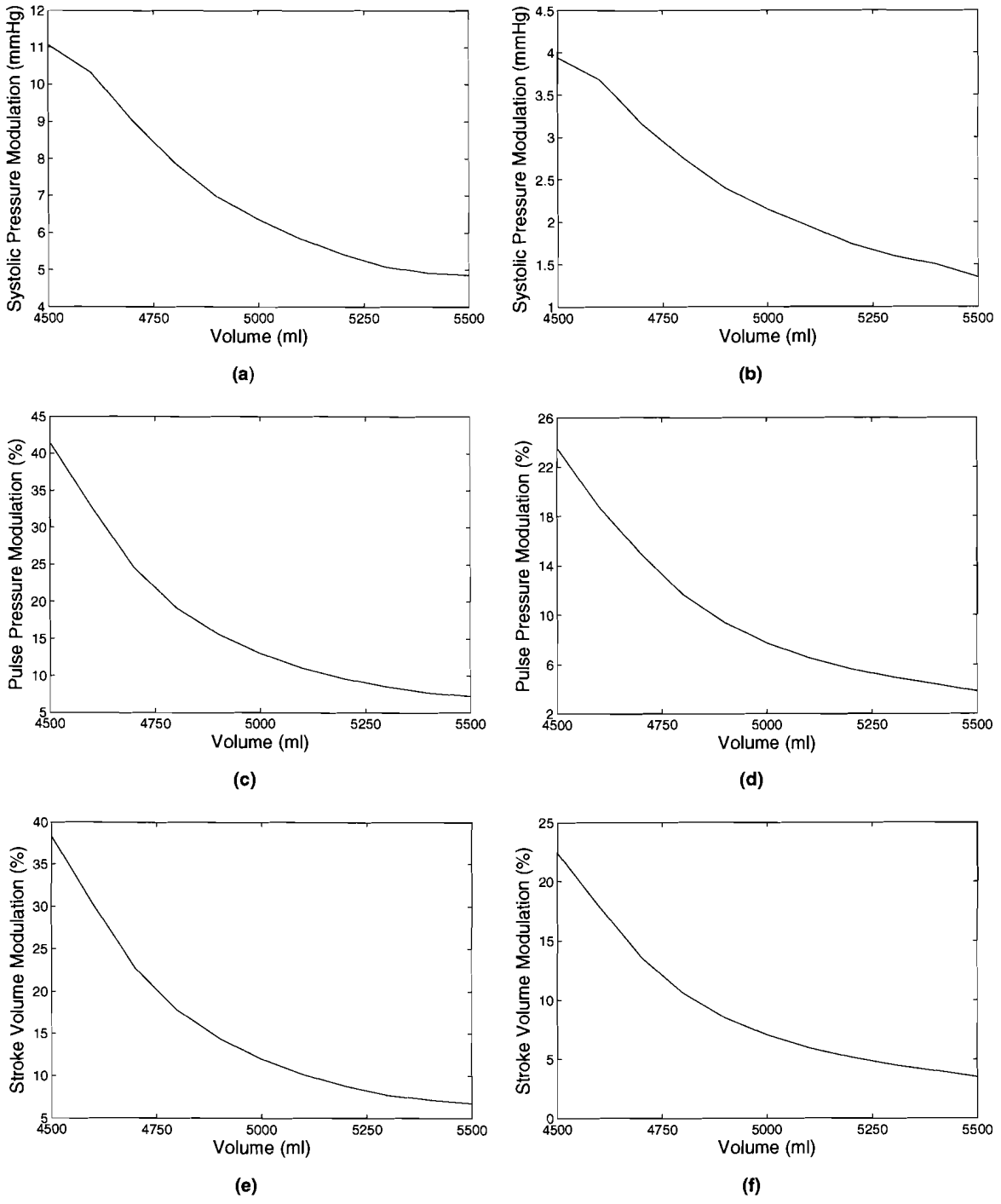

Figure 6.9: *Simulated measures of respiratory induced variations in ABP during stepwise fluid loading: systolic pressure modulation for (a) the normal heart and (b) the stiff heart, pulse pressure modulation for (c) the normal heart and (d) the stiff heart and stroke volume modulation for (e) the normal heart and (f) the stiff heart. The volume is the total blood volume in the model.*

Inspiratory : Expiratory time ratio

It is expected that if one shortens the time of inspiration (I), the circulatory system is influenced differently, because the same air volume has to be pumped into the lungs in a shorter time, resulting in higher driving pressures. The latter, in turn, result in a higher intrathoracic pressure. During the enlarged expiratory time (E), the values should return to the stationary level more quickly.

Ratios were changed from 1:2 until 1:5. The inspiratory pause was constant and set to 0.5 seconds. The ventilation period was set to six seconds and was followed by an apnea period of six seconds. The simulated systolic pressure modulation envelopes of the model's normal functioning heart for the different I:E time ratios are drawn in Figure 6.10(a). The simulated envelopes of the model's stiffened heart are drawn in Figure 6.10(b).

In Figure 6.10(b), it can be seen that for the stiff heart the extended respiratory period is still too short to let the systolic peaks return to their equilibrium value. Therefore, a new simulation for the stiff heart was done. in this simulation, the total respiratory period was extended to twenty seconds. The resulting modulation envelopes for this simulation are shown in Figure 6.11.

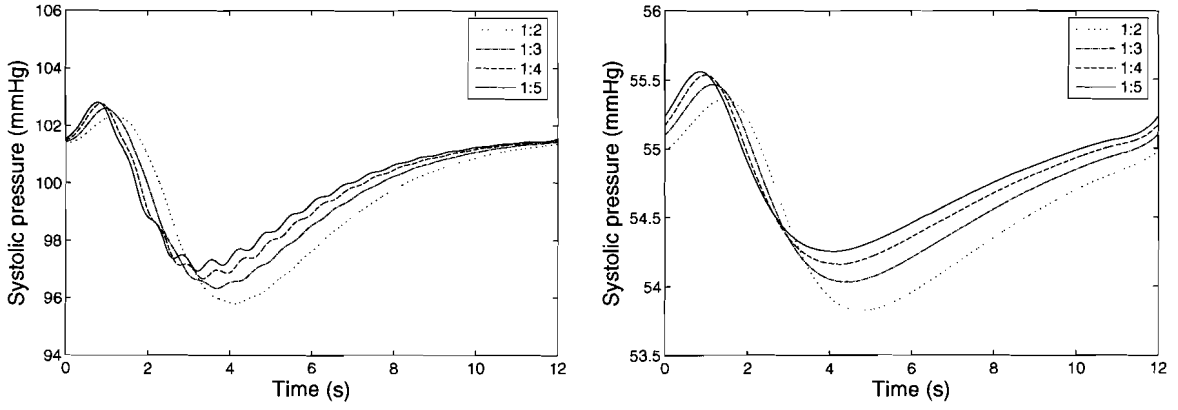

Figure 6.10: *Simulated systolic pressure modulation envelopes for changing I:E time ratio for (a) the normal heart and (b) the stiff heart.*

According to the envelopes in Figure 6.10(a) and Figure 6.11, the SPM for both types of heart decrease when the I:E time ratio is decreased.

In Figure 6.10 it can furthermore be observed that the smooth shape of the modulation envelope gets progressively more influenced by a high-frequency component for decreasing I:E time ratio. This observation will be examined in more detail in the next subsection.

Tidal volume

Just like decreasing I:E time ratio increases driving pressures, increasing tidal volumes results in increased (end inspiratory) intrathoracic pressure. To simulate the model's response to increased tidal volumes, the tidal pressure (which is linearly related to the tidal volume) was increased. Four different

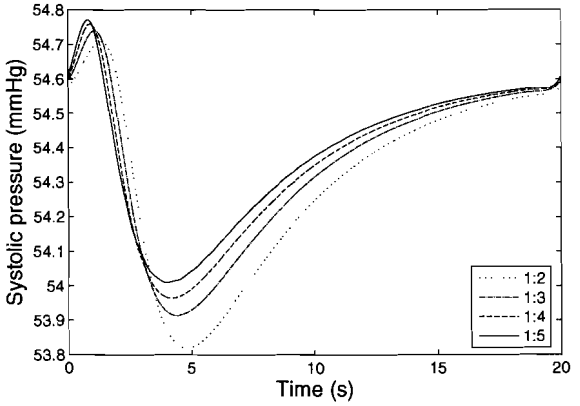

Figure 6.11: *Simulated systolic pressure modulation envelopes for changing I:E time ratio for the stiff heart using a longer respiratory period.*

tidal pressures were used. The resulting systolic pressure modulation envelopes for the normal and stiff hearts are shown in Figure 6.12(a) and (b), respectively.

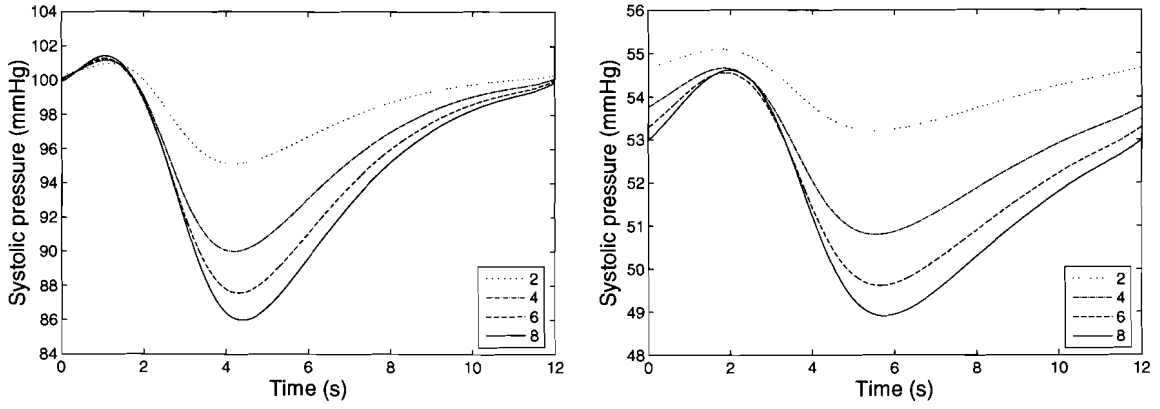

Figure 6.12: *Simulated systolic pressure modulation envelopes for changing tidal volume for (a) the normal heart and (b) the stiff heart.*

The drawn modulation envelopes in Figure 6.12 indicate that, according to the model, increasing the tidal volume results in increases in SPM amplitudes. This holds for both the normal and the stiff hearts. Note that the extended ventilatory period for the stiff heart is still too short.

In Figure 6.12(b), it can be seen that for the stiff heart the extended respiratory period is still to short to let the systolic peaks return to their equilibrium value. Therefore, a new simulation for the stiff heart was done using a period which was extended to twenty five seconds. The result of this simulation is shown in Figure 6.13.

In Figure 6.12 and Figure 6.13 it can furthermore be observed that the modulation envelopes have a typical shape: a peak component, a valley component and a smooth return to 'baseline'-level. This

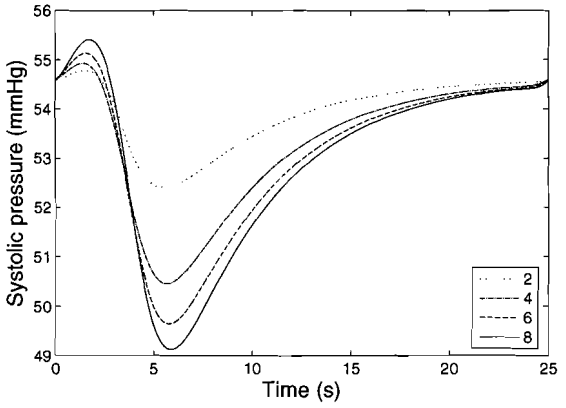

Figure 6.13: *Simulated systolic pressure modulation envelopes for changing tidal volume for the stiff heart using a longer respiratory period.*

observation will be examined in more detail in the next subsection.

One has to keep in mind that the simulation results have to be compared to patient data as well. As will be explained in the next chapter, the (inspiratory) tidal volume cannot just be changed, because a certain respiratory minute volume has to be maintained. The respiratory minute volume is the product of the tidal volume and the respiratory rate. Decreasing the tidal volume therefore implies that the respiratory rate has to increase and vice versa.

To be able to do a qualitative comparison with the patient data, the tidal volume simulations were therefore performed a second time. This time, the product of tidal volume and respiratory rate was kept constant. However, the same apnea period was used. Furthermore, the product of tidal pressure and respiratory rate was kept at 20 mm Hg/minute. In Figure 6.14, the results of the second simulation are shown.

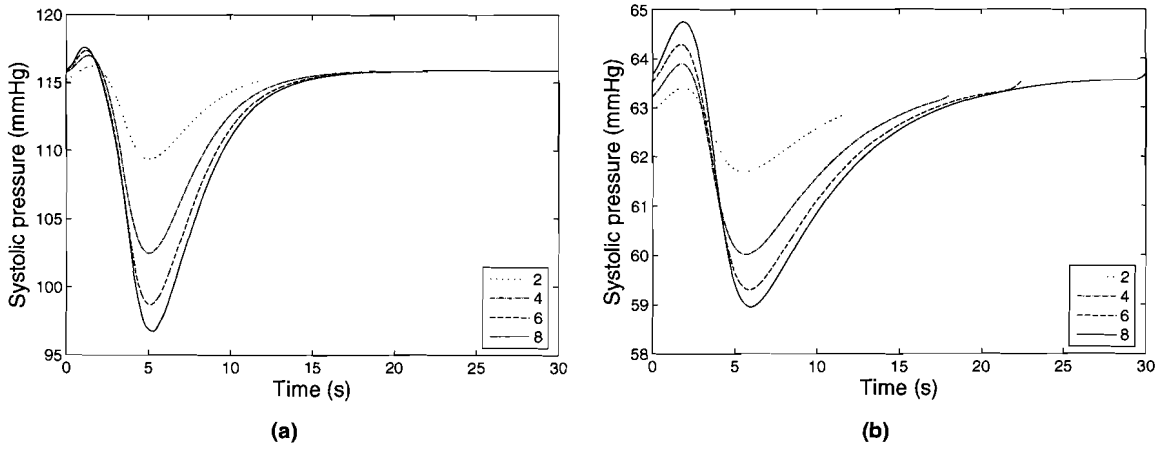

Figure 6.14: *Simulated systolic pressure modulation envelopes for changing tidal 'volume' with constant respiratory minute volume for (a) the normal heart and (b) the stiff heart.*

As can be seen in Figure 6.14, in both types of heart the increase in tidal volume (and decrease of respiratory rate) results in an increase of the SPM.

Level of Positive End Expiratory Pressure

The last condition that was changed, was the level of PEEP. Increasing values of PEEP result in increased pulmonary pressure during the whole respiratory period. As described earlier, this yields that left ventricular preload decreases. This implies that the working point changes and that the magnitude of the modulation envelope increases.

A PEEP level of 0 mm Hg would result in a baseline alveolar pressure of 0 mm Hg as well. According to Equation 6.5, this would mean that the pulmonary capillary resistance R_{pc} would be equal to 0 mm Hg/ml. Therefore, this situation was never simulated. Other levels of PEEP were therefore used: 4 mm Hg, 8 mm Hg, 12 mm Hg, 16 mm Hg 20 mm Hg and 24 mm Hg. The resulting systolic modulation envelopes for the model's normal functioning and stiffened hearts are drawn in Figure 6.15(a) and (b), respectively. The numbers in the legend denote the baseline pressure level (i.e. the sum value of P_0 and .5 * PEEP).

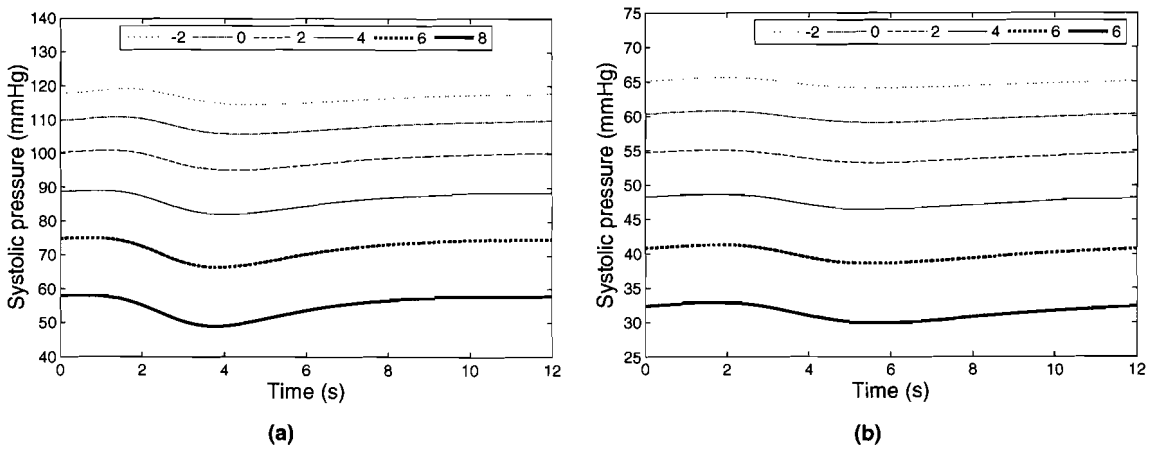

Figure 6.15: *Simulated systolic pressure modulation envelopes for changing PEEP for (a) the normal heart and (b) the stiff heart.*

It was said earlier that the model does not adapt the systemic resistance to significant changes in ABP. Therefore, the magnitudes of the modulation envelopes are most probably smaller than they should be, because increasing the systemic resistance should result in a downwards shift of the working point on the Frank-Starling curve [Smith, 2003]. However, the results drawn in Figure 6.15 show that the SPM increases when the PEEP is increased.

6.2.3 Observations

High-frequency component in valley of the envelope

The simulation results show that the down-slope and valley of the modulation envelope have a high-frequency component. This was especially the case when the I:E time ratio was decreased, as can be

clearly seen in Figure 6.10(a).

Since the component starts to occur when the intrathoracic pressure decreases, simulations with the way the intrathoracic pressure decreases were carried out to further investigate the phenomenon. In the first simulation, the intrathoracic pressure returned to the resting value instantaneously (which is of course not possible in patients). In the second and third simulations, a slow and fast exponential decrease was used, respectively. In the fourth simulation, a very slow linear decrease was used. The resulting modulation envelopes (with the high-frequency component) are drawn in Figure 6.16.

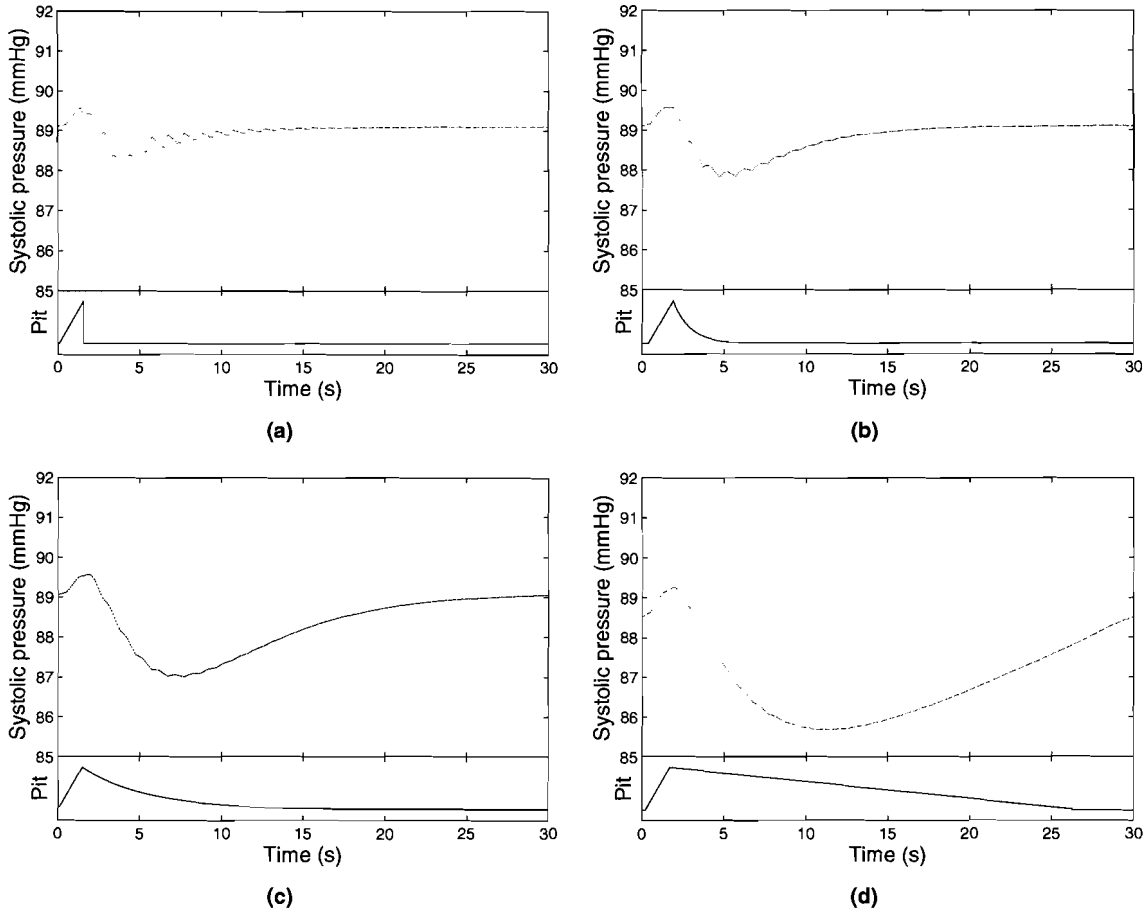

Figure 6.16: *Unexpected high-frequency component in simulated modulation envelopes for different types of expiration: (a) instantaneous expiration, (b) fast expiration, (c) slow expiration, and (d) very slow linear expiration.*

In Figure 6.16 it can be seen that the influence of the high-frequency component is related to the way the intrathoracic pressure decreases, the speed with which it decreases in particular. Currently it is not clear if this is due to assumptions (e.g. neglecting the inertia of blood near the valves) or to aspects related to the implementation (e.g. the used units for volume and pressure).

One may expect that the component is related to the chosen time step. However, when the time step was decreased, the component was still present.

Return to equilibrium

Another observation is the characteristic shape of the modulation envelopes. A typical example of this shape is drawn in Figure 6.17. It seems that during the apnea period that succeeds the ventilation period, the amplitude of the modulation envelope seems to increase exponentially to its stationary value. This holds for all the modulation types (i.e. SPM, PPM, and SVM). The characteristic shape of the envelopes is drawn in Figure 6.17.

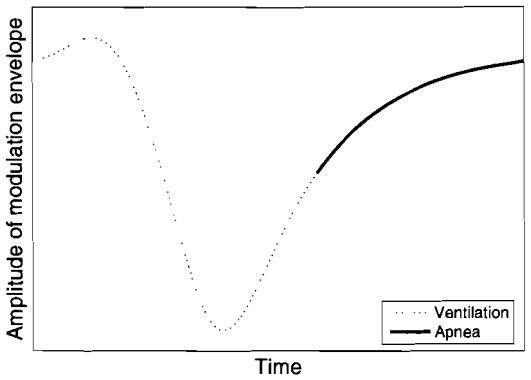

Figure 6.17: *Typical shape of the modulation envelope: small inspiratory rise, followed by a decrease. After the ventilation part, the amplitude seems to increase exponentially to its stationary value during the apnea part.*

If one looks at the preload/SV relation of the model and the modulation envelope simultaneously, one can see that the relation between the preload and SV is pushed away from the steady state relation of Figure 6.4 during the true ventilation period. During apnea the SVs (slowly) return to their equilibrium values again. During this return, the successive preload/SV pairs 'climb' over the previously measured curve to the equilibrium.

It could be the case that the time constant of this return reveals information about the functioning of the heart as well, much like the manoeuvre proposed by Perel et al. [2005].

6.3 Summary

The derived respiratory and circulatory models are based on already verified models. Therefore, only the coupled model's response to (changing) ventilation was simulated. The simulations were carried out for qualitative testing rather than for both qualitative and quantitative testing, because a parameter estimation routine was not created. The latter is necessary to compare quantitative simulation results with results obtained from patient data.

The simulations were carried out using a LabVIEW implementation of the model and made use of a Forward-Euler integration method and parameter values found in literature. Because of the qualitative testing background and the fact that simulations were done to simulate the response of the circulatory model to changing intrathoracic pressure, not the whole respiratory model was implemented, but only a function describing a basic intrathoracic pressure curve was implemented. This function is constructed

using five ventilatory settings and two patient specific parameters.

Based on aspects that influence the respiratory induced variations in arterial blood pressure, four tests were carried out to determine the model's response to changing ventilator conditions: total volume, the ratio of inspiratory and expiratory times, the tidal volume and the level of PEEP. Although there are more influencing aspects, one should keep in mind that not all of them can be tested on patients for cross-validation. Since in stiff hearts the amplitude of the respiratory induced variations in ABP should be lower than for normal hearts, the simulations were carried out for the a normal model heart and a stiffened model heart. According to the simulations, the amplitude of the modulation envelopes should decrease for increasing volume, increase for increasing tidal volume, decrease for decreasing I:E time ratios and increase for increasing level of PEEP.

Besides the direct results of the simulations, two other observations can be made if one looks at the modulation envelopes that were constructed. The first observation is that during expiration, an unexpected high-frequency component is present in the modulation envelope. The magnitude of this component seems to depend on the speed with which the intrathoracic pressure decreases to its resting value. This may be due to used assumptions and/or the implementation. A second observation is that the modulation envelopes have characteristic shapes. During the simulations, it became apparent that the modulation envelopes have characteristic shapes that can be split up into a ventilation part and an apnea part. The shape of the apnea part, particularly the time constant of the increase in pressure during this period, might be another interesting value for the assessment of fluid loading responsiveness.

chapter 7

Limiting factors for obtaining patient data

To compare the model results to patient data, patient data has to be obtained. However, when obtaining patient data, one is limited by several factors. For example, all kinds of preventive measures are taken (e.g. sufficient supply of oxygen), so tidal volume and respiratory rate cannot just be changed. Also, not all needed signals may be present. In this chapter an overview of general limiting factors and the ones that applied to the project is listed.

7.1 Respiratory minute volume

The respiratory minute volume (RMV) is the product of the respiratory rate f and the inspiratory tidal volume TV_i:[1]

$$f_r * TV_i = RMV \tag{7.1}$$

For a given stable situation the RMV should remain constant in order to keep the partial pressure of CO_2 at a constant level [Reuter et al., 2003]. This implies that when f_r is changed TV_i should change as well and vice versa.

Most parts of the body consume oxygen in order to perform their tasks. The consumption of oxygen is expressed as a volume per mass per unit of time. For a patient, this mass can be defined as the weight of the parts of the body that consume oxygen. An approximation for this mass is called the lean body mass (LBM) and is defined as the body weight minus the weight of the fat. Since the percentage of oxygen in the ventilation gases is practically constant, the supply of oxygen is proportional to the respiratory minute volume (RMV):

$$\frac{RMV}{LBM} = c \tag{7.2}$$

Here c is proportional to the supply of oxygen. The state of the patient may change, resulting in different needs for oxygen. If the need for oxygen is higher than the supply, the fraction has to be increased. Also, if the need for oxygen is lower than the supply, the fraction may be adjusted. Since the LBM is constant, changes can only be achieved by changing the RMV. Moreover, when the supply of oxygen

[1] One has to make a correction for the effective tidal volume: because of the dead space not the whole inspiratory tidal volume reaches the alveoli.

is not sufficient, clinicians only use TV_i to change the supply:

$$\frac{TV_i}{LBM} = BMTV \tag{7.3}$$

Here BMTV is the body mass scaled tidal volume. In the Catharina Hospital, the staff tries to keep its value at 8 ml/kg. As said before, for stable situations, adjusting TV_i implies adjusting f_r as well. However, one should be careful with adjusting f_r too much. If for successive respiratory cycles the expiration time is too short, an increasing air volume remains in the lungs. This volume results in a pressure called intrinsic PEEP and has to be avoided. Another important value is the peak inspiratory pressure P_{ip}. If this value becomes too high (a maximum of 30 cm H_2O is usually used by the staff, but it should certainly not exceed 35 cm H_2O), lung tissue may get damaged. The same holds for the peak inspiratory flow F_i which may also not be too high.

If during the recordings TV_i is changed, f_r thus changes as well. Determining the system's response to either changes in TV_i or changes in f_r only is therefore difficult.

7.2 Available time and location

In the hospital, the medical staff is primarily concerned with the well being of their patients. The condition of these patients should at least not worsen. Clinicians may therefore not have the proper time available to perform the tests, if these tests can even be performed.

The patient data can be obtained from patients who are sedated and fully ventilated. Measurements can therefore only take place at the hospital's operating room (OR) and intensive care unit (ICU). During surgery, the state of the patient is usually unstable (e.g. due to losses of blood). Furthermore, the data obtained from the OR may contain many artifacts which result from interfering sources (e.g. distortion due to used equipment). This makes it difficult and maybe even impossible to distinguish between changes due to the test performed and those due to other (interfering) sources. Therefore, only data obtained from the ICU was used.

A limiting factor of the data obtained from the ICU is the respiratory signal. The monitors do not measure a pressure, but instead measure the bioelectric impedance of the thorax. This impedance is presented as a surrogate of the pressure in the lungs. In fact, an approximation for the volume in the lungs is measured, because the impedance varies proportional to this volume (approximately 1 to 2 ohms per liter of lung volume) [Patterson, 2000]. The volume in the lungs is, in turn, proportional to the pressure in the lungs.

The measured signal is much noisier than for example the pressure measured by the patient monitor in the OR. This is partly due to the fact that thorax impedance depends on more processes than just the ventilation (even small fluctuations due to blood pressure pulses are reflected in the signal). An example of a period of a 'clean' respiration signal as measured on the ICU is shown in Figure 7.1(a). For comparison, a 'clean' period of a respiration signal as measured on the OR is shown in Figure 7.1(b). Note that the signal from the ICU is an approximate for the pressure inside the lungs, whereas the signal measured at the OR is the airway pressure measured in the trachea. Therefore, the actual shapes cannot be compared directly. However, it is clear that the signal measured on the ICU is much

noisier.

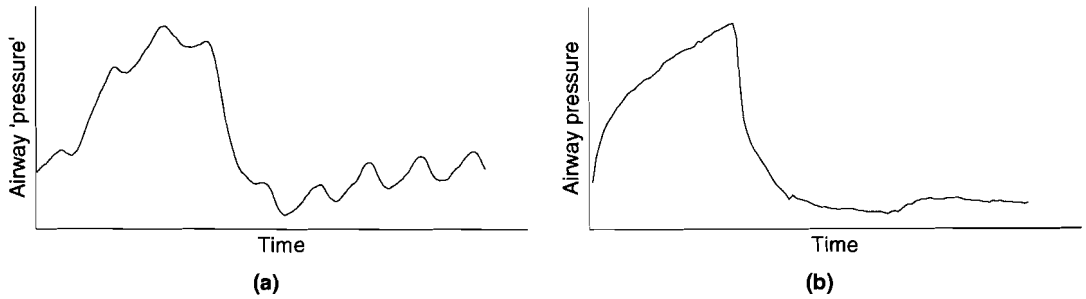

Figure 7.1: *Difference between clean respiration signals from (a) ICU and (b) OR.*

The significant influences of the blood pressure pulses on the respiratory signal make it difficult to validate the period using the method described in Appendix B. However, although noisy, the respiratory period can still be extracted. This becomes more difficult when the sensor comes loose, which was often the case (this became evident during processing). Therefore, the measured airway 'pressure' signals were unusable for period extraction. Instead, the periodicity of the respiratory signal was obtained differently. An obvious solution would be to use the periodicity as specified by the ventilator, however, the specified value did not match the measured period length exactly. Therefore, the ABP signal was used to determine the respiratory period.

Furthermore, the ventilators at the ICU seem to have some 'intelligence' since every once in a while it starts a new respiratory cycle while the previous one has not finished yet.

7.3 Number of patients

The fact that patients need to be sedated and ventilated in order to use respiratory induced variations in ABP for assessment of fluid loading responsiveness, limits the number of patients that can be included in tests. Not all patients on the ICU are fully ventilated, or even sedated. Keeping the patients unnecessarily sedated and ventilated may harm them. Here ethical questions play a role.

If one wants to obtain patient data (during tests) in a systematic manner (e.g. in academic research), patients (or their relatives) should give written informed consent. Moreover, an extensive measurement protocol has to be approved by the medical-ethical committee before testing is allowed. In the current project, there was no time to create an extensive measurement protocol, let alone getting such a protocol approved.

Therefore, no tests with changing settings were performed. Only the patient signals were recorded. Fortunately, due to circumstances, clinicians changed settings during the recordings. This resulted in one recording per type of setting change that was mentioned in the previous chapter.

7.4 Summary

The way experiments can be performed and processed are limited by precautions and several other aspects. It is very important that the patients do not get harmed as a result of the tests. An important value in this context is the respiratory minute volume, which is the product of inspiratory tidal volume and respiratory rate. If one of the ventilator settings is changed, the other setting should change as well, because the minute volume must remain constant. Tests on tidal volume therefore reflect changes due to varying respiratory rate, as well as changes due to varying inspiratory tidal volume.

Due to interfering sources during surgery, identifying the changes due to a test may be difficult and even impossible. Therefore, it was chosen to obtain data from the ICU only. Unfortunately, the respiratory signal from the ICU is noisy. This is mainly because not a pressure, but the thorax impedance is measured. This value is proportional to the lung volume (and pressure), but depends on many other processes as well. Also, the respiratory rate as specified by the ventilator did not always match the measured rate. Therefore, the respiratory rate was obtained from the ABP signal.

If tests on patients are performed in a systematic manner, written informed consent from the patient and approval of the medical-ethical committee is necessary. Since there was no time for this consent and approval in the project, patient signals were only recorded and no test was carried out. Fortunately, due to circumstances, one recording for all setting changes mentioned in the previous chapter was obtained.

chapter 8

Trends in patient data

To be able to do a qualitative verification of the model, the trends in simulation results have to be compared to the trends found in patient data. In the previous chapter it was said that no systematic testing could be performed. Instead, several recordings of patient data were obtained. Fortunately, due to circumstances settings were changed during the recordings. The same settings were adjusted as in the simulations. The adjustments were very small and far within the limits. Also, one recording was done while fluid was added to a patient.

Due to time and practical limitations, only one recording per change of setting was obtained. Unfortunately, it was impossible to test beforehand whether patients would be responders or not. In order to extend the limited dataset, trends obtained from literature were used as well.

At first glance, comparing the trends in simulation data with patient data obtained from the recordings and from literature seems like comparing apples to pears, because during the recordings the extended respiratory cycles of the simulations were not used. However, most literature studies mentioned in this chapter use the $\triangle_{down}$ component as well. This implies that at least several extended measurements were performed to determine baseline systolic pressure values. Therefore, the comparison based on the shorter periods will be done nevertheless.

Each of the adjustments that were presented in Chapter 6 is discussed in a separate section. Each section is divided into two parts. The first part describes the trends as found in literature and the second part describes the trends found in the recorded dat.

The results were calculated from the recorded signals using the system described in Appendix B. To make sure that patients would not suffer from the adjustments, the parameters mentioned in the previous chapter and several others were monitored continuously. For each type of adjustment a table containing the monitored settings and values accompanies the results. The values that were adjusted are highlighted in these tables.

Prior to the recordings in which the previously mentioned settings were adjusted, the first section describes a recording with the respiratory rate. This was used to determine whether changes in the phase of the modulation envelope occurred.

8.1 Changes in respiratory rate

One cannot just change and extend the respiratory period as described in the previous chapter, certainly not for prolonged tests. However, one recording contained two different respiratory rates. This data can thus be used to verify the effect that was shown in Figure 6.8.

The respiratory rate was changed from 10 to 15 per minute (in fact, the respiratory period of the slower rate was an extended version of the period of the faster rate, because all other ventilation settings, including I:E time ratio and TV_i, were kept constant). In Figure 8.1 several successive respiratory periods and the simultaneously recorded ABP periods for both rates are shown.

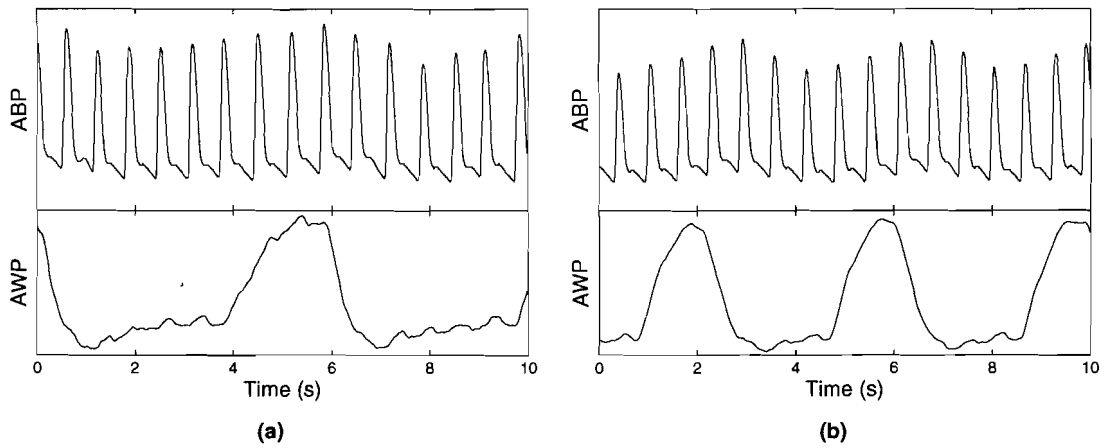

Figure 8.1: *The ventilation period influences the shape and phase of the modulation envelope. (a) For slow ventilation rates the start of the inspiratory period coincides with a point on the upslope of the (imaginary) envelope. (b) For faster rates the start of the inspiratory period coincides with a position near the valley of the envelope.*

Like the short period in Figure 6.8, the start of inspiration seems to coincide with the minimum value of the (imaginary) modulation envelope for the faster respiratory rate (see Figure 8.1(b)), whereas the start of inspiration for the slower rate coincides with a position on the upslope of the envelope (see Figure 8.1(a)), much like the normal period in Figure 6.8.

The respiratory rate thus has influence on the phase of the modulation envelope. Several studies report negative $\triangle_{up}$ values, which indicate that also the shape of the envelope is affected [Pizov et al., 1996; Weiss et al., 1999; Jardin, 2004]. It would thus be better to use extended periods, because then the effects due to a changing parameter become more clear than in the current situation. The effects as will be seen in the other recordings might have been different if other respiratory rates were used. It is however expected that only amplitudes will differ, as can be seen in the stiff heart's simulation results for the I:E time ratio test. When the respiratory period was too short (see Figure 6.10(b)), the trend in amplitude was the same as the trend seen for a respiratory period that was long enough (see Figure 6.11).

8.2 Adding fluid

Literature

Perel et al. [1987] found that the SPV is a sensitive indicator of hypovolemia. By subjecting dogs to gradual hemorrhage, they found that the SPV increases for decreasing blood volume. Preisman et al. [2002] had similar findings with gradual hemorrhage and retransfusion in pigs. The results were also confirmed by numerous other studies (e.g. for dogs by Szold et al. [1989], Preisman et al. [1997] and Fujita et al. [2004] and for humans by Bennett-Guerrero et al. [2002] and Reuter et al. [2002]).

Recording

The recorded signals were from a patient whose lean body mass (LBM) was estimated to be 55kg. During the recording 1l of fluid was added to the patient's blood volume. The speed of infusion was set to 1l/hour. The volume came in two 0.5 l bags. Therefore, two successive sessions were held. Between the two sessions a short pause (approximately 15 minutes) was inserted to let the patient adapt to the new situation.

The ventilation settings that were used during the recording are listed in Table 8.1. Since no ventilation settings were adjusted, they were set to convenient values. The times indicated in Table 8.1 are related to the start and end points of the fluid addition (the fluid was added using a pump that was set to 1l per hour).

Table 8.1: *Monitored ventilation settings and values during the addition of fluid.*

Time	BMTV (ml/kg)	TV_i (ml)	f (per minute)	I:E	RMV (l)	F_i (l/min)
15:57	10	550	15	1:2	8.25	50
16:27	10	550	15	1:2	8.25	50
16:43	10	550	15	1:2	8.25	50
16:15	10	550	15	1:2	8.25	50

The resulting SPM values for the first session are shown in Figure 8.2(a). It can be seen that during the first part of infusion, the SPM decreases. Just before the infusion stops, an increase in SPM can be observed. After the infusion, the system takes a little time to adapt itself. In Figure 8.2(b), the resulting SPM values during the infusion of the second 0.5 l are shown. Since a decrease in SPM values is not directly noticeable, a line was fitted through the values. Before the fitting, SPM values belonging to amplitudes of wrongly approximated curves (see for example the points in Figure 8.2(a)) were removed. As with the first session, after infusion the system is not stable, but adapts itself. This resulted in increasing SPM values.

8.3 Adjusting Inspiratory : Expiratory time ratio

Literature

In nine volume controlled ventilated patients, Vedrinne et al. [1997] changed I:E time ratio from 1:1 to 1:3, while the BMTV remained constant. They found that the SPV was higher for the 1:1 test than for

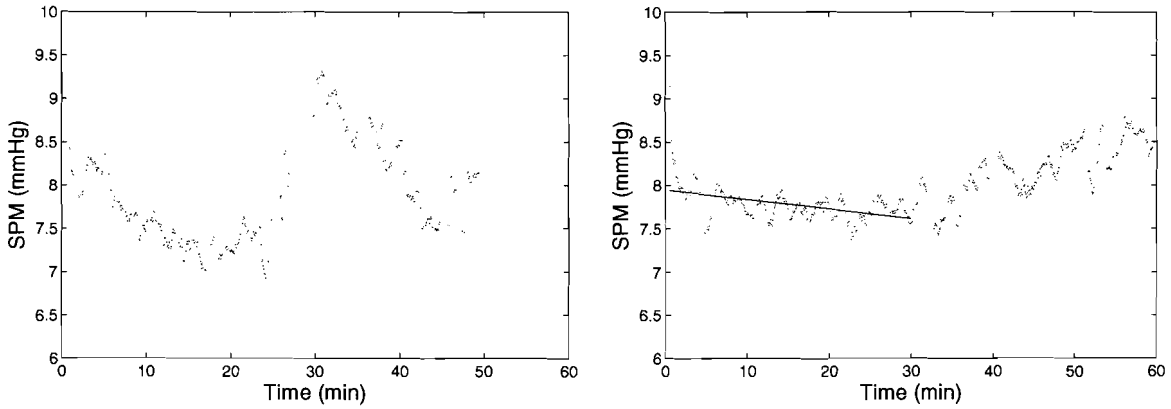

Figure 8.2: *SPM values of the fluid addition recording: (a) first 0.5 l and (b) second 0.5 l. Values below 7 mm Hg were ignored in the linear approximation of the second session. Fluid was added with 1 l per hour.*

the 1:3 test, which suggests that when the I:E time ratio is decreased, the SPV decreases as well.

Recording

The recorded signals were from the same patient as the previous recording. The ventilation settings that were used during the recording are listed in Table 8.2. The times indicated in Table 8.2 are related to the times at which the I:E time ratio was changed. When decreasing the inspiratory time, the same volume has to be pumped into the lungs faster, resulting in a higher (peak) inspiratory flow F_i. To make sure that this value did not increase too much, this value was monitored carefully during the recording.

Table 8.2: *Monitored ventilation settings and values during the I:E time ratio recording.*

Time	BMTV (ml/kg)	TV_i (ml)	f (per minute)	I:E	RMV (l)	F_i (l/min)	P_{ip} (cm H_2O)
16:17	10	800	10	**1:2**	7.7	50.0	28
16:35	10	780	10	**1:3**	7.5	63.0	29
16:49	10	780	10	**1:4**	8.0	79.0	29
17:02	10	790	10	**1:5**	8.0	96.0	31
17:12	10	800	10	**1:2**	8.2	48.5	27

The calculated SPM values of the recording are shown in Figure 8.3. It can be seen that for decreasing I:E time ratio the amplitude of the SPM envelope decreases. Also, the SPM values for the last setting are approximately equal to the values of the same setting at the beginning of the recording. Clear plateaus for each of the I:E time ratio settings can however not be observed.

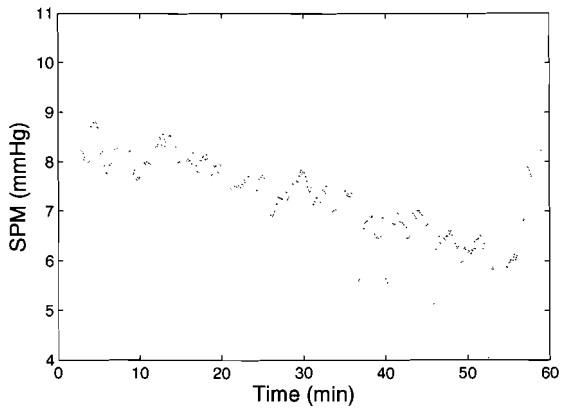

Figure 8.3: *SPM values during the I:E time ratio recording.*

8.4 Adjusting Tidal Volume

Literature

After a test where the BMTV was changed and the respiratory minute volume was kept constant, Reuter et al. [2003] concluded that the variations in stroke volume (and the accompanying variations in arterial blood pressure) highly correlated with the BMTV.[1] With a base value of 10 ml/kg, they found that the SVV decreased for a BMTV of 5 ml/kg, whereas it increased for a BMTV of 15 ml/kg. Szold et al. [1989] found that in dogs the SPV increased when the BMTV was increased from 15 ml/kg to 25 ml/kg.

Recording

For this recording, the data of a patient with an LBM of 80kg was used (for comparison: the total body mass was found to be 100kg). To make sure that the respiratory minute volume remained constant, the adjustment of inspiratory tidal volume (TV_i) was accompanied by simultaneous changes in the respiratory rate (see Equation 7.1 and Equation 7.3). Three levels of BMTV were used: 8 ml/kg, 10 ml/kg and 12 ml/kg.

The ventilation settings that were used are listed in Table 8.3. The times indicated in Table 8.3 are related to the times at which the BMTV was changed.

Table 8.3: *Monitored ventilation settings and values during the tidal volume recording.*

Time	BMTV (ml/kg)	TV_i (ml)	f (per minute)	I:E	RMV (l)	P_{ip} (cm H_2O)
15:15	8	**640**	**13**	1:2	8.0	23
15:30	10	**800**	**10**	1:2	8.3	28
15:44	12	**970**	**8**	1:2	7.3	32
15:59	8	**640**	**13**	1:2	8.0	24

[1] Like in many clinical studies, the term tidal volume is assigned to the BMTV in this study.

Unfortunately, processing the ABP signal and constructing the modulation envelope of the systolic peaks was impossible. The respiratory signal was noisy and the respiratory rate was not constant. Therefore, only variation values can be given that were visually observed in the obtained data. The observed values are listed in Table 8.4.

Table 8.4: *SPV values during the tidal volume recording as visually observed*

BMTV (ml/kg)	SPV (mm Hg)
8	5
10	8
12	10
8	5

Of course, the values that were visually inspected are not as accurate as the values the system would normally extract. However, an increase in SPV is observed for increasing tidal volume and a decrease in SPV was clearly visible when the BMTV was decreased from 12 ml/kg to 8 ml/kg. This suggests that increasing the tidal volume, decreases SPV values.

8.5 Adjusting level of Positive End Expiratory Pressure

Literature

Michard et al. [1999] found that by applying PEEP, the respiratory induced variations in ABP increased compared to the variations as seen during zero end expiratory pressure. In the results of Pizov et al. [1996], it can be seen that, at least for dogs, PEEP decreases cardiac output and induces a shift to the left on the Frank-Starling curve. The latter results in higher SPV values.

Recording

Signals from the same patient as the tidal volume recording were recorded. The ventilation settings that were used are listed in Table 8.5. The times indicated in Table 8.5 are related to the times at which the level of PEEP was changed.

Table 8.5: *Monitored ventilation settings and values during the PEEP recording.*

Time	PEEP (cm H_2O)	TV_i (ml)	f (per minute)	I:E	RMV (l)	F_i (l/min)	P_{ip} (cm H_2O)
17:15	**10**	784	10	1:2	7.8	46.3	27
17:22	**8**	802	10	1:2	8.0	48.5	24
17:34	**5**	786	10	1:2	8.3	48.5	21
17:45	**3**	794	10	1:2	8.5	46.8	18
17:56	**0**	785	10	1:2	8.5	48.0	17
18:14	**5**	800	10	1:2	8.0	47.0	23

The calculated SPM values are shown in Figure 8.4. It can be seen that the SPM values slightly decrease for decreasing level of PEEP. Like with the I:E time ratio recording, no clear plateaus for

each of the PEEP settings can be observed. After an hour, the level of PEEP was increased to an intermediate level. The resulting SPM values also return to an intermediate value. However, like with the fluid addition recording, the system seems to adapt itself and the SPM values slightly decrease.

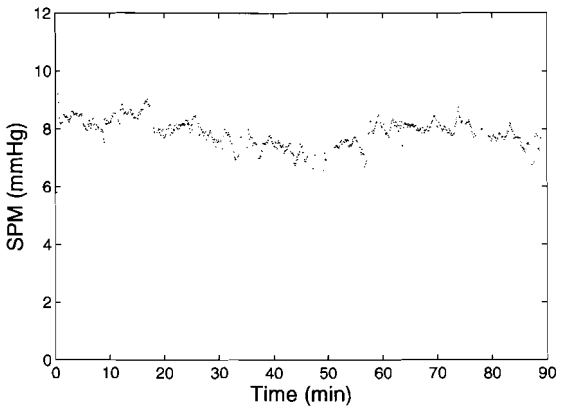

Figure 8.4: *SPM values of during the PEEP recording.*

8.6 Summary

In order to be able to do a qualitative verification of the model, trends in patient data were obtained. Since only one recording was used for each of the changes mentioned in Chapter 6, results obtained from literature were used to extend the dataset.

According to the results of one recording, the respiratory rate influences the phase of the modulation envelope, as was seen in the simulations. However, because the respiratory period could not be extended, 'normal' respiratory rates were used. It is expected that this only affects the amplitudes of the modulations, but that the observed trends remain the same.

For each of the adjusted settings that was mentioned in Chapter 6, the trends in patient data were obtained.

chapter 9 Results

In this chapter the results of the project in relation to the research objectives are given. The last objective, adding a parameter estimation routine, was not met and will therefore not be discussed in this chapter. In the last section of this chapter general results of the project are given.

9.1 Coupled model of the respiratory and circulatory system

The main research objective of the project was to model the respiratory induced variations in arterial blood pressure (ABP). The coupled model is based on already existing models of the respiratory and circulatory systems. However, the coupled model itself still needs to be validated. It was mentioned earlier that a full validation of the developed model was not done in the project and that only a preliminary qualitative verification between simulation results and patient data was possible. This qualitative verification is given in this section.

Settings were changed in the model and trends in resulting systolic modulation envelopes were found. Patient data of situations during which similar changes in settings occurred was processed to obtain trends. To extend the limited data set, trends found in literature that describe similar studies are used as well.

9.1.1 Respiratory rate

In the simulations it was found that when the respiratory period was changed/extended, the shape and phase of the systolic modulation envelopes changed. In Figure 9.1 the simulated systolic modulation envelopes for three different respiratory periods (short, normal, and extended) are shown.

In two of the collected recordings the respiratory period was changed as well. Although no extended periods were used, the influence of the respiratory period on the shape and phase of the systolic modulation envelopes seems to be confirmed by these recordings. In Figure 9.2(a) the ABP signal is shown for a situation where the respiratory period was set to six seconds. For convenience, the respiratory signal is shown as well. As can be seen, the minimum of the imaginary systolic pressure modulation envelope falls somewhere around the middle of the respiratory period. In Figure 9.2(b) the ABP signal of the same recording during a situation where the respiratory period was set to four seconds is shown. In this situation, the minimum of the imaginary systolic pressure modulation envelope falls at the start of the respiratory period.

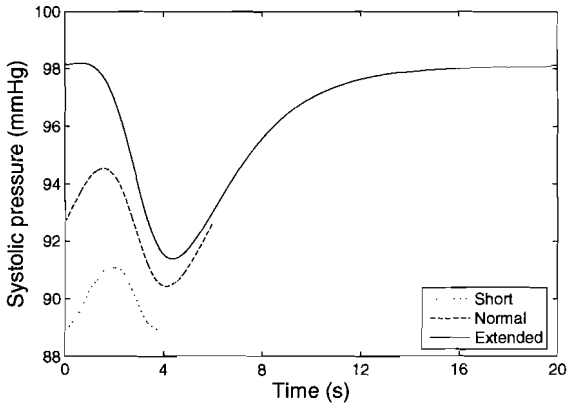

Figure 9.1: *The ventilation period influences the shape and offset of the modulation envelope. In the short period the envelope starts at its minimum, whereas this is not the case for the normal and extended respiratory periods.*

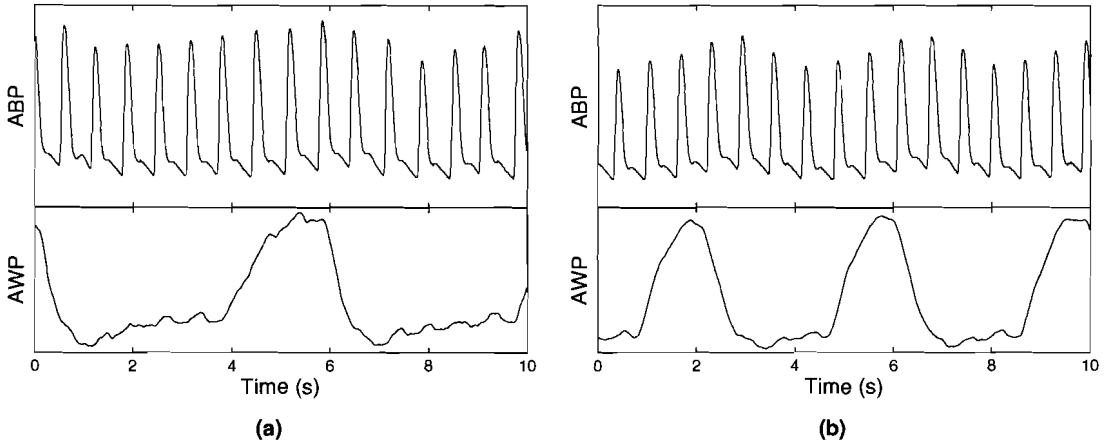

Figure 9.2: *The ventilation period influences the shape and phase of the modulation envelope. (a) For slow ventilation rates the start of the inspiratory period coincides with a point on the upslope of the (imaginary) envelope. (b) For faster rates the start of the inspiratory period coincides with a position near the valley of the envelope.*

Although the respiratory periods were changed in only two of the recordings, these recordings seem to confirm the simulation results. Whether the differences in shape and phase of the modulation envelopes for successive respiratory cycles indeed reveal relevant information in clinical practice yet remains unclear.

9.1.2 Adding fluid

In the simulation, the total blood volume was increased from 4500 ml to 5500 ml. The simulations were performed for both a normal heart and a stiffened heart. The resulting Systolic Pressure Modulation (SPM) values are shown in Figure 9.3(a) for the normal heart and in Figure 9.3(b) for the stiff heart.

According to the simulation results, the SPM decreases when the total blood volume is increased.

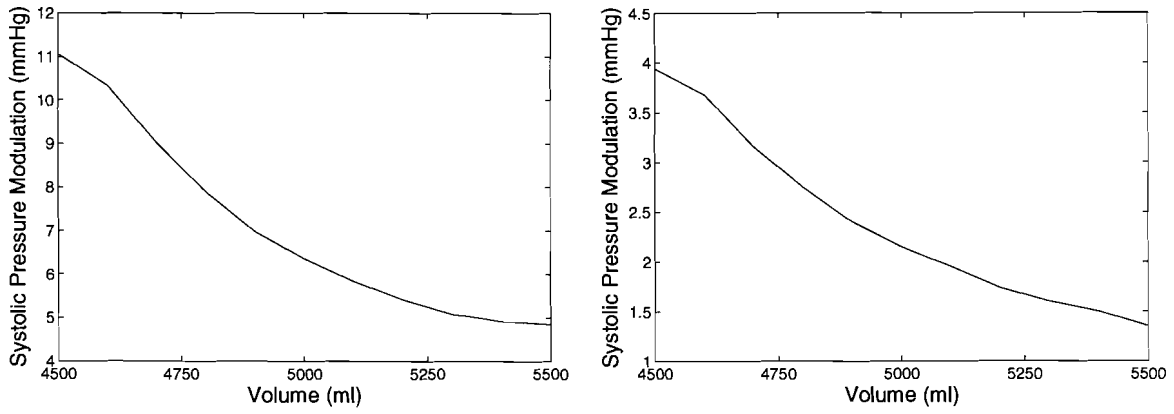

Figure 9.3: *Simulated systolic pressure modulation for (a) the normal heart and (b) the stiff heart.*

A recording was performed during fluid addition to a patient. The fluid was added in two successive sessions of 0.5 l. The speed of infusion was set to 1.0 l per hour. In Figure 9.4 the SPM values that were measured during the first infusion are shown. It can be seen that during the infusion the SPM decreases. At the end of infusion the SPM increases again. This probably has to do with adaptations within the body.

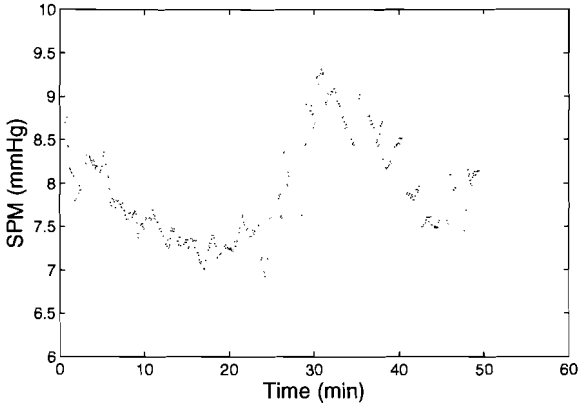

Figure 9.4: *SPM values of the fluid addition recording*

In literature it was found that the Systolic Pressure Variation (SPV) decreases for increasing blood volume in human patient and animal subject studies [Perel et al., 1987; Szold et al., 1989; Preisman et al., 1997, 2002; Bennett-Guerrero et al., 2002; Reuter et al., 2002; Fujita et al., 2004] .

For changing blood volume, the trends in the simulation results are confirmed by the trends in patient data, so the qualitative response of the model seems to be correct.

9.1.3 Adjusting Inspiratory : Expiratory time ratio

In the simulations the I:E time ratio was changed from 1:2 to 1:3, 1:4, and 1:5. The simulations were performed for both a normal heart and a stiffened heart. The resulting SPM values are shown in Figure 9.5(a) for the normal heart and in Figure 9.5(b) for the stiff heart. According to the simulation results, the SPM decreases when the I:E time ratio is decreased.

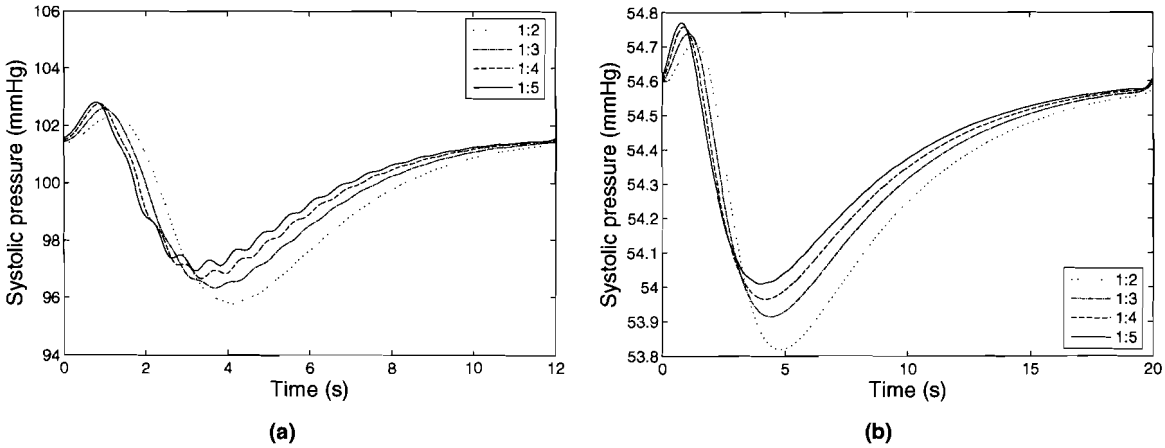

Figure 9.5: *Simulated systolic pressure modulation envelopes for changing I:E time ratio for (a) the normal heart and (b) the stiff heart.*

A recording was performed while the I:E time ratio was changed from 1:2 to 1:3, 1:4 and 1:5. At the end the ratio was set back to 1:2 again. In Figure 9.6 the SPM values that were measured during the recording are shown. Although no clear plateaus of SPM values are present, it can be seen that the SPM decreases when the I:E time ratio decreases.

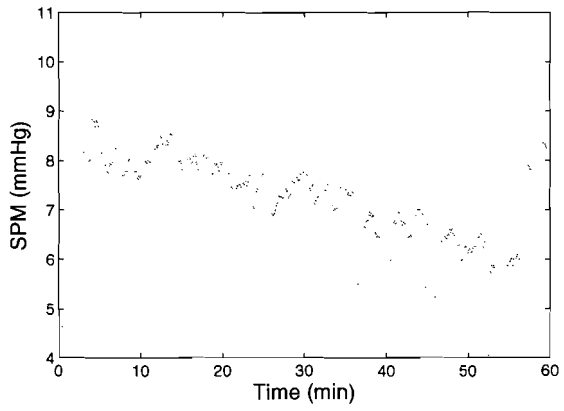

Figure 9.6: *SPM values during the I:E time ratio recording.*

In literature it was found that the SPV decreased when the I:E time ratio was changed from 1:1 to 1:3 [Vedrinne et al., 1997].

For changing I:E time ratio, the trend in the simulation results are confirmed by the trends in patient data, so the qualitative response of the model seems to be correct.

9.1.4 Adjusting Tidal Volume

As mentioned in Chapter 7, changing the inspiratory tidal volume involves changing the respiratory rate as well.

In the model tidal pressure is used instead of tidal volume. However, since these values are linearly related in the model, changing the tidal volume is the same as changing the tidal pressure. In the simulations the tidal pressure was changed from 2 mm Hg to 8 mm Hg with steps of 2 mm Hg. The product of the tidal pressure and the unextended respiratory period was kept constant. The simulations were performed for both a normal heart and a stiffened heart. The resulting SPM values are shown in Figure 9.7(a) for the normal heart and in Figure 9.7(b) for the stiff heart. According to the simulation results, the SPM increases when the tidal pressure is increased.

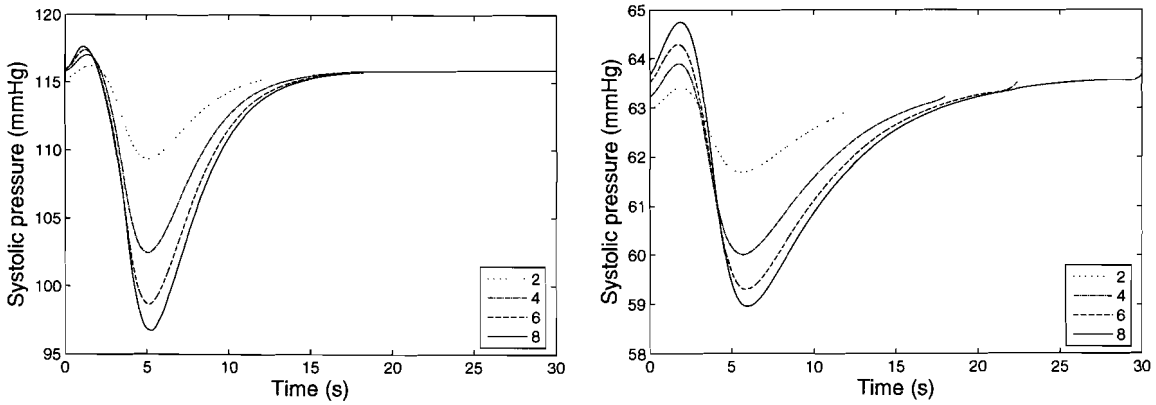

Figure 9.7: *Simulated systolic pressure modulation envelopes for changing tidal pressure with constant product of respiratory rate and tidal pressure for (a) the normal heart and (b) the stiff heart.*

A recording was performed while the body mass scaled tidal volume (BMTV) and respiratory rate were changed. The BMTV was changed between from 8 to 12 ml/kg with steps of 2 ml/kg, while the product of inspiratory tidal volume and the respiratory rate was kept at approximately 8 l per minute. At the end, the BMTV was set to 8 ml/kg again. Since the respiratory rate was not constant and the respiratory signal was very noisy, processing the signals was impossible. Therefore, only visual observations can be given. In Table 9.1 the SPV values that were observed for the different BMTVs are listed. In the table it can be seen that the SPV increases when the tidal volume increases.

In literature it was found that the SPV increased when the BMTV increased in human patient and animal subject studies [Szold et al., 1989; Reuter et al., 2003].

For changing tidal volume, the trend in the simulation results are confirmed by the trends in patient data, so the qualitative response of the model seems to be correct.

Table 9.1: *SPV values during the tidal volume recording as visually observed*

BMTV (ml/kg)	SPV (mm Hg)
8	5
10	8
12	10
8	5

Note that two parameters were changed. If possible, it would be better to just change the inspiratory tidal volume to see the response to this one parameter!

9.1.5 Adjusting level of Positive End Expiratory Pressure

In the simulations the level of positive end expiratory pressure (PEEP) was changed from 4 mm Hg, to 24 mm Hg with steps of 4 mm Hg. The simulations were performed for both a normal heart and a stiffened heart. The resulting SPM values are shown in Figure 9.8(a) for the normal heart and in Figure 9.8(b) for the stiff heart. The values in the legend denote the baseline pressure level (i.e. the sum value of the intrathoracic resting pressure and .5 * PEEP).

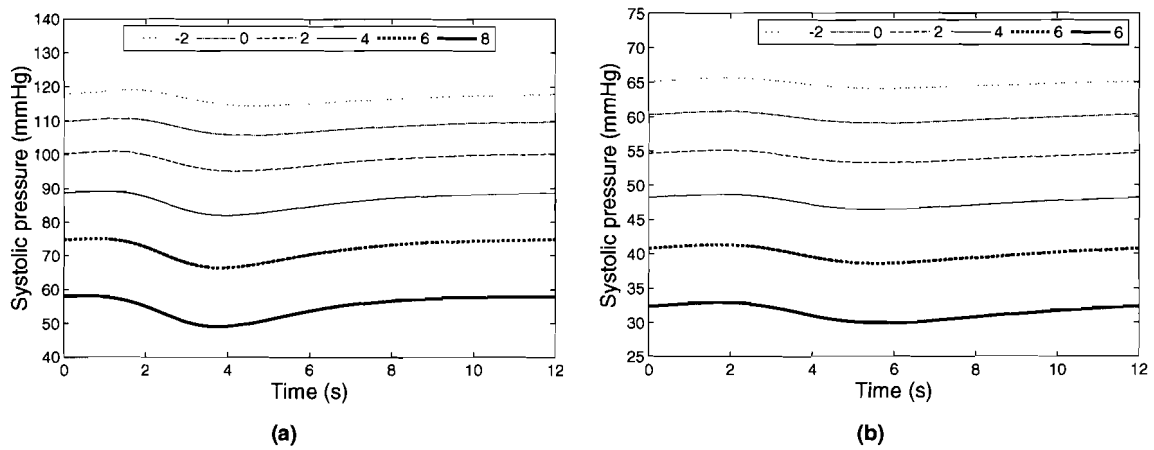

Figure 9.8: *Simulated systolic pressure modulation envelopes for changing level of PEEP for (a) the normal heart and (b) the stiff heart.*

In the model the systemic resistance is not adjusted when the blood pressure drops significantly (which it does when a higher level of PEEP is applied). According to Smith [2003], such an increase in resistance results in a shift leftwards on the Frank-Starling curve, which suggests that the SPM values increase even more for a higher level of PEEP. Since the results will be qualitatively compared, this is not important here. According to the simulation results, the SPM increases when the level of PEEP is increased.

A recording was performed while the level PEEP was stepwise decreased from 10 cm H_2O to 0 cm H_2O. After this level, the level of PEEP was set to 5 cm H_2O. In Figure 9.9 the SPM values that were measured during the recording are shown. Although no clear plateaus of SPM values are present, it

can be seen that the SPM decreases when the I:E time ratio decreases.

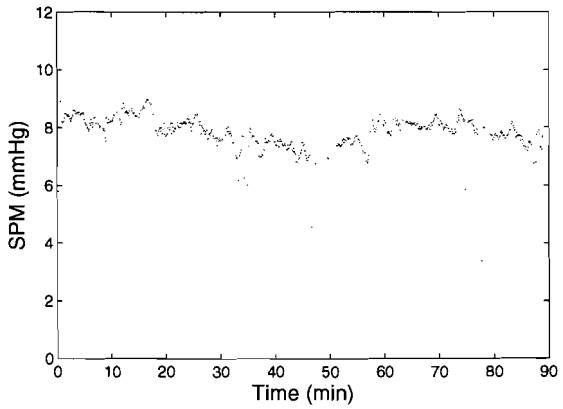

Figure 9.9: *SPM values of during the PEEP recording.*

In literature it was found that the SPV increased when the level of PEEP was increased in human patient and animal subject studies [Pizov et al., 1996; Michard et al., 1999].

For changing level of PEEP, the trend in the simulation results are confirmed by the trends in patient data, so the qualitative response of the model seems to be correct.

9.1.6 Qualitative verification

For each of the changes in settings, the trends in the modulation envelopes of the model are the same as the trends found in patient data. Therefore, the qualitative response of the model seems correct. However, because only a limited data set was used, a full qualitative verification needs to confirm these results. Also, a quantitative verification has to take place in order to fully validate the model.

9.2 Calculating the respiratory induced variations in arterial blood pressure

The second research objective involved calculation of respiratory induced variations in arterial blood pressure. For this calculation a new approach was introduced. This approach makes use of modulation envelopes that have the same periodicity as the respiratory signal. Prior to constructing these envelopes, the ABP signal is filtered to suppress neural influences in the ABP signal. In this section, a comparison between calculation based on the SPV and calculation based on the new approach, the SPM, is given.

During a period in which the state of the patient is stable, successive SPM values should not fluctuate as much as successive SPV values. Successive SPV values that were calculated during a stable period one minute are shown in Figure 9.10(a). The SPM values that were calculated using a filtered version of the same data are shown in Figure 9.10(b). In Figure 9.10(a) and Figure 9.10(b) it can be seen that the successive SPM fluctuate less than the SPV values.

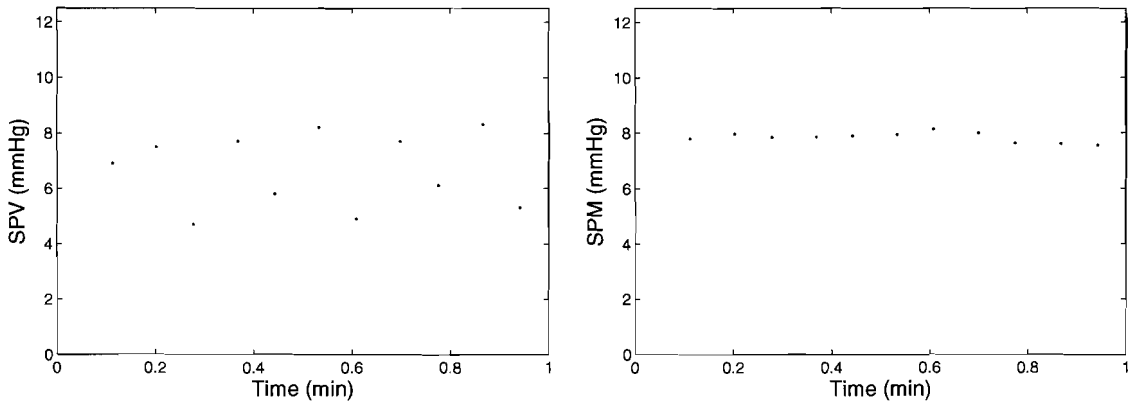

Figure 9.10: *Successive (a) SPV and (b) SPM values that were calculated using the same data. Prior to SPM calculation the ABP was filtered to suppress low-frequency neural distortions. The history window for the SPM calculation was set to sixty seconds.*

The standard deviation of successive SPM values should be lower than the standard deviation of the corresponding SPV values. Also, the average of these SPM values should be higher than the average of the SPV values. For five patients the mean and standard deviation of successive SPV and SPM values that were measured during a stable period of one minute are listed in Table 9.2.

Table 9.2: *Comparison between mean (μ) and standard deviation (σ) of SPV and SPM values during one minute using a SPM history window of one minute (values in mm Hg; adapted from Diepen et al. [2005]).*

Patient	μ_{SPV} (σ_{SPV})	μ_{SPM} (σ_{SPM})
1	2.07 (0.60)	2.59 (0.22)
2	6.62 (1.87)	7.20 (0.22)
3	6.04 (1.18)	6.39 (0.40)
4	7.00 (0.97)	7.57 (0.27)
5	3.60 (1.96)	3.42 (0.25)

As can be seen in Table 9.2, the standard deviation of the SPM values is in all cases at least three times smaller than that of the SPV values. Furthermore, the average SPM values are up to 25% higher than the average SPV values for four patients. The average value of the last patient is higher for the SPV calculation than for the SPM calculation. However, as the standard deviation of the SPV calculation for this patient is almost eight times the standard deviation of the SPM, questions regarding its significance should be raised. In fact, an extreme value that occurred during the measurement affected the SPV calculation, while it did not affect the SPM calculation too much.

The SPM was presented at the annual conference of the European Society for Computing and Technology in Anesthesia and Intensive Care (Aalborg, Denmark 2005).

9.3 General project results

For the project it was necessary to acquire patient data. Although it was possible in the Catharina Hospital to store data in the Operating Room (OR) and Intensive Care Unit (ICU) settings, the acquisition infrastructure needed to be extended in order to be used. Especially the software used in the OR did not allow for online processing of the data. Therefore, a LabVIEW component was written that can be used either as a stand-alone program, for example to store data, or it can be used in a system that processes the acquired signals. Like the model, the program was developed in cooperation with E.P.A. Verheijen.

Besides the data acquisition, a system was developed to process the ABP and airway pressure (AWP) signals of patients and measure the respiratory induced variations in ABP. The system is able to process data from a previously recorded file and from an online connection with the patient monitor. The ABP and AWP waveforms are validated to extract periods. For each validated respiratory cycle systolic peaks, pulse pressures, and estimates of stroke volumes are used to approximate a modulation envelope. The envelope construction is only done if all ABP periods within the respiratory cycle were found valid as well. Based on the envelopes, the values of the measures of respiratory induced variations in ABP are calculated and presented.

9.4 Summary

The results related to the research objectives are discussed in this chapter. Since the last objective, the parameter estimation routine, was not met, it is not discussed. Also, general project results are given.

A coupled model of the respiratory and circulatory systems was developed. According to a preliminary qualitative verification, trends in simulation results for changing ventilator settings and blood volume correspond to trends that were found in patient data. The trends in patient data were both measured and found in literature.

For the calculation of measures of respiratory induced variations in ABP it was found that a new approach was necessary. The developed approach is based on modulation envelopes. For successive cycles, this approach results in less fluctuating values. Also, the mean value of the successive calculated values is higher with the new approach.

To extend the data acquisition infrastructure in the Catharina Hospital, a program was written in LabVIEW. Based on this program, data processing can be done online in the OR. Furthermore, a program was written to calculate the respiratory induced variations in measured ABP signals.

chapter 10

Conclusions and recommendations

10.1 Conclusions

A coupled model was constructed based on already existing and verified models for both the respiratory and circulatory systems and significant influences that the respiratory system has on the circulation as described in literature.

The derived model was only qualitatively verified. This verification showed that the trends in the respiratory induced variations in ABP of the model due to changing settings (i.e. changing tidal volume, ratio of inspiratory and expiratory times, level of positive end expiratory pressure, and blood volume) agrees well with trends found in recordings and in literature. Although the verification was only preliminary due to limitations the results indicate that further research based on more recordings and maybe even clinical experiments, is recommended. Due to the nature of some of the tests (e.g. prolonged tests with extended respiratory periods) there are experiments that might have to be conducted on animal subjects instead of human patients. According to the preliminary qualitative verification the model has the potential to assist a clinician in assessing a patient's fluid loading responsiveness.

A quantitative verification was not performed. This is mainly because the previous step in the process, the qualitative verification, is not completed yet. Furthermore, a quantitative verification needs a reliable parameter estimation routine. Such a routine was not developed in the project.

To process the patient data, a system was developed in LabVIEW. The system obtains and validates arterial blood pressure (ABP) and airway pressure signals. Using validated periods of both signals, respiratory induced variations in ABP are measured. The system works online and can be used near the bedside. The measures are based on a new approach, which extends the currently used measures. Systolic pressures, diastolic pressures, and stroke volumes are thought of as samples of modulation envelopes. Instead of using the difference between the maximum and minimum systolic pressures, pulse pressures, and stroke volumes of each respiratory cycle, the difference between maximum and minimum values of the envelopes are used. With this approach the mean value of the measures of successive respiratory cycles increases, while at the same time the standard deviation decreases, thereby reducing the fluctuations.

Although it was shown that the modulation approach improves upon the traditional approach to measure respiratory induced variations in ABP, an important conclusion is that the measures of these variations based on the modulation approach still cannot be used to do a reliable assessment of fluid loading responsiveness: as long as the changes in preload (or an equivalent value) cannot be measured, the functioning of the heart (expressed using the Frank-Starling relation) cannot be determined well.

Since the quantitative verification was not done due to lacking of the parameter estimation routine, it can be concluded that not all project objectives were met. On the other hand, it was found that before model output could be compared to patient signals, first a new approach was necessary to suppress the fluctuations in successive measures of respiratory induced variations in ABP.

10.2 Recommendations and future work

In the project it was found that successive values of measures of respiratory induced variations in ABP can fluctuate highly. When the amplitude of the fluctuations becomes too high, the fluctuations may cause the indication of fluid loading responsiveness to vary each respiratory cycle. Therefore, it is recommended to use the modulation approach, which results in more consistent results for successive respiratory cycles. Future work may include improving the envelope approximation routine, because the currently used routine sometimes fails.

The ABP signals that were used, were all measured invasively. The invasive measurement limits the applicability of the respiratory induced variations in ABP for fluid loading responsiveness assessment. To broaden the applicability, the usage of a noninvasive finger pressure can be investigated. Since the arterial system has a transfer function, the pressure variations in the finger pressure measurement are most probably different than the invasive pressure variations. Therefore, research has to be done in this area.

Only few recordings were used to verify simulation results. One of the reasons for this is the fact that within the project there was no time for creation, approval, and putting into effect of an extensive measurement protocol. Since the results obtained from the recordings agreed with the simulation results, extensive testing can be recommended in order to make a good comparison and validate the model. This implies that such a protocol and approval is necessary.

As for right now, only a qualitative comparison is available. However, in order to correctly validate the model, quantitative comparisons also have to be carried out. These comparisons can only be performed if patient-specific parameters can be estimated reliably. Thus, a parameter estimation routine has to be integrated into the system. This routine should be able to estimate the parameters based on only few measured signals. If possible, measuring (intrathoracic) blood flows as well is recommended. When both pressures and flows are known, characterization of the parameters (impedances) should be possible. Eventually, the routine should work in real-time, so the model can be used to assist clinicians. Measuring the blood flows can also be useful to estimate variations in ventricular preload. In combination with the respiratory induced variations in ABP, an estimate of the functioning of the heart, based on the Frank-Starling curve, can be determined.

For both verification types, it holds that problems and limitations related to the experimental settings have to be solved. For instance, respiratory related signals should be obtained from the ventilator, instead of using the thorax impedance measurement.

According to the model results and the results obtained from patient data, the respiratory rate may influence the shape and position of the modulation envelope significantly: in some cases this may even lead to negative $\triangle_{up}$ components. For different ventilatory periods, the respiratory induced variation/modulation methods produce different values. A study has to be performed to check whether (and, if so, how) this affects the sensitivity and specificity of the methods.

The simulations showed that the modulation envelope that can be constructed for each (extended) respiratory period, has a characteristic shape. Especially the last part of the envelope, which seems to be an exponential increase to the baseline level, might reveal interesting information on the functioning of the heart. If so, measurements of preload might not be necessary. Perhaps this study can be combined with the RSVT-method as proposed by Perel et al. [2005], because this method lets the minimal value of the modulation envelope decrease for successive respiratory cycles. This could shed some light on the exponential increase that was observed. Also other characteristics of the shape should be further investigated (e.g. the position of the maximum with respect to the start of the respiratory cycle; the width of the positive lobe).

Some of the modulation envelopes constructed in the simulations had an unexpected high-frequency component. Currently it is not clear whether this component is due to aspects concerning the implementation, or due to assumptions (e.g. the inertia of blood). It was found that for the current model and its implementation, the speed of intrathoracic pressure decrease was an important factor, but it did not depend on the step size. However, a study has to be done to fully determine the reason and, if possible, find a solution, because such components were not seen in the recorded data.

References

Aben M. Model of the respiratory system, 2003. Internal report traineeship Technische Universiteit Eindhoven.

Beale RJ, Hollenberg SM, Vincent JL and Parrillo JE. Vasopressor and inotropic support in septic shock: An evidence-based review. Critical Care Medicine, 32, 455–465, 2004.

Bendjelid K and Romand JA. Fluid responsiveness in mechanically ventilated patients: a review of indices used in intensive care. Intensive Care Medicine, 29, 352–360, 2003.

Bennett-Guerrero E, Kahn RA, Moskowitz DM, Falcucci O and Bodian CA. Comparison of arterial systolic pressure variations with other clinical parameters to predict the response to fluid challenges during cardiac surgery. The Mount Sinai Journal of Medicine, 69, 96–100, 2002.

Berkenstadt H, Friedman Z, Preisman S, Marx R and Perel A. Stroke Volume Variation (SVV) Reflects Changes in Preload during Hemorrhage and Retransfusion in Dogs. In Book of Abstracts of the Annual Meeting. American Society of anesthesiologists (ASA), 2001, 2001.

Beyar R, Hausknecht MJ, Halperin HR, Yin FC and Weisfeldt ML. Interaction bewteen cardiac chambers and thoracic pressure in intact circulation. American Journal of Physiology, 22, H1240–H1252, 1987.

Blom JA. The SIMPLEXYS experiment: real time expert systems in patient monitoring. Ph.D. thesis, Technische Universiteit Eindhoven, 1990.

Blom JA. Monitoring of respiration and circulation. CRC Press, London, 1st ed., 2004.

Boldt J, Lenz M, Kumle B and Papsdorf M. Volume replacement strategies on intensive care units: results from a postal survey. Intensive Care Medicine, 24, 147–151, 1998.

Cannesson M, Besnard C, Durand PG, Bohé J and Jacques D. Relation between respiratory variations in pulse oximetry plethysmographic waveform amplitude and arterial pulse pressure in ventilated patients. Critical Care, 9, R562–R568, 2005.

Diepen S, Korsten HHM and Blom JA. Systolic Pressure Modulation. In Book of Abstracts of the Annual Conference. European Society of Computing and Technology in Anesthesia and Intensive Care (ESCTAIC), 2005.

Ferrari G, Lazarri CD, Mimmo R, Tosti G and Ambrosi D. A modular numerical model of the cardiovascular system for studying and training in the field of cardiovascular physiopathology. Journal of Biomedical Engineering, 14, 91–107, 1992.

Fujita Y, Sari A and Yamamoto T. On-line monitoring of Systolic Pressure Variation. Anesthesia & Analgesia, 96, 1529–1530, 2003.

Fujita Y, Yoshioka N, Hinenoya H, Yamamoto T and Sano I. A comparison of changes in cardiac preload variables during graded hypovolemia and hypervolemia in mechanically ventilated dogs. Anesthesia & Analgesia, 99, 1780–1786, 2004.

Gouvêa G and Gouvêa FG. Measurement of Systolic Pressure Variation on a Datex AS/3 Monitor. Anesthesia & Analgesia, 100, 1864–1864, 2005.

Guyton AC and Hall JE. TEXTBOOK OF MEDICAL PHYSIOLOGY. W.B. Saunders Company, Philadelphia, London, New York, St. Louis, Sydney, Toronto, 10th ed., 2000.

Guyton AC and Harris JW. Pressoreceptor-autonomic oscillation: a probable cause of vasomotor waves. American Journal of Physiology, 165, 158–166, 1951.

Guyton AC, Jones CE and Coleman TG. CIRCULATORY PHYSIOLOGY: Cardiac Output and its Regulation. W.B. Saunders Company, Philadelphia, London, Toronto, 2nd ed., 1973.

Jansen JRC, Schreuder JJ, Mulier JP, Smith NT, Settels JJ and Wesseling KH. A comparison of cardiac output derived from the arterial pressure wave against thermodilution in cardiac surgery patients. British Journal of Anaesthesia, 87, 212–222, 2001.

Jardin F. Cyclic changes in arterial pressure during mechanical ventilation. Intensive Care Medicine, 30, 1047–1050, 2004.

Kemp B, Värri A, Rosa AC, Nielsen KD and Gade J. A simple format for exchange of digitized polygraphic recordings. Electroencephalography and Clinical Neurophysiology, 82, 391–393, 1992.

Kentgens SAL. Coronary circulation teaching model. Master's thesis, Technische Universiteit Eindhoven, 2001.

Lu K, Clark JW, Ghorbel FH, Ware DL and Bidani A. A human cardiopulmonary system model applied to the analysis of the Valsava maneuver. American Journal of Physiology - Heart and Circulatory Physiology, 281, 2661–2679, 2001.

Magder S. Clinical usefulness of respiratory variations in arterial pressure. American Journal of Respiratory and Critical Care Medicine, 169, 151–155, 2004.

Malpas SC. Neural influences on cardiovascular variability: possibilities and pitfalls. American Journal of Physiology - Heart and Circulatory Physiology, 282, 6–20, 2002.

Massumi RA, Mason DT, Vera Z, Zelis R, Otero J and Amsterdam EA. Reversed pulsus paradoxus. New England Journal of Medicine, 289, 1272–1275, 1973.

McDonald DA. Blood flow in arteries. Arnold, London, 2nd ed., 1974.

Michard F. Changes in Arterial Pressure during Mechanical Ventilation. Anesthesiology, 103, 419–428, 2005.

Michard F, Chemla D, Richard C, Wysocki M, Pinsky MR, Lecarpentier Y and Teboul JL. Cinical use of respiratory changes in arterial pulse pressure to monitor the hemodynamic effects of PEEP. American Journal of Respiratory and Critical Care Medicine, 159, 935–939, 1999.

Michard F and Teboul JL. Predicting Fluid Responsiveness in ICU Patients: A Critical Analysis of the Evidence. Chest, 121, 2000–2008, 2002.

Milnor WR. Cardiovascular Physiology. OXFORD UNIVERSITY PRESS, New York, Oxford, 1st ed., 1990.

Morelot-Panzini C, Lefort Y and an T Similowski JPD. Simplified method to measure respiratory-related changes in arterial pulse pressure in patients receiving mechanical ventilation. Chest, 124, 665–670, 2003.

Niranjan SC, Bidan A, Ghorbbel F, Zwischenberger JB and Clark JW. Theoretical Study of Inspiratory Flow Waveforms during Mechanical Ventilation on Pulmonary Blood Flow and Gas Exchange. Computers and Biomedical Research, 32, 355–390, 1999.

Norton JM. Toward consistent definitions for preload and afterload. Advances in physiology education, 25, 53–61, 2001.

Oczenski W, Werba A and Andel H. Atmen-Atemhilfen: Atemphysiologie und Beatmungstechnik. Blackwell Wissenschafts-Verlag Berlin Wien, Oxford, Edinburgh, Boston, London, Melbourne, Paris, Yokohama, 3rd ed., 1996.

Parry-Jones AJD and Pittman JAL. Arterial pressure and stroke volume variability as measurements for cardiovascular optimisation. International journal of intensive care, 10, 67–72, 2003.

Patterson R. The Biomedical Engineering Handbook, chap. Bioelectric Impedance Measurements. CRC Press, London, 2nd ed., 2000.

Perel A. The value of functional hemodynamic parameters in hemodynamic monitoring of ventilated patients. Anaesthesist, 52, 1003–1004, 2003.

Perel A, Minkovich L, Preisman S, Abiad M, Segal E and Coriat P. Assessing fluid-responsiveness by a standardized ventilatory maneuver: the Respiratory Systolic Variation Test. Anesthesia & Analgesia, 100, 942–945, 2005.

Perel A, Pizov R and Cotev S. Systolic blood pressure variation is a sensitive indicator of hypovolemia in ventilated dogs subjected to graded hemorrhage. Anesthesiology, 67, 498–502, 1987.

Pizov R, Cohen M, Weiss Y, Segal E, Cotev S and Perel A. Positive end-expiratory pressure-induced hemodynamic changes are reflected in the arterial pressure waveform. Critical Care Medicine, 24, 1381–1387, 1996.

Pizov R, Segal E, Kaplan L, Floman Y and Perel A. The use of systolic pressure variation in hemodynamic monitoring during deliberate hypotension in spine surgery. Journal of Clinical Anesthesia, 2, 96–100, 1990.

Pizov R, Ya'ari Y and Perel A. The arterial pressure waveform during acute ventricular failure and synchronized external chest compression. Anesthesia & Analgesia, 68, 150–156, 1989.

Preisman S, DiSegni E, Vered Z and Perel A. Left ventricular preload and function during graded haemorrhage and retransfusion in pigs: analysis of arterial pressure waveform and correlation with echocardiography. British Journal of Anaesthesia, 88, 716–718, 2002.

Preisman S, Kogan S, Berkenstadt H and Perel A. Predicting fluid responsiveness in patients undergoing cardiac surgery: functional haemodynamic parameters including the Respiratory Systolic Variation Test and static preload indicators. British Journal of Anaesthesia, 95, 746–755, 2005.

Preisman S, Pfeiffer U, Lieberman N and Perel A. New monitors of intravascular volume: a comparison of arterial pressure waveform analysis and the intrathoracic blood volume. Intensive Care Medicine, 23, 651–657, 1997.

Pybus A. The 'St. George' Guide To Pulmonary Artery Catheterisation. http://www.manbit.com/PAC, [Accessed: October 15, 2005].

Reinsch CH. Smoothing by Spline Functions. Numerische Mathematik, 10, 177–183, 1967.

Reuter DA, Bayerlein J, Goepfert MSG, Weis FC, Kilger E, Lamm P and Goetz AE. Influence of tidal volume on left ventricular stroke volume variation measured by pulse contour analysis in mechanically ventilated patients. Intensive Care Medicine, 29, 476–480, 2003.

Reuter DA, Felbinger TW, Kilger E, Schmidt C, Lamm P and Goetz AE. Optimizing fluid therapy in mechanically ventilated patients after cardiac surgery by on-line monitoring of left ventricular stroke volume variations. Comparison with aortic systolic pressure variations. British Journal of Anaesthesia, 88, 124–126, 2002.

Rick JJ and Burke SS. Respirator paradox. Southern Medical Journal, 71, 1376–1378, 1978.

Scharf SM, Brown R, Saunders N and Green LH. Hemodynamic effects of positive-pressure inflation. Journal of Applied Physiology, 49, 124–131, 1980.

Schott RHA. Real-time computation of respiratory effort during ventilation weaning. Master's thesis, Technische Universiteit Eindhoven, 2005.

Schwid HA and Rooke GA. Systolic blood pressure at end-expiration measured by the automated systolic pressure variation monitor is equivalent to systolic blood pressure during apneavariation is a sensitive indicator of hypovolemia in ventilated dogs subjected to graded hemorrhage. Journal of Clinical Monitoring and Computing, 16, 115–120, 2000.

Segers P, Stergiopulos N, Schreuder JJ, Westerhof BE and Westerhof N. Left ventricular wall stress normalization in chronic pressure-overloaded heart: a mathematical model study. American Journal of Physiology - Heart and Circulatory Physiology, 279, 1120–1127, 2000.

Senzaki H, Chen CH and Kass DA. Single-beat estimation of end-systolic pressure-volume relation in humans. A new method with the potential for noninvasive application. Circulation, 94, 2497–2506, 1996.

Shoemaker WC, Wo CCJ, Thangathurai D, Velmahos G, Belzberg H, Asensio JA and Demetriades D. Hemodynamic patterns of survivors and nonsurvivors during high risk elective surgical operations. World Journal of Surgery, 23, 1264–1271, 1999.

Smith BW. Minimal Haemodynamic Modelling of the Heart & Circulation for Clinical Application. Ph.D. thesis, University of Canterbury, New Zealand, 2003.

Smith BW, Chase JG, Nokes RI, Shaw GM and Wake G. Minimal haemodynamic system model including ventricular interaction and valve dynamics. Medical Engineering & Physics, 26, 131–139, 2004.

Smith BW, Chase JG, Nokes RI, Shaw GM and Wake G. Experimentally verified minimal cardiovascular system model for rapid diagnostic assistance. Control Engineering Practice, 13, 1183–1193, 2005.

Sun Y, Beshara M, Lucariello RJ and Chiaramida SA. A comprehensive model for right-left heart interaction under the influence of pericardium and baroreflex. American Journal of Physiology - Heart and Circulatory Physiology, 272, 1499–1515, 1997.

Szold A, Pizov R, Segal E and Perel A. The effect of tidal volume and intravascular volume state on systolic pressure variation in ventilated dogs. Intensive Care Medicine, 15, 368–371, 1989.

Tsitlik JE, Halperin HR, Popel AS, Shoukas AA, Yin FC and Westerhof N. Modeling the circulation with three-terminal electrical networks containing special nonlinear capacitors. Annals of Biomedical Engineering, 20, 595–616, 1992.

Van den Berg PCM. Cardiopulmonary Interaction: The Effects of Transient Airway Pressure Increase on Cardiac Function. Ph.D. thesis, Universiteit van Amsterdam, The Netherlands, 1991.

Vedrinne JM, Duperret S, Decaillot F, Gratadour P and Motin J. Haemodynamic changes induced by two I:E ratios: a transoesophageal echocardiographic study. Canadian Journal of Anesthesia, 44, 354–359, 1997.

Weiss YG, Oppenheim-Eden A, Gilon D, Sprung CL, Muggia-Sullam M and Pizov R. Systolic Pressure Variation in Hemodynamic Monitoring After Severe Blast Injury. Journal of Clinical Anesthesia, 11, 132–135, 1999.

Wesseling KH, de Wit B, Weber JAP and Smith NT. A simple device for the continuous measurement of cardiac output. Advanced Cardiovascular Physics, 5, 16–52, 1983.

Wesseling KH, Jansen JRC, Settels JJ and Schreuder JJ. Computation of aortic flow from pressure in humans using a nonlinear, three-element model. Journal of Applied Physiology, 74, 2566–2573, 1993.

appendix A

Used model parameter values

All parameters and their values that were used for the simulations, are listed below. They are grouped using the three derived systems (respiratory system, circulatory system and coupled system). Only the values for the basic simulation are given. The values of the parameters that were used to change conditions, are given Chapter 6.

A.1 Respiratory system parameters

The most important part of the respiratory system during the project, was the intrathoracic pressure. This pressure can be written as a function of time, using several parameters. The curve and its parameters are shown in Figure A.1.

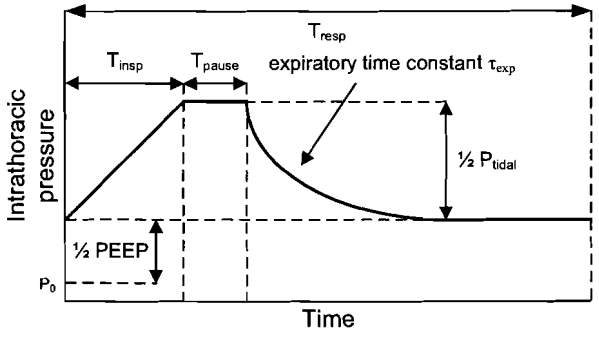

Figure A.1: *Basic intrathoracic pressure curve shape and its parameters. The respiratory period (T_{resp}) consists of an inspiratory period (T_{insp}), an inspiratory pause (T_{pause}) and an expiratory period. The expiratory time constant depends on the patient's lung and airway physiology. Intrathoracic pressure varies between the pressure when no ventilatory signal is applied (P_0) plus a half times the PEEP value and this sum value plus a tidal pressure.*

The parameters can be categorized into parameters related to pressure and to time. The basic curve was constructed using the following values:

times

T_{resp}	12	s
T_{insp}	2	s
T_{pause}	1	s
τ_{exp}	0.75	s

pressures

P_0	-4	mm Hg
PEEP	6	mm Hg
P_{tidal}	4	mm Hg

A.2 Circulatory system parameters

The derived circulatory system can be split up into six separate compartments. Each compartment has several parameters, depending on the type of compartment (passive/active). All values were obtained from Smith [2003]; Smith et al. [2004, 2005].

left ventricle

E	454.3526	10^{+6}	Nm^{-5}
P_0	168.2353	10^{0}	Nm^{-2}
V_D	5.0	10^{-6}	m^3
V_0	5.0	10^{-6}	m^3
λ	15	10^{+3}	m^{-3}

right ventricle

E	87.10099	10^{+6}	Nm^{-5}
P_0	154.8903	10^{0}	Nm^{-2}
V_D	5.0	10^{-6}	m^3
V_0	5.0	10^{-6}	m^3
λ	15	10^{+3}	m^{-3}

Pulmonary artery

E	45.29830	10^{+6}	Nm^{-5}
V_0	160	10^{-6}	m^3

Pulmonary vein

E	829.0998	10^{+3}	Nm^{-5}
V_0	200	10^{-6}	m^3

Systemic artery

E	94.66374	10^{+6}	Nm^{-5}
V_0	800	10^{-6}	m^3

Systemic vein

E	1.451072	10^{+6}	Nm^{-5}
V_0	2.830	10^{-3}	m^3

The compartments are connected through resistive paths:

R_{mt}	63.45997	10^{+3}	Nsm^{-5}
R_{av}	1.432370	10^{+6}	Nsm^{-5}
$R_{systemic}$	140.9251	10^{+6}	Nsm^{-5}
R_{tc}	175.7974	10^{+3}	Nsm^{-5}
R_{pv}	482.4593	10^{+3}	Nsm^{-5}
$R_{pulmonary}$	19.38203	10^{+6}	Nsm^{-5}

Remains the pericardial compartment:

V_0	200.0	10^{0}	m^3
P_0	66.6612	10^{0}	Nm^{-2}
λ	30.0	10^{+3}	m^{-3}

As can be seen, the mentioned values are given in SI units. However, for presentation of the values, different units were used. The multiplication factor between the used and SI units are listed in Table A.1.

Table A.1: *Multiplication factor between used and SI units (SI = used * mult.)*

	Used unit	SI unit	mult.
pressure	mm Hg	Nm^{-2}	133.32239
volume	ml	m^3	$1\ 10^{-6}$

Finally, there are two other parameters: the heart rate and the total blood volume. The former was set to 93 beats per minute and the latter to 5000 ml.

The iteration step-size was set to 0.005 s.

A.3 Coupled system specific parameters

The only parameters involved in the coupling are the values that alter the pulmonary resistance. Consistent values for the parameters where not found in literature. However, a maximum inspiratory (alveolar) pressure of 30 mm Hg was used, based on the limits used during the recordings. The value of the scaling factor was found by adjusting its value until the modulation amplitude gave reasonable results: 10 mm Hg ml^{-1} s^{-1}.

appendix B

Patient data acquisition and processing

Patient data that was used during the project, was obtained from the Catharina Hospital in Eindhoven, The Netherlands. This document describes how the patient data was acquired and processed in the project. It starts with a description of where and how the necessary signals were obtained. It then continuous with how the acquired signals were validated. Finally, the calculation of the respiratory induced variations in arterial blood pressure (ABP) is discussed.

The total system was implemented in National Instruments' LabVIEW (National Instruments, USA) and therefore the system will be described from a LabVIEW point of view whenever this is required by aspects concerning the implementation.

B.1 Acquisition

Patient data were obtained from the hospital's Operating Room (OR) and Intensive Care Unit (ICU). Below a short description of how data can be obtained in these settings is given.

B.1.1 Operating Room

In the OR of the hospital S/5 Anesthesia Delivery Units from Datex/Ohmeda (Datex/Ohmeda, Finland) are used. Besides the ability to monitor patient-specific waveforms (e.g. (invasive) arterial blood pressure, airway pressure), the machines are capable of administering anesthetic gases. Furthermore, the machines are able to present results not only on their built-in displays, but they can also communicate with other devices using a RS232 communication port.

Using the RS232 communication, the monitor can send a maximum of eight waveforms simultaneously to another device. Furthermore, the total number of waveform samples that can be transferred each second is 600. For the current project only two signals are necessary: ABP and airway pressure (AWP). The ABP signal comes with 100 samples per second, whereas the AWP comes with 25 per second. Therefore, there should be no problem in receiving the samples correctly.

When a device requests waveforms, the machine does not send new samples to the requesting device whenever they are recorded by the sensors. Instead, it keeps internal buffers for all requested waveforms. The samples recorded by the sensors are added to these buffers. Each second the oldest

elements in the buffers are cleared and send to the requesting device. So, if the ABP and AWP signals are requested, the monitor sends 100 + 25 = 125 samples per second.

B.1.2 Intensive Care Unit

In the ICU of the hospital patient monitors from Hewlett-Packard (Hewlett-Packard Company, USA) are used. Unfortunately, these monitors cannot be accessed directly to obtain waveforms. The monitors are connected to a central server through which the waveforms can be obtained.

Like the monitors in the OR, the central server can only send groups of waveform samples at specified time intervals. However, instead of 1 second time intervals like the OR's anesthesia monitors, the intervals last 1.024 seconds. Another difference with the OR's anesthesia monitor is that all signals have the same sample rate. Every 1.024 the machine sends 128 samples per signal (i.e. a sample rate of 125 Hz).

B.1.3 Online vs offline

Eventually, determining the magnitude of the variations in ABP should occur online near the bedside. Unfortunately, as said before, the waveforms recorded in the ICU are only available through the central server which is not located near the bedside. Furthermore, during development, it is not convenient to test the program in the OR every time a new feature has been added or an existing feature has been improved.

The system therefore had to be designed in such a way that both the online OR and offline ICU data could be used. Also, usage of offline data from the OR should be possible. Fortunately, in the hospital software is used that can store the signals (both in OR and ICU) using the European Data Format (EDF) [Kemp et al., 1992]. This is a file format designed for storing biomedical waveforms. The system should thus be able to make connections to EDF files to process the offline data previously recorded by the hospital's software.

In the EDF format, all signals are stored in records, which have a specified length T. In one record, all samples that occurred during the period T are stored per signal. For example, a record contains two signals. Signal A is a 25 Hz signal and Signal B a 100 Hz signal. A 1 second record then contains 125 samples: 25 samples of Signal A, followed by 100 samples of Signal B.

Like the online connection, samples thus come in groups. Therefore, the system should only distinguish in its connection (i.e. the connection to a file or to a patient monitor) and the accompanying properties. The way it passes the samples through to the processing part, however, does not have to be different.

Connection to the patient monitor

The software that is able to store patient signals in the OR, makes use of a component that provides communication with the pc and the patient monitor. The component was written in Delphi (Borland, United States) by Dr. Leo van Wolfswinkel. Instead of writing the specific commands of the communication in LabVIEW (which can become very complicated quickly), it was chosen to use this component.

Due to the fact that the component only works in a Delphi environment and not (directly) in the LabVIEW environment, an external library containing the component was created in Delphi. The library is linked to the LabVIEW system and provides an initialization routine in which the wanted waveforms can be requested. A second routine is used to pass the waveform samples to the system developed in LabVIEW. A third routine in the library, which is not visible for the system in LabVIEW, is triggered by the anesthesia monitor when it has new samples available. The samples of the requested waveforms are then obtained and stored in an internal buffer. Since the monitor sends the trigger each second, new data will only be available each second and therefore, the LabVIEW system calls the passing routine each second. The passing routine then passes the buffered samples to the LabVIEW program.

Connection to an EDF file

According to the EDF file format, EDF files consist of a header and multiple signal records. The header contains all kind of meta information regarding the recording (e.g. patient identification, date-/timestamps, recording duration, record duration). Beside this information, also properties of the recorded signals are given (e.g. signal name, number of samples per record). The records contain the signal data as described above.

During initialization, the system reads the header information. This is mainly used to determine the sample rates of the ABP and AWP signals. When this is finished, the system starts to read records.

In the online connection the system waits for new samples each second, as the anesthesia monitor provides new samples every second. A similar approach was used in the EDF file connection: the system reads a record and waits for the duration of the record (as specified in the file header) before it reads the next record.

When creating an EDF file, the range of values that a signal can have is scaled to a two-byte signed integer value (big endian; two's complement). Therefore, before samples can be passed for further processing, they need to be parsed back to their original values, using scaling factors which are specified in the signals part of the header.

B.1.4 Getting data ready for processing

The connection (either online or offline) provides groups of samples for further processing in the LabVIEW system. However, because the processing has to occur sample by sample, the groups have to be buffered. The processing mechanism can then take a sample from the buffer each timestep. The buffer is implemented as a FIFO buffer, because the validation needs the samples to come in the correct order.

When a sample is obtained from the buffer, the buffer size should decrease. This implies that the processing part of the system needs to 'write' to the buffer variable. Since the connection part also writes to the buffer, errors may occur when both parts want to write to the buffer simultaneously. To avoid this, a mechanism provided by LabVIEW, called semaphores, was used. If the sampling proces wants to write to the buffer, it needs to acquire the right for writing (i.e. the semaphore). If the sample processing loop already has this right, the sampling proces has to wait until the sample processing proces has finished writing. When the sample processing proces finishes writing, it releases the

semaphore, so the sampling process can gain access to the buffer. The sample processing process now has to wait for the sampling process to finish writing before it can write to the buffer again.

B.2 Signal validation

Before calculations can be performed on the ABP and AWP waveforms, they need to be validated. For quasi-periodic biomedical waveforms, Blom [1990] proposed a validation method. This method is used in the graduation project. A short description of this method will be given below. However, prior to validation, the data are filtered. This is to reduce neural influenced distortions on the RIM. This influence can be expected in the 0.03–0.06 Hz range. Therefore, a third-order Butterworth bandstop filter (f_{low} = 0.015 Hz; f_{high} = 0.07 Hz) was used.

The validation method is based on properties of each period in the signal. Since the signal is quasi-periodic, properties of successive periods cannot change too much (e.g. minimum value, maximum value, period length). This implies that some kind of slowly changing model of the properties can be created, which can be updated each period: model = model $*$ x + (1$--$x) $*$ $value_{this\ period}$ (for $0 < x < 1$). If calculated properties differ too much from the model value and/or some predefined settings, the model has to be initialized again using these predefined settings.

Using the properties, each period can be split up into several parts. During a part, the current period's propertie can be derived. The partial parts can be seen as states of a finite state machine (FSM). The value of a sample is then used to determine whether the system stays in the current state, or that a transition to the next state has to take place.

For example, some properties of the ABP are the systolic and diastolic pressures, the period duration and the pulse pressure (both up and down). It is known that from the diastolic pressure the blood pressure rises to the systolic pressure pretty fast. After it has reached the systolic pressure, it falls down to a diastolic value again. However, this transition is much slower. Also, a dicrotic notch may be present in the pressure waveform.

Since the shape of the ABP period is known, it can be characterized and split up into several parts. For example, separate states for minimum and maximum detection can be defined. Thresholds can be used for state transitions.

To be able to create a model, some initialization is necessary. This initialization takes a predefined time (e.g. the maximum time a period of the ABP should last within which correct minimum and maximum values should be found). The minimum and maximum levels of the ABP are searched during this time. If the found values fall within a predefined range, they are copied to the model values. The model period is set as the maximum time a period should last. The initialization can end at any given position of a period. This means that validation algorithm has to get in phase with the pressure waveform. In order to do this, the state machine is extended with two synchronization states.

The time to stay in each state depends on the model's period. If the stay in a period takes too long, a transition to the initialization state takes place. Also, if the calculated properties are wrong (i.e. they exceed a predefined limit or they differ too much from the model's property), a transition to the initialization state takes place.

Arterial blood pressure

Blom [1990] proposes six states with three different transition values. Each period, the transition levels are calculated as 25%, 50% and 75% of the pressure between the model's minimum and maximum pressures. So, the new minimum should be below the 25% threshold, while the new maximum should be above the 75% threshold.

Instead of using the minimum (diastolic) pressure as the start of the period, the FSM detects a new period when it passes the 75% threshold [Blom, 1990].

In Figure B.1, the used FSM is drawn.

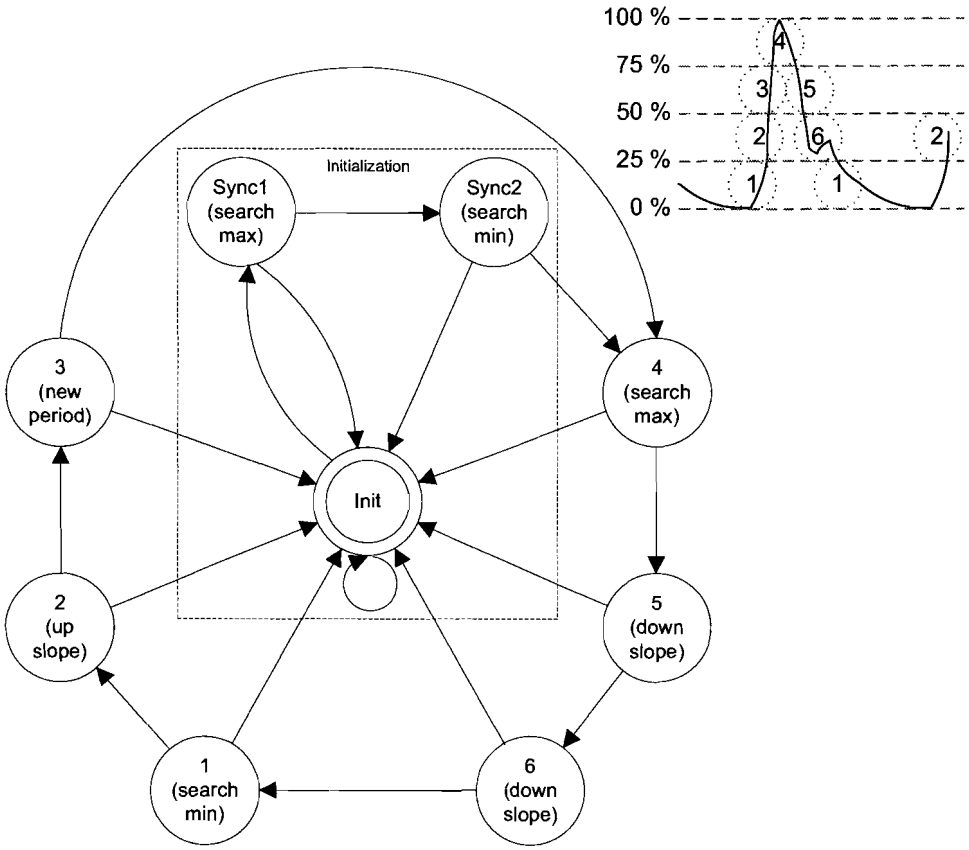

Figure B.1: *Finite state machine for ABP validation and the relation of the states to the typical ABP period.*

The method is implemented in a loop which runs synchronously with the sampling process. The time between two iterations of the loop is set to the reciprocal of the sample rate of the signal.

When the system is in track (i.e. no initialization/synchronization), the samples that are processed are buffered. When the state makes a transition from state 3 to state 4, the system has detected a new period. The index of the sample, however, is not the end point of the ABP period. The true end point

of the period is the diastolic index that preceded the transition (note that the end point also marks the beginning of the new period). If the preceding period was also found, a valid period is detected. Using the period, several parameters (period length, pulse pressure, systolic pressure, diastolic pressure) are calculated, which in turn are used to update the model. The pressure samples that were buffered for the newly found period are extracted from the buffer and used for calculation of SV based on modelflow [Wesseling et al., 1993].

The program thus has to process a lot of information when a new period is detected. This processing may become too heavy for the validation loop causing it to slow down. Eventually, this may result in the unwanted desynchronization of the sampling and sample processing loops. A better solution would be a mechanism that can process the information in parallel, which is triggered when the new period is detected. Actually, this is an event-driven approach for which LabVIEW has built-in functionality. Using this functionality, an event handler was created that starts processing the period when the new period event is triggered by the processing loop. The validation loop now only processes/uses the maximum and minimum pressures and the period length to update the model.

The built-in functionality provides an interface for event triggering that enables passing data together with the event itself. So, whenever a new period was found, the event that is triggered, is accompanied by the pressure values extracted from the buffer and the current index (the event handler has to determine the true start and end of the period).

The event handler thus contains the functionality as previously described (i.e. all processing after the new period was detected). More about the event handler will be discussed in the next section.

Airway pressure

The AWP processing is nearly identical to the processing of the ABP signal. However, because the shape of an AWP period is different than a period of the ABP signal, the number of states in the FSM differ. Also, the AWP has different features and properties. In Figure B.2 an example of the shape of a typical AWP period is drawn. The shape has two main levels: the low and high level.

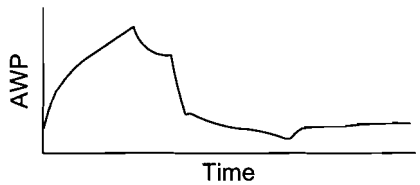

Figure B.2: *Shape of a typical AWP period (pressure in arbitrary units, time in s).*

The smooth decrease near the maximum value (just before the pressure falls down), which occurs at the inspiratory pause, is not always clearly visible. Therefore, the implementation only distinguishes between two levels: a high level and a low level. Instead of six tracking states, the FSM for the AWP therefore contains two tracking states.

The signals are not always as smooth as the shape drawn in Figure B.2. If the same transition levels from the low to high state and vice versa are then used, a small fluctuation around this transition level

may cause false validation. Therefore, a hysteresis was used: the transition from the low to the high pressure level occurs at a higher pressure than the other transition.

Similar to the ABP validation part of the system, the AWP validation detects a new period later than the period started. The real start occurs when the pressure goes up, while the new period is detected somewhere later on the rising edge. However, this is not important for the validation process: when the period is detected, the validation proces generates an event which is handled by the event handler using the obtained pressures and the index of detection.

B.3 Calculation

B.3.1 Event handler

In the previous section it was mentioned that both the respiratory and circulatory validation processes generate an event when a new period was validated. The event trigger is accompanied with the pressures seen during the period and an index that, using the respective sample frequencies, specifies the time at which the new period was detected.

For both signals, the event handler has to process the information contained within one period. For the ABP values systolic and pulse pressures have to be calculated. Using the pressure values, the SV has to be calculated as well. The most important part of the AWP signal that is needed for the measures of respiratory induced variations in ABP, is the length of the period.

It was already mentioned that the event is generated a little time after the actual or true end (/beginning) of the period. This means that before properties can be extracted, first the true period has to be found. The part of the true end until the time of triggering belongs to the next period. Likewise, the part between the true end and the triggering point of the previous period belongs to the current one. The event handler therefore stores this part.

The true end/beginning of an ABP period is the index at which the signal starts with the up slope. The system finds this point by searching backwards in the pressure array (starting at the end) until the found value is higher than the previous value (which is its follower in the pressure array). The same approach is used to determine the true end/beginning index of the AWP period.

With the pressures of the true ABP period, the event handler determines the diastolic pressure (i.e. the first value), the systolic pressure (i.e. the maximum value), and the SV. Also, the indexes of these values are determined. For the diastolic and systolic pressures this is the index of their occurrence, for the SV this is the index at which the dicrotic notch occurs. The latter is obtained from the modelflow-based SV calculation.

The indexes are used to find the phase within the respiratory cycle. If a new AWP period is found, the phase is the difference between the index and the start of the respiratory cycle. When the whole respiratory cycle is found and also the properties of the ABP periods within this cycle are calculated, the respiratory induced variations and modulations can be calculated.

B.3.2 Respiratory induced variations in ABP

The last part of the program involves the calculation and presentation of the measures of respiratory induced variations in ABP. This part of the systeem is also a loop, which runs in parallel with the other loop processes. Whenever new information becomes available from the event handler, the system calculates the SPV, PPV and SVV values using the methods found in literature [Michard, 2005].

For the calculation of the SPM, PPM and SVM, information from the past is needed for the envelope approximation. Therefore, a recent history has to be kept. It is not yet clear what the optimal length of the history should be so it was chosen to make this value variable: the length can be set by the user (a default value of sixty seconds is used).

The system keeps track of the history by assigning an intensity value of 1 to the points when they are provided by the event handler. Each iteration, the intensities ($0.01 < \text{intensity} < 1$) are multiplied by a weighting factor w, which depends on the length of the history window. The factor is set using the following relation:

$$w^{\frac{\text{window length}}{\text{iteration time}}} = 0.01 \tag{B.1}$$

Here 0.01 is a predefined threshold. Whenever the intensity of a point becomes lower than this value, this means that the time at which the point was obtained from the event handler, falls out of the time window. Therefore, it is removed from the history.

Although a trivial solution would be just remembering the times at which the points were provided, the intensities are needed for further calculations as well. The used curve approximation algorithm ([Reinsch, 1967]), has two inputs. It uses a vector of time instances and a vector of the corresponding values (pressures/volumes). The algorithm was chosen because it can approximate curves of which no a-priori shape information is present for non-equidistant time vectors. A drawback of the algorithm is that it needs the time vector to be strictly monotonic. It could be that the points (which are synchronized on one respiratory cycle) have the same time value and different pressure/volume values. When this happens, a single value has to be determined. When for a time value N synchronized values are present, the value used for calculation (V_w) is determined as follows:

$$V_w = \frac{\sum_{j=1}^{N} v_j * i_j}{\sum_{i=1}^{N} i_j} \tag{B.2}$$

Here $v_{1\ldots N}$ are the N values that are present for the time value and $i_{1\ldots N}$ the corresponding intensities. The intensities can thus also be used to give more weight to more recently found values.

Using the weighted values and their corresponding timings, the system constructs a modulation envelope for the systolic pressures, the diastolic pressures and the stroke volumes using the algorithm. Next, the formulae for the SPV and SVV are applied to the systolic envelope and the SV envelope, to calculate the SPM and SVM, respectively. For the calculation of the PPM, the systolic and diastolic envelopes are used.

Since there is a delay between the systolic and diastolic points, the diastolic envelope is shifted forwards. The shift is determined using the time difference of the systolic and diastolic value of the first pulse pressure seen in the newly arrived points. The PPM is now calculated as the PPV applied to the difference of the systolic envelope and the shifted diastolic envelope.

The weighting, curve approximation and calculation are only performed during iterations in which new points have arrived. The multiplication of the intensities is performed each iteration.

The SPM calculation uses the envelope approximation only once, while it is used twice to calculate the PPM values. The SVM calculation uses the approximation once too, however the SVs are already approximated values (the calculation of the SVs is based on the pressure curve). Since the approximation is not always optimal, the current implementation is most reliable for the SPM.